

FEDERAL SCIENCE CENTRE  
INSTITUTE FOR HIGH ENERGY PHYSICS

IHEP 94-81

S.S.Gershtein, V.V.Kiselev, A.K.Likhoded, A.V.Tkabladze

**Physics of  $B_c$  mesons**

Protvino 1994

arXiv:hep-ph/9504319v1 18 Apr 1995

**Abstract**

Gershtein S.S., Kiselev V.V., Likhoded A.K., Tkabladze A.V. Physics of  $B_c$  mesons: IHEP Preprint 94-81. – Protvino, 1994. – p. 82, figs. 23, tables 28.

In the framework of potential models for heavy quarkonium the mass spectrum for the system  $(\bar{b}c)$  is considered. Spin-dependent splittings, taking into account a change of a constant for effective coulomb interaction between the quarks, and widths of radiative transitions between the  $(\bar{b}c)$  levels are calculated. In the framework of QCD sum rules, masses of the lightest vector  $B_c^*$  and pseudoscalar  $B_c$  states are estimated, scaling relation for leptonic constants of heavy quarkonia is derived, and the leptonic constant  $f_{B_c}$  is evaluated. The  $B_c$  decays are considered in the framework of both the potential models and the QCD sum rules, where the significance of Coulomb-like corrections is shown. The relations, following from the approximate spin symmetry for the heavy quarks in the heavy quarkonium, are analysed for the form factors of the semileptonic weak exclusive decays of  $B_c$ . The  $B_c$  lifetime is evaluated with the account of the corrections to the spectator mechanism of the decay, because of the quark binding into the meson. The total and differential cross sections of the  $B_c$  production in different interactions are calculated. The analytic expressions for the fragmentational production cross sections of  $B_c$  are derived. The possibility of the practical  $B_c$  search in the current and planning experiments at electron-positron and hadron colliders is analysed.

## 1. Introduction

A complete picture for both precise tests of the Standard Model [1] and a search of effects from new physics supposes a direct measurement of the three-boson electroweak vertex, searches of higgs particles [2], the supermultiplets [3] etc. at colliders of super high energies (LEP200, LHC) as well as a study of the  $CP$  violation and a measurement of the fundamental parameters of the electroweak theory (first of all, in the heavy quark sector).

In the nearest decade, the centre of efforts, directed to the realization of this program, will certainly be in the field of the heavy quark physics at both the running colliders (LEP and Fermilab) and the  $B$  meson factories, being planned in SLAC, KEK and at HERA-B. In this case, the extraction of effects, related with high values of the energy scale, will be essentially determined by an accuracy of the theoretical and empirical knowledge on mechanisms of the quark interactions at non high energy and, first of all, about effects, caused by the QCD dynamics [4]. Therefore, the experimental researches of processes with the heavy  $c$ -,  $b$ -,  $t$ -quarks take a special importance.

The presence of the small parameter  $\Lambda_{QCD}/m_Q$ , where  $\Lambda_{QCD}$  is the scale of the quark confinement and  $m_Q$  is the heavy quark mass, has allowed one to develop the powerful tools for the study of the QCD dynamics in the heavy quark interactions, such methods as the phenomenological potential models [5–10], the QCD sum rules [11–13] and Effective Heavy Quark Theory (EHQT) [14], that is successfully applied for the study of hadrons, containing a single heavy quark. Thus, the investigation of the processes with the heavy quarks allows one to extract and to study nonperturbative QCD effects, causing the quark hadronization, by means of the use of the heavy quark as the "marked" atoms. A successful realization of such program of studies becomes possible due to the progress in the experimental technique of the detecting and the identification of particles (mainly, it is related with the invention and the improvement of the vertex detectors, allowing one to observe the heavy quark particles due to its running gap from the primary vertex of the interaction).

Among the heavy quarkonia ( $Q\bar{Q}'$ ), the  $(\bar{b}c)$  system with the open charm and beauty takes a particular place. In contrast to the hidden charm ( $c\bar{c}$ ) and beauty ( $b\bar{b}$ ) families, studied in details experimentally [15] and being quite accurately described theoretically

[13,16,17], the heavy quarkonium ( $\bar{b}c$ ), the family of  $B_c$  mesons, has some specific production and decay mechanisms and the spectroscopy, whose study allows one to extend and to enforce the quantitative understanding of the QCD dynamics as well as to step forward in the study of the most important parameters of the electroweak theory.

From the spectroscopy viewpoint, the ( $\bar{b}c$ ) system is the heavy quarkonium, whose spectrum can be quite reliably calculated in the framework of the QCD-motivated non-relativistic potential models as well as in the QCD sum rules. ( $\bar{b}c$ ) is the only system, composed of two heavy quarks, where the description of this system mass spectrum can test the selfconsistency for the potential models and the QCD sum rules, whose parameters (the quark masses, for instance) have been fixed from the fitting of the spectroscopic data on the charmonium and bottomonium. Thus, the study of the  $B_c$  family spectroscopy can serve for the essential improvement of the quantitative characteristics of the quark models and the QCD sum rules, which are intensively applied in other fields of the heavy quark physics (for example, when one extracts values of elements in the matrix of mixings of the heavy quark weak charged currents and one estimates contributions, interfering with the effects of the  $CP$  invariance violation, in the heavy hadron decays [18]).

Moreover, there is a problem of the precise description of the  $P$ -wave level splittings in the charmonium and bottomonium, when the experimental measurement has found an essential deviation from the values, which have been expected in some well-acknowledged quark models [19]. The study of the  $B_c$  meson family can help in a solution of this problem.

In addition, the ( $\bar{b}c$ ) system is interesting due to that it allows one, in a new way, to use the phenomenological information, obtained from the detailed experimental study of the charmonium and bottomonium. So, for example, ( $\bar{b}c$ ) takes an intermediate place between the charmonium and bottomonium in respect to both the system level masses and the values of average distances between the heavy quarks. As has been clarified, in the region of the average distances in the ( $c\bar{c}$ ) and ( $b\bar{b}$ ) systems, the heavy quark potential possesses the simple scaling properties [8,20,57], which state that the kinetic energy of the heavy quarks is practically a constant value, independent of the quark flavours and the excitation level in the heavy quarkonium system. Furthermore, this leads to that the heavy quarkonium level density (the distance between the  $nL$  and  $n'L$  levels) does not depend on the flavours of quarks, composing the heavy quarkonium. This regularity is quite accurately valid empirically for the ( $c\bar{c}$ ) and ( $b\bar{b}$ ) systems and it can be used in the framework of the QCD sum rules, where a scaling relation, connecting the leptonic constants of the  $S$ -wave levels in the different quarkonia [21,22], is derived.

Further, having no strong and electromagnetic annihilation channels of decays, the excited ( $\bar{b}c$ ) system levels, being below the threshold of the decay into the  $BD$  meson pair, will decay into the lightest basic pseudoscalar state  $B_c^+(0^-)$  due to the radiative cascade transitions into the underlying levels. Therefore, the widths of the electromagnetic ( $\gamma$ ) and hadronic ( $\pi\pi, \eta, \dots$ ) radiative decays of the given excitation into the other levels will compose its total width. As a result, the total widths of the excited levels in the ( $\bar{b}c$ ) system turn out two orders of magnitude less than the total widths of the charmonium and bottomonium excited levels, for which the annihilation channels are essential. Moreover, maybe, the data on the radiative hadronic decays in the ( $\bar{b}c$ ) family give a possibility for one to solve some problems on the theory of the hadronic transitions in the heavy

quarkonia (for example, the problem on the anomalous distribution over the  $\pi\pi$  pair invariant mass in the decay of  $\Upsilon'' \rightarrow \Upsilon\pi\pi$  [23–28]).

Thus, on the one hand, the methods, applied in the heavy quark physics, are able quite reliably to point out the spectroscopic characteristics of the  $(\bar{b}c)$  system for one to make a purposefully-directed experimental search of the given heavy quarkonium, and, on the other hand, the measurement of the spectroscopic data in the  $B_c$  family would allow one to improve these methods approaches for the extraction of the fundamental parameters of the Standard Model from both the  $B_c$  meson physics and the other fields of the heavy quark physics.

Like the other mesons with the open flavour, the basic state of the  $B_c$  meson family, the pseudoscalar meson  $B_c^+(0^-)$ , is the long-living particle, decaying due to the weak interaction and having the life time, comparable with the lifetimes of  $B$  and  $D$  mesons, so this feature essentially distinguishes  $B_c$  from the heavy quarkonia  $\eta_c$  and  $\eta_b$ . Therefore, the study of  $B_c$  meson decays is the rich field of the heavy quark physics, where one extracts an important information about both the QCD dynamics and the weak interactions. The spectroscopic  $B_c$  meson characteristics such as the leptonic constant, determining the width of the wave package of the  $(\bar{b}c)$  system in the basic state, essentially determine the description of the  $B_c$  decay modes, in which some specific features and effects are observed.

First of all, the presence of the valent heavy quark-spectator leads to a large probability for the  $B_c$  decay modes with the heavy mesons in the final state, i.e. in the decays  $B_c \rightarrow \psi(\eta_c)$  and  $B_c \rightarrow B_s^{(*)}$  [29–36]. The large  $\psi$  particle yield is interesting, in addition, by that the  $\psi$  particle has the perfect experimental signature in the leptonic decay mode.

Further, in the consideration of the semileptonic  $B_c^+ \rightarrow \psi(\eta_c)l^+\nu$  decays, the non-relativistic heavy quark motion inside the quarkonia leads to an essential effect, caused by large Coulomb-like corrections, which notably change the calculation results for these decays in the framework of the QCD sum rules [31]. Only the taking into the account these corrections makes the results of the QCD sum rules and the potential quark models to be consistent.

Recently, considering the semileptonic transitions of the heavy quarks  $Q \rightarrow Q'l\nu$  in the framework of the Effective Heavy Quark Theory (EHQT) for hadrons with a single heavy quark ( $Q\bar{q}$ ,  $Qqq$ ), one has stated the universal regularities [14], which serve, for example, for the model independent extraction of the Kobayashi–Maskawa matrix element value  $|V_{bc}|$ . This universality in the limit of  $\Lambda_{QCD}/m_Q \rightarrow 0$  is caused by the heavy quark flavour-independence of the light quark motion in the gluon field of the static source (the heavy quark), so that the wave functions of such hadrons are universal. In the case of the heavy quarkonium with two heavy quarks, the distances between the quarks depend on the values and ratios of its masses, i.e. the wave functions of the heavy quarkonia are not universal and depend on the quark flavours. However, in this case, one can neglect a low value of the spin-dependent splitting in the heavy quarkonium and suppose the wave functions of the  $nL_J$  quarkonia to be  $J$ -independent. This fact finds the expression in an approximate spin-symmetry for the heavy quarks, so it puts some relations on the form factors of the weak semileptonic exclusive decays of  $B_c$  [37]. Such relations for the form factors are universal and characteristic for the  $B_c$  meson and reflect the high power of understanding the heavy quark decay dynamics, needing a direct experimental

verification.

Considering the  $B_c$  decays with the spectator  $b$ -quark, one has particularly to note an essential role of the effects, caused by that the  $c$ -quark is not in the free state, but in the bound one. The decrease of the phase space for the  $c$ -quark decay within the heavy quarkonium makes the probability of the decay to be 40 % less than the probability in the  $D$  and  $D_s$  meson decays [34]. The annihilation channel of the weak  $B_c$  meson decay [52], allowing one to determine the value of the quark wave function at the origin  $|\Psi(0)|^2$ , acquires the important meaning, too.

As in the case of the  $(\bar{b}c)$  system spectroscopy, the heavy quark theory is able to make the basic predictions on the mechanisms of the  $B_c$  meson decays, whose characteristics measurement would allow one essentially to develop the methods of its description and also to use these methods for the precise investigations of the Standard Model as well as possible deviations from predictions of the latter.

In the case of the  $B_c$  meson production, a low value of the  $\Lambda_{QCD}/m_Q$  ratio and, hence, the low value of the quark-gluon coupling  $\alpha_S \sim 1/\ln(m_Q/\Lambda_{QCD}) \ll 1$  allow one to make the consideration of the pair production of the  $b\bar{b}$  and  $c\bar{c}$  quarks, from which the  $B_c$  meson is formed, in the framework of the perturbative QCD theory, and also, in a way, to factorize contributions, caused by the perturbative production of heavy quarks and forthcoming nonperturbative binding of the latter into the heavy quarkonium. So, to calculate the cross sections of the  $S$ -wave  $B_c$  state production in the  $Z$  boson peak is enough to compute the matrix elements for the joint production of the  $b\bar{b}$  and  $c\bar{c}$  pairs in the colour-singlet state of the  $(\bar{b}c)$  pair with the fixed total spin of quarks ( $S = 0, 1$ ), when the quarks, being bound into the meson, move with one and the same velocity, equal to the meson velocity. After that, one has to multiply these matrix elements by the nonperturbative factor, whose value is determined by the spectroscopic characteristics of the bound state (the quark masses and the leptonic constant, related with the probability of the observation of quarks at the zero distance between them in the bound state) [38–47]. The last notion is caused by that the characteristic virtualities of heavy quarks inside the heavy quarkonium are much less than its masses, since the heavy quarks inside the bound states are moving nonrelativistically, otherwise the quark virtualities in its production are of the order of its masses. Therefore, considering the  $B_c$  production, one can assume, that, inside the meson, the  $\bar{b}$ - and  $c$ -quarks are close to the mass shell and practically at rest in respect to each other. Thus, after the extraction of the nonperturbative factor, the analysis of the  $B_c$  heavy quarkonium production is determined by the consideration of the matrix elements, calculated in the perturbation theory of QCD.

Note first of all, that the necessity of the two pair production of heavy quarks in the electromagnetic and strong processes for the  $B_c$  yield leads to that the leading order of the perturbative QCD has an additional factor of the suppression  $\sim \alpha_S^2$  in respect to the leading order of the perturbation theory for the production of the single flavour heavy quarks, for example, the  $b\bar{b}$  pair (see Figures 7, 9), so  $\sigma(B_c)/\sigma(b\bar{b}) \sim \alpha_S^2 |\Psi(0)|^2/m_c^3$ . This causes the low yield of the  $B_c$  mesons in respect to the  $B$  meson production.

The analysis of the leading approximation in the perturbative QCD for the  $B_c$  meson production allows one to derive a number of analytical expressions for the  $B_c$  production cross sections [38,39], where one has especially to stress the expressions for the functions of the heavy quark fragmentation into the heavy quarkonium in the scaling limit  $M^2/s \rightarrow 0$ ,

so these functions are determined by the values of  $\alpha_S$ , the quark masses and the leptonic constant of the meson [42–44]. Thus, the fragmentational  $B_c$  production can be reliably described by the analytical expressions, so this opens new possibilities in the study of the QCD dynamics, essential in the complete picture of the heavy quark physics. As one can show, the fragmentational  $B_c$  production certainly dominates in the  $Z$  boson decays [44], so that it can be straightforwardly studied at the LEP facilities. Moreover, one can analytically study notable spin effects in the fragmentation into the vector  $B_c^*$  meson [48], decaying electromagnetically  $B_c^* \rightarrow B_c \gamma$ .

In the hadronic  $B_c$  production, patron processes at the energies, comparable with the  $B_c$  mass, dominate, so that the processes, having the character of the fragmentational and also recombinational type [38,46] (see Figure 9), are essential.

Further, the numerical estimates of the  $B_c$  meson yield at the colliders LEP and Tevatron show that the fraction of the  $B_c$  mesons in the production of the beauty hadrons is of the order of  $10^{-3}$  [38–47,49]. This leads to that at the current experimental facilities, a quite large number of the  $B_c$  mesons are being produced.

Thus, one can point out the expected number of the  $B_c$  mesons, being produced at different colliders, and the differential  $B_c$  characteristics, whose experimental study would significantly clarify the picture of the QCD interactions of heavy quarks.

A solution of the problem on the experimental discovery and study of the  $B_c$  mesons is determined, first, by the theoretical description of the characteristics of the  $B_c$  meson family (the spectroscopy, the production and decay mechanisms), so that the present review is devoted to this purpose. Second, this program is determined by the experimental methodics at the current detectors, so that the latter would allow one to observe the events with the  $B_c$  production and decays, predicted by the theory. As for the second part of the problem, at present there is, as mentioned, the colossal progress, related with the use of the electronic vertex detectors, possessing the fast operation and allowing one to isolate the processes with the long living particles ( $B$ ,  $B_c$ ,  $D$ ) from the production processes (the technique of distinguishing the primary and secondary vertices), and also accurately to reconstruct the decay vertices of the particles in space [50]. The presence of distinct signatures in the  $B_c$  meson decays and the practical possibility for the registration of these decay modes have led to the real chance of the  $B_c$  meson discovery at the LEP and Fermilab detectors [51] as well as to the sharp rise of the theoretical interest to the  $(\bar{b}c)$  system. The latter has reflected in the achievement of a large number of the essential results in the consideration of the heavy quark interaction mechanisms at the example of  $B_c$  mesons. So, the present paper is devoted to the review of these results.

## 2. Spectroscopy of $B_c$ mesons

Some preliminary estimates of the bound state masses of the  $(\bar{b}c)$  system have been made in [5,6], devoted to the description of the charmonium and bottomonium properties, as well as in ref.[52]. Recently in refs.[53] and [35], the revised analysis of the  $B_c$  spectroscopy has been performed in the framework of the potential approach and QCD sum rules.

In the present section we consider the  $(\bar{b}c)$  spectroscopy with account of the change of the effective Coulomb interaction constant, defining spin-dependent splittings of the

quarkonium levels. We calculate the widths of radiative transitions between the levels and analyse the leptonic constant  $f_{B_c}$  in the framework of the QCD sum rules in the scheme, allowing one to derive scaling relation for the leptonic constants of the heavy quarkonia.

## 2.1. Mass spectrum of $B_c$ mesons

The  $B_c$  meson is the heavy  $(\bar{b}c)$  quarkonium with the open charm and beauty. It occupies an intermediate place in the mass spectrum of the heavy quarkonia between the  $(\bar{c}c)$  charmonium and the  $(\bar{b}b)$  bottomonium. The approaches, applied to the charmonium and bottomonium study, can be used to describe the  $B_c$  meson properties, and experimental observation of  $B_c$  could serve as a test for these approaches and it could be used for the detailed quantitative study of the mechanisms of the heavy quark production, hadronization and decays.

In the following we obtain the results on the  $B_c$  meson spectroscopy. We will show that below the threshold for the hadronic decay of the  $(\bar{b}c)$  system into the  $BD$  meson pair, there are 16 narrow bound states, cascadingly decaying into the lightest pseudoscalar  $B_c^+(0^-)$  state with the mass  $m(0^-) \approx 6.25$  GeV.

### 2.1.1. Potential

The mass spectra of the charmonium and the bottomonium are experimentally studied in details [15] and they are properly described in the framework of phenomenological potential models of nonrelativistic heavy quarks [5–8,10]. To describe the mass spectrum of the  $(\bar{b}c)$  system, one would prefer to use the potentials, whose parameters do not depend on the flavours of the heavy quarks, composing a heavy quarkonium, i.e. one would use the potentials, which rather accurately describe the mass spectra of  $(\bar{c}c)$  as well as  $(\bar{b}b)$ , with one and the same set of potential parameters. The use of such potentials allows one to avoid an interpolation of the potential parameters from the values, fixed by the experimental data on the  $(\bar{c}c)$  and  $(\bar{b}b)$  systems, to the values in the intermediate region of the  $(\bar{b}c)$  system.

As it has been shown in ref.[20], with an accuracy up to an additive shift, the potentials, independent of heavy quark flavours [5–8,10], coincide with each other in the region of the average distances between heavy quarks in the  $(\bar{c}c)$  and  $(\bar{b}b)$  systems, so

$$0.1 \text{ fm} < r < 1 \text{ fm} , \quad (1)$$

although those potentials have different asymptotic behaviour in the regions of very low ( $r \rightarrow 0$ ) and very large ( $r \rightarrow \infty$ ) distances.

In Cornell model [5] in accordance with asymptotic freedom in QCD, the potential has the Coulomb-like behaviour at low distances, and the term, confining the quarks, rises linearly at large distances

$$V_C(r) = -\frac{4}{3} \frac{\alpha_S}{r} + \frac{r}{a^2} + c_0 , \quad (2)$$

so that

$$\alpha_S = 0.36 ,$$



$$\begin{aligned}
a &= 2.34 \text{ GeV}^{-1}, \\
m_c &= 1.84 \text{ GeV}, \\
c_0 &= -0.25 \text{ GeV}.
\end{aligned}
\tag{3}$$

The Richardson potential [7] and its modifications in refs.[10] and [54] also correspond to the behaviour, expected in the framework of QCD, so

$$\begin{aligned}
V_R(r) &= - \int \frac{d^3q}{(2\pi)^3} e^{i\mathbf{r}\mathbf{q}} \frac{4}{3} \frac{48\pi^2}{11N_c - 2n_f} \frac{1}{q^2 \ln(1 + q^2/\Lambda^2)} \\
&= - \int \frac{d^3q}{(2\pi)^3} e^{i\mathbf{r}\mathbf{q}} \frac{4}{3} \frac{48\pi^2}{27} \left( \frac{1}{q^2 \ln(1 + q^2/\Lambda^2)} - \frac{\Lambda^2}{q^4} \right) + \frac{8\pi}{27} \Lambda^2 r,
\end{aligned}
\tag{4}$$

with

$$\Lambda = 0.398 \text{ GeV} . \tag{5}$$

In the region of the average distances between heavy quarks (1), the QCD-motivated potentials allow the approximations in the forms of the power (Martin) or logarithmic potentials.

The Martin potential has the form [8]

$$V_M(r) = -c_M + d_M(\Lambda_M r)^k, \tag{6}$$

so that

$$\begin{aligned}
\Lambda_M &= 1 \text{ GeV}, \\
k &= 0.1, \\
m_b &= 5.174 \text{ GeV}, \\
m_c &= 1.8 \text{ GeV}, \\
c_M &= 8.064 \text{ GeV}, \\
d_M &= 6.869 \text{ GeV}.
\end{aligned}
\tag{7}$$

The logarithmic potential is equal to [9]

$$V_L(r) = c_L + d_L \ln(\Lambda_L r), \tag{8}$$

so that

$$\begin{aligned}
\Lambda_L &= 1 \text{ GeV}, \\
m_b &= 4.906 \text{ GeV}, \\
m_c &= 1.5 \text{ GeV}, \\
c_L &= -0.6635 \text{ GeV}, \\
d_L &= 0.733 \text{ GeV}.
\end{aligned}
\tag{9}$$

The approximations of the nonrelativistic potential of heavy quarks in the region of distances (1) in the form of the power (6) and logarithmic (8) laws, allow one to study its scaling properties.

In accordance with the virial theorem, the average kinetic energy of the quarks in the bound state is determined by the following expression

$$\langle T \rangle = \frac{1}{2} \left\langle \frac{rdV}{dr} \right\rangle . \quad (10)$$

Then, the logarithmic potential allows one to conclude, that for the quarkonium states one gets

$$\langle T_L \rangle = \text{const} \quad (11)$$

independently of the flavours of the heavy quarks, composing the heavy quarkonium,

$$d_L/2 = \text{const} \approx 0.367 \text{ GeV} .$$

In the Martin potential, the virial theorem (10) allows one to obtain the expression

$$\langle T_M \rangle = \frac{k}{2+k} (c_M + E) , \quad (12)$$

where  $E$  is the binding energy of the quarks in the heavy quarkonium. Phenomenologically, one has  $|E| \ll c_M$  (for example,  $E(1S, c\bar{c}) \approx -0.5 \text{ GeV}$ ), so that, neglecting the binding energy of the heavy quarks inside the heavy quarkonium, one can conclude that the average kinetic energy of the heavy quarks is a constant value, independent of the quark flavours and the number of the radial or orbital excitation. The accuracy of such approximation for  $\langle T \rangle$  is about 10%, i.e.  $|\Delta T/T| \sim 30 \div 40 \text{ MeV}$ .

From the Feynman-Hellmann theorem for the system with the reduced mass  $\mu$ , one has

$$\frac{dE}{d\mu} = - \frac{\langle T \rangle}{\mu} , \quad (13)$$

and, in accordance with condition (11), it follows that the difference of the energies for the radial excitations of the heavy quarkonium levels does not depend on the reduced mass of the  $Q\bar{Q}'$  system

$$E(\bar{n}, \mu) - E(n, \mu) = E(\bar{n}, \mu') - E(n, \mu') . \quad (14)$$

Thus, in the approximation of both the low value for the binding energy of quarks and the zero value for the spin-dependent splittings of the levels, the heavy quarkonium state density does not depend on the heavy quark flavours

$$\frac{dn}{dM_n} = \text{const} . \quad (15)$$

The given statement has been also derived in ref.[21] using the Bohr–Sommerfeld quantization of the S-wave states for the heavy quarkonium system with Martin potential [8].

Relations (14)-(15) are phenomenologically confirmed for the vector S-levels of the  $(b\bar{b})$ ,  $(c\bar{c})$ ,  $(s\bar{s})$  systems [15] (see Table 1).

Thus, the structure of the nonsplitted S-levels of the  $(\bar{b}c)$  system must repeat not only qualitatively, but quantitatively the structure of the S-levels for the  $(\bar{b}b)$  and  $(\bar{c}c)$  systems, with an accuracy up to the overall additive shift of masses.

Table 1.

The mass difference (in MeV) for the two lightest vector states of different heavy systems,  $\Delta M = M(2S) - M(1S)$

System	$\Upsilon$	$\psi$	$B_c$	$\phi$
$\Delta M$	563	588	585	660

Moreover, in the framework of the QCD sum rules, the universality of the heavy quark nonrelativistic potential (the independence on the flavours and the scaling properties (11), (14), (15)) allows one to obtain the scaling relation for the leptonic constants of the S-wave quarkonia [21]

$$\frac{f^2}{M} = \text{const} \quad (16)$$

independently of the heavy quark flavours in the regime, when

$$|m_Q - m_{Q'}| \text{ is restricted, } \frac{\Lambda_{QCD}}{m_{Q,Q'}} \ll 1,$$

i.e., when one can neglect the heavy quark mass difference. On the other hand, in the regime, when the mass difference is not low, one has

$$\frac{f^2}{M} \left( \frac{M}{4\mu} \right)^2 = \text{const}, \quad (17)$$

where

$$\mu = \frac{m_Q m_{Q'}}{m_Q + m_{Q'}}.$$

Consider the mass spectrum of the  $(\bar{b}c)$  system with the Martin potential [8].

Solving the Schrödinger equation with potential (6) and the parameters (7), one finds the  $B_c$  mass spectrum and the characteristics of the radial wave functions  $R(0)$  and  $R'(0)$ , shown in Tables 2 and 3, respectively.

The average kinetic energy of the levels, lying below the threshold for the  $(\bar{b}c)$  system decay into the  $BD$  pair, is presented in Table 4, wherein one can see that the term, added to the radial potential due to the orbital rotation,

$$\Delta V_l = \frac{\mathbf{L}^2}{2\mu r^2} \quad (18)$$

Table 2.

The energy levels of the  $(\bar{b}c)$  system, calculated without taking into account relativistic corrections, in GeV

$n$	[52]	[55]	[54]	$n$	[52]	[55]	[54]	$n$	[52]	[55]	[54]
1S	6.301	6.315	6.344	2P	6.728	6.735	6.763	3D	7.008	7.145	7.030
2S	6.893	7.009	6.910	3P	7.122	–	7.160	4D	7.308	–	7.365
3S	7.237	–	7.024	4P	7.395	–	–	5D	7.532	–	–

Table 3.

The characteristics of the radial wave functions  $R_{nS}(0)$  (in  $\text{GeV}^{3/2}$ ) and  $R'_{nP}(0)$  (in  $\text{GeV}^{5/2}$ ), obtained from the Schrödinger equation

$n$	Martin	[53]
$R_{1S}(0)$	1.31	1.28
$R_{2S}(0)$	0.97	0.99
$R'_{2P}(0)$	0.55	0.45
$R'_{3P}(0)$	0.57	0.51

weakly influences the value of the average kinetic energy, and the binding energy for the levels with  $L \neq 0$  is essentially determined by the orbital rotation energy, which is approximately independent of the quark flavours (see Table 5), so that the structure of the nonsplit levels of the  $(\bar{b}c)$  system with  $L \neq 0$  must quantitatively repeat the structure of the charmonium and bottomonium levels, too.

### 2.1.2. Spin-dependent splitting of the $(\bar{b}c)$ quarkonium

In accordance with the results of refs.[55,56], one introduces the additional term to the potential to take into the account the spin-orbital and spin-spin interactions, causing the splitting of the  $nL$  levels ( $n$  is the principal quantum number,  $L$  is the orbital momentum), so it has the form

$$\begin{aligned}
V_{SD}(\mathbf{r}) = & \left( \frac{\mathbf{L} \cdot \mathbf{S}_c}{2m_c^2} + \frac{\mathbf{L} \cdot \mathbf{S}_b}{2m_b^2} \right) \left( -\frac{dV(r)}{rdr} + \frac{8}{3} \alpha_S \frac{1}{r^3} \right) + \\
& + \frac{4}{3} \alpha_S \frac{1}{m_c m_b} \frac{\mathbf{L} \cdot \mathbf{S}}{r^3} + \frac{4}{3} \alpha_S \frac{2}{3m_c m_b} \mathbf{S}_c \cdot \mathbf{S}_b 4\pi \delta(\mathbf{r}) \\
& + \frac{4}{3} \alpha_S \frac{1}{m_c m_b} (3(\mathbf{S}_c \cdot \mathbf{n})(\mathbf{S}_b \cdot \mathbf{n}) - \mathbf{S}_c \cdot \mathbf{S}_b) \frac{1}{r^3}, \quad \mathbf{n} = \frac{\mathbf{r}}{r}.
\end{aligned} \tag{19}$$

where  $V(r)$  is the phenomenological potential, confining the quarks, the first term takes into account the relativistic corrections to the potential  $V(r)$ ; the second, third and fourth terms are the relativistic corrections, coming from the account of the one gluon exchange between the  $b$  and  $c$  quarks;  $\alpha_S$  is the effective constant of the quark-gluon interaction inside the  $(\bar{b}c)$  system.

The value of the  $\alpha_S$  parameter can be determined in the following way.

Table 4.

The average kinetic and orbital energies of the quark motion in the  $(\bar{b}c)$  system, in GeV

$nL$	1S	2S	2P	3P	3D
$\langle T \rangle$	0.35	0.38	0.37	0.39	0.39
$\Delta V_l$	0.00	0.00	0.22	0.14	0.29

The splitting of the S-wave heavy quarkonium ( $Q_1\bar{Q}_2$ ) is determined by the expression

$$\Delta M(nS) = \alpha_S \frac{8}{9m_1m_2} |R_{nS}(0)|^2, \quad (20)$$

where  $R_{nS}(0)$  is the value of the radial wave function of the quarkonium, at the origin. Using the experimental value of the S-state splitting in the  $(c\bar{c})$  system [15]

$$\Delta M(1S, c\bar{c}) = 117 \pm 2 \text{ MeV}, \quad (21)$$

and the  $R_{1S}(0)$  value, calculated in the potential model for the  $(c\bar{c})$  system, one gets the model-dependent value of the  $\alpha_S(\psi)$  constant for the effective Coulomb interaction of the heavy quarks (in the Martin potential, one has  $\alpha_S(\psi) = 0.44$ ).

In ref.[53] the effective constant value, fixed in the described way, has been applied to the description of not only the  $(c\bar{c})$  system, but also the  $(\bar{b}c)$  and  $(\bar{b}b)$  quarkonia.

In the present paper we take into account the variation of the effective Coulomb interaction constant versus the reduced mass of the system ( $\mu$ ).

In the one-loop approximation at the momentum scale  $p^2$ , the "running" coupling constant in QCD is determined by the expression

$$\alpha_S(p^2) = \frac{4\pi}{b \ln(p^2/\Lambda_{QCD}^2)}, \quad (22)$$

where  $b = 11 - 2n_f/3$ , and  $n_f = 3$ , when one takes into account the contribution by the virtual light quarks,  $p^2 < m_{c,b}^2$ .

In the model with the Martin potential, for the kinetic energy of quarks  $(c\bar{c})$  inside  $\psi$ , one has

$$\langle T_{1S}(c\bar{c}) \rangle \approx 0.357 \text{ GeV}, \quad (23)$$

so that, using the expression for the kinetic energy,

$$\langle T \rangle = \frac{\langle p^2 \rangle}{2\mu}, \quad (24)$$

one gets

$$\alpha_S(p^2) = \frac{4\pi}{b \ln(2\langle T \rangle \mu / \Lambda_{QCD}^2)}, \quad (25)$$

so that  $\alpha_S(\psi) = 0.44$  at

$$\Lambda_{QCD} \approx 164 \text{ MeV}. \quad (26)$$

Table 5. The average energy of the orbital motion in the heavy quarkonia, in the model with the Martin potential, in GeV

System	$\bar{c}c$	$bc$	$bb$
$\Delta V_l(2P)$	0.23	0.22	0.21

Table 6.

The leptonic decay constants of the heavy quarkonia, the values, measured experimentally and obtained in the model with the Martin potential, in the model with the effective Coulomb interaction and from the scaling relation (SR), in MeV

Model	Exp.[15]	Martin	Coulomb	SR
$f_\psi$	$410 \pm 15$	$547 \pm 80$	$426 \pm 60$	$410 \pm 40$
$f_{B_c}$	–	$510 \pm 80$	$456 \pm 70$	$460 \pm 60$
$f_\Upsilon$	$715 \pm 15$	$660 \pm 90$	$772 \pm 120$	$715 \pm 70$

As it has been noted in the previous section, the value of the kinetic energy of the quark motion weakly depends on the heavy quark flavours, and it, practically, is constant, and, hence, the change of the effective  $\alpha_S$  coupling is basically determined by the variation of the reduced mass of the heavy quarkonium. In accordance with eqs.(25)-(26) and Table 4, for the  $(\bar{b}c)$  system one has

$$\begin{array}{cccccc} nL & 1S & 2S & 2P & 3P & 3D \\ \alpha_S & 0.394 & 0.385 & 0.387 & 0.382 & 0.383. \end{array}$$

Note, the Martin potential leads to the  $R_{1S}(0)$  values, which, with the accuracy up to  $15 \div 20\%$ , agrees with the experimental values of the leptonic decay constants for the heavy  $(c\bar{c})$  and  $(b\bar{b})$  quarkonia. The leptonic constants are determined by the expression

$$\Gamma(Q\bar{Q} \rightarrow l^+l^-) = \frac{4\pi}{3} e_Q^2 \alpha_{em}^2 \frac{f_{Q\bar{Q}}^2}{M_{Q\bar{Q}}}, \quad (27)$$

where  $e_Q$  is the heavy quark charge.

In the nonrelativistic model one has

$$f_{Q\bar{Q}} = \sqrt{\frac{3}{\pi M_{Q\bar{Q}}}} R_{1S}(0). \quad (28)$$

For the effective Coulomb interaction of the heavy quarks in the basic 1S-state one has

$$R_{1S}^C(0) = 2 \left( \frac{4}{3} \mu \alpha_S \right)^{3/2}. \quad (29)$$

One can see from Table 6, that, taking into account the variation of the effective  $\alpha_S$  constant versus the reduced mass of the heavy quarkonium (see eq.(25)), the Coulomb wave functions give the values of the leptonic constants for the heavy 1S-quarkonia, so that in the framework of the accuracy of the potential models, those values agree with the experimental values and the values, obtained by the solution of the Schrödinger equation with the given potential.

The consideration of the variation of the effective Coulomb interaction constant becomes especially essential for the  $\Upsilon$  particles, for which  $\alpha_S(\Upsilon) \approx 0.33$  instead of the fixed value  $\alpha_S = 0.44$ .

Thus, calculating the splitting of the  $(\bar{b}c)$  levels, we take into account the  $\alpha_S$  dependence on the reduced mass of the heavy quarkonium.

As one can see from eq.(19), in contrast to the  $LS$ -coupling in the  $(\bar{c}c)$  and  $(\bar{b}b)$  systems, there is the  $jj$ -coupling in the heavy quarkonium, where the heavy quarks have different masses (here,  $\mathbf{L}\mathbf{S}_c$  is diagonalized at the given  $\mathbf{J}_c$  momentum,  $(\mathbf{J}_c = \mathbf{L} + \mathbf{S}_c, \mathbf{J} = \mathbf{J}_c + \mathbf{S}_b)$ ,  $\mathbf{J}$  is the total spin of the system). We use the following spectroscopic notations for the splitted levels of the  $(\bar{b}c)$  system,  $-n^{2j_c}L_J$ .

One can easily show, that independently of the total spin  $J$  projection one has

$$\begin{aligned} |^{2L+1}L_{L+1}\rangle &= |J = L + 1, S = 1\rangle, \\ |^{2L-1}L_{L-1}\rangle &= |J = L - 1, S = 1\rangle, \\ |^{2L+1}L_L\rangle &= \sqrt{\frac{L}{2L+1}}|J = L, S = 1\rangle + \sqrt{\frac{L+1}{2L+1}}|J = L, S = 0\rangle, \\ |^{2L-1}L_L\rangle &= \sqrt{\frac{L+1}{2L+1}}|J = L, S = 1\rangle - \sqrt{\frac{L}{2L+1}}|J = L, S = 0\rangle, \end{aligned} \quad (30)$$

where  $|J, S\rangle$  are the state vectors with the given values of the total quark spin  $\mathbf{S} = \mathbf{S}_c + \mathbf{S}_b$ , so that the potential terms of the order of  $1/m_c m_b$ ,  $1/m_b^2$  lead, generally speaking, to the mixing of the levels with the different  $J_c$  values at the given  $J$  values. The tensor forces (the last term in eq.(19)) are equal to zero at  $L = 0$  or  $S = 0$ .

To calculate values of the level shifts, appearing due to the spin-spin and spin-orbital interactions, one has to take the averaged expression (19) over the wave functions of the corresponding states.

The averaging over the angle variables can be performed in the following standard way. Let us represent the matrix element of the unit vector  $\mathbf{n} = \mathbf{r}/r$  pair in the form

$$\langle L, m | n^p n^q | L, m' \rangle = a(L^p L^q + L^q L^p)_{mm'} + b \delta^{pq} \delta_{mm'}, \quad (31)$$

where  $\mathbf{L}$  are the orbital momentum matrices in the corresponding irreducible representation.

From the conditions of the normalization of the unit vector,  $\langle n^p n^q \rangle \delta^{pq} = 1$ , the orthogonality of the radius-vector to the orbital momentum,  $n^p L^p = 0$ , the commutation relations for the angle momentum,  $[L^p; L^q] = i \epsilon^{pq} L_l$ , one finds the values of constants  $a$  and  $b$  in eq.(31)

$$a = -\frac{1}{4\mathbf{L}^2 - 3}, \quad (32)$$

$$b = \frac{2\mathbf{L}^2 - 1}{4\mathbf{L}^2 - 3}. \quad (33)$$

Note further, that from the condition for the quark spins  $S_c^p S_c^q + S_b^p S_b^q = \frac{1}{2} \delta^{pq}$  it follows, that

$$3(n^p n^q - \frac{1}{3} \delta^{pq}) S_c^p S_b^q = \frac{3}{2} (n^p n^q - \frac{1}{3} \delta^{pq}) S^p S^q. \quad (34)$$

Thus, (see also ref.[57])

$$\langle 6(n^p n^q - \frac{1}{3} \delta^{pq}) S_c^p S_b^q \rangle = -\frac{1}{4\mathbf{L}^2 - 3} (6(\mathbf{L}\mathbf{S})^2 + 3(\mathbf{L}\mathbf{S}) - 2\mathbf{L}^2 \mathbf{S}^2). \quad (35)$$

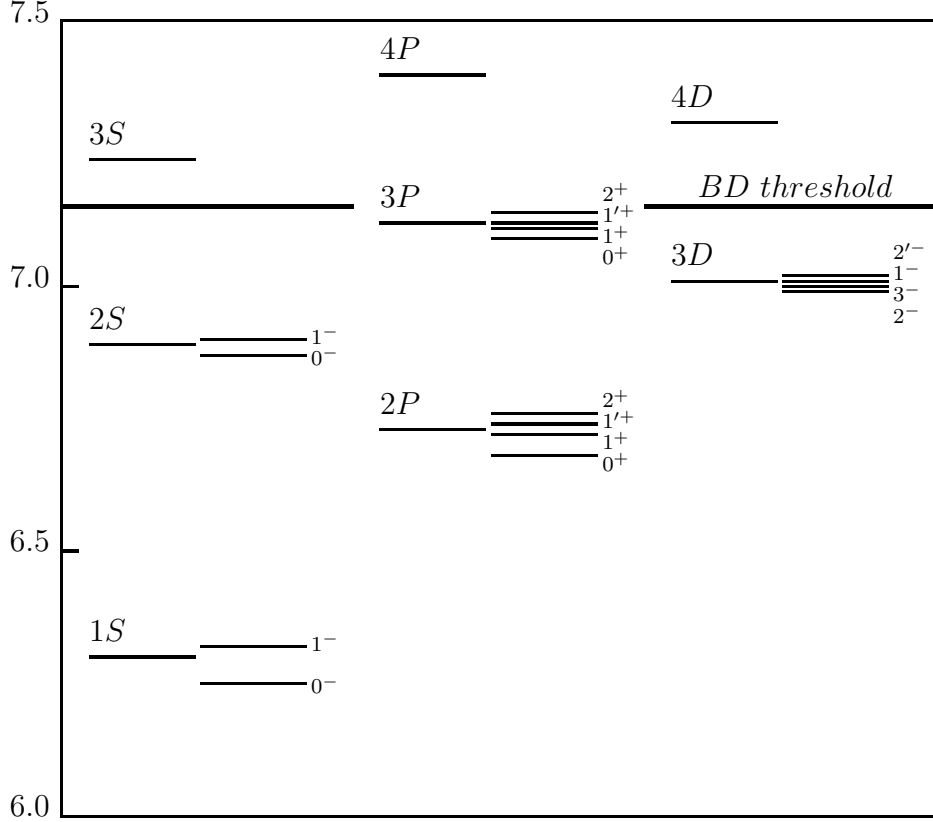


Fig. 1. The mass spectrum of the  $(\bar{b}c)$  system with account of splittings.

Using eqs.(30), (35), for the level shifts, calculated in the perturbation theory at  $S = 1$ , one gets the following formulae

$$\Delta E_{n^1S_0} = -\alpha_S \frac{2}{3m_c m_b} |R_{nS}(0)|^2, \quad (36)$$

$$\Delta E_{n^1S_1} = \alpha_S \frac{2}{9m_c m_b} |R_{nS}(0)|^2, \quad (37)$$

$$\Delta E_{n^3P_2} = \alpha_S \frac{6}{5m_c m_b} \langle \frac{1}{r^3} \rangle + \frac{1}{4} \left( \frac{1}{m_c^2} + \frac{1}{m_b^2} \right) \left\langle -\frac{dV(r)}{rdr} + \frac{8}{3} \alpha_S \frac{1}{r^3} \right\rangle, \quad (38)$$

$$\Delta E_{n^1P_0} = -\alpha_S \frac{4}{m_c m_b} \langle \frac{1}{r^3} \rangle - \frac{1}{2} \left( \frac{1}{m_c^2} + \frac{1}{m_b^2} \right) \left\langle -\frac{dV(r)}{rdr} + \frac{8}{3} \alpha_S \frac{1}{r^3} \right\rangle, \quad (39)$$

$$\Delta E_{n^5D_3} = \alpha_S \frac{52}{21m_c m_b} \langle \frac{1}{r^3} \rangle + \frac{1}{2} \left( \frac{1}{m_c^2} + \frac{1}{m_b^2} \right) \left\langle -\frac{dV(r)}{rdr} + \frac{8}{3} \alpha_S \frac{1}{r^3} \right\rangle, \quad (40)$$

$$\Delta E_{n^3D_1} = -\alpha_S \frac{92}{21m_c m_b} \langle \frac{1}{r^3} \rangle - \frac{3}{4} \left( \frac{1}{m_c^2} + \frac{1}{m_b^2} \right) \left\langle -\frac{dV(r)}{rdr} + \frac{8}{3} \alpha_S \frac{1}{r^3} \right\rangle, \quad (41)$$

where  $R_{nS}(0)$  are the radial wave functions at  $L = 0$ ,  $\langle \dots \rangle$  denote the average values, calculated under the wave functions  $R_{nL}(r)$ . The mixing matrix elements have the forms

$$\langle {}^3P_1 | \Delta E | {}^3P_1 \rangle = -\alpha_S \frac{2}{9m_c m_b} \langle \frac{1}{r^3} \rangle +$$



Table 7.

The masses (in GeV) of the lightest pseudoscalar  $B_c$  and vector  $B_c^*$  states in different models (\* is the present paper)

State	*	[55]	[54]	[58]	[6]	[59]	[65,21]
$0^-$	6.253	6.249	6.314	6.293	6.270	6.243	6.246
$1^-$	6.317	6.339	6.354	6.346	6.340	6.320	6.319
State	[53]	[60]	[61]	[62]	[63]	[64]	[35]
$0^-$	6.264	6.320	6.256	6.276	6.286	–	6.255
$1^-$	6.337	6.370	6.329	6.365	6.328	6.320	6.330

$$\left( \frac{1}{4m_c^2} - \frac{5}{12m_b^2} \right) \left\langle -\frac{dV(r)}{rdr} + \frac{8}{3} \alpha_S \frac{1}{r^3} \right\rangle, \quad (42)$$

$$\begin{aligned} \langle {}^1P_1 | \Delta E | {}^1P_1 \rangle &= -\alpha_S \frac{4}{9m_c m_b} \left\langle \frac{1}{r^3} \right\rangle + \\ &\left( -\frac{1}{2m_c^2} + \frac{1}{6m_b^2} \right) \left\langle -\frac{dV(r)}{rdr} + \frac{8}{3} \alpha_S \frac{1}{r^3} \right\rangle, \end{aligned} \quad (43)$$

$$\begin{aligned} \langle {}^3P_1 | \Delta E | {}^1P_1 \rangle &= -\alpha_S \frac{2\sqrt{2}}{9m_c m_b} \left\langle \frac{1}{r^3} \right\rangle \\ &- \frac{\sqrt{2}}{6m_b^2} \left\langle -\frac{dV(r)}{rdr} + \frac{8}{3} \alpha_S \frac{1}{r^3} \right\rangle, \end{aligned} \quad (44)$$

$$\begin{aligned} \langle {}^5D_2 | \Delta E | {}^5D_2 \rangle &= -\alpha_S \frac{4}{15m_c m_b} \left\langle \frac{1}{r^3} \right\rangle + \\ &\left( \frac{1}{2m_c^2} - \frac{1}{5m_b^2} \right) \left\langle -\frac{dV(r)}{rdr} + \frac{8}{3} \alpha_S \frac{1}{r^3} \right\rangle, \end{aligned} \quad (45)$$

$$\begin{aligned} \langle {}^3D_2 | \Delta E | {}^3D_2 \rangle &= -\alpha_S \frac{8}{15m_c m_b} \left\langle \frac{1}{r^3} \right\rangle + \\ &\left( -\frac{3}{4m_c^2} + \frac{9}{20m_b^2} \right) \left\langle -\frac{dV(r)}{rdr} + \frac{8}{3} \alpha_S \frac{1}{r^3} \right\rangle, \end{aligned} \quad (46)$$

$$\begin{aligned} \langle {}^5D_2 | \Delta E | {}^3D_2 \rangle &= -\alpha_S \frac{2\sqrt{6}}{15m_c m_b} \left\langle \frac{1}{r^3} \right\rangle \\ &- \frac{\sqrt{6}}{10m_b^2} \left\langle -\frac{dV(r)}{rdr} + \frac{8}{3} \alpha_S \frac{1}{r^3} \right\rangle, \end{aligned} \quad (47)$$

As one can see from eq.(37), the S-level splitting is essentially determined by the  $|R_{nS}(0)|$  value, which can be related to the leptonic decay constants of the S-states ( $0^-$ ,  $1^-$ ). Section 2.3 is devoted to the calculation of these constants in different ways. We only note here, that with enough accuracy, the predictions of different potential models on the  $|R_{1S}(0)|$  value are in agreement with each other as well as with predictions in other approaches.

For the  $2P$ ,  $3P$  and  $3D$  levels, the mixing matrices of the states with the total quark

spin  $S = 1$  and  $S = 0$  have the forms

$$|2P, 1'^+\rangle = 0.294|S = 1\rangle + 0.956|S = 0\rangle, \quad (48)$$

$$|2P, 1^+\rangle = 0.956|S = 1\rangle - 0.294|S = 0\rangle, \quad (49)$$

so that in the  $1^+$  state the probability of the total quark spin value  $S = 1$  is equal to

$$w_1(2P) = 0.913. \quad (50)$$

For the  $3P$  level one has

$$|3P, 1'^+\rangle = 0.371|S = 1\rangle + 0.929|S = 0\rangle, \quad (51)$$

$$|3P, 1^+\rangle = 0.929|S = 1\rangle - 0.371|S = 0\rangle, \quad (52)$$

so that

$$w_1(3P) = 0.863, \quad (53)$$

For the  $3D$  level one gets

$$|3D, 2'^-\rangle = -0.566|S = 1\rangle + 0.825|S = 0\rangle, \quad (54)$$

$$|3D, 2^-\rangle = 0.825|S = 1\rangle + 0.566|S = 0\rangle, \quad (55)$$

so that

$$w_2(3D) = 0.680. \quad (56)$$

With account of the calculated splittings, the  $B_c$  mass spectrum is shown in Figure 1 and Table 8.

The masses of the  $B_c$  mesons have been also calculated in papers of ref.[66].

As one can see from Tables 2 and 7, the place of the 1S-level in the  $(\bar{b}c)$  system ( $m(1S) \approx 6.3$  GeV) is predicted by the potential models with the rather high accuracy  $\Delta m(1S) \approx 30$  MeV, and the 1S-level splitting into the vector and pseudoscalar states is about  $m(1^-) - m(0^-) \approx 70$  MeV.

### 2.1.3. $B_c$ meson masses from QCD sum rules

Potential model estimates for the masses of the lightest  $(\bar{b}c)$  states are in agreement with the results of the calculations for the vector and pseudoscalar  $(\bar{b}c)$  states in the framework of the QCD sum rules [35,36,67], where the calculation accuracy is lower, than the accuracy of the potential models, because the results essentially depend on both the modelling of the nonresonant hadronic part of the current correlator (the continuum threshold) and the parameter of the sum rule scheme (the moment number for the spectral density of the current correlator or the Borel transformation parameter),

$$m^{SR}(0^-) \approx m^{SR}(1^-) \approx 6.3 \div 6.5 \text{ GeV}. \quad (57)$$

As it has been shown in [11], for the lightest vector quarkonium, the following QCD sum rules take place

$$\frac{f_V^2 M_V^2}{M_V^2 - q^2} = \frac{1}{\pi} \int_{s_i}^{s_{\text{th}}} \frac{\Im m \Pi_V^{\text{QCD}(\text{pert})}(s)}{s - q^2} ds + \Pi_V^{\text{QCD}(\text{nonpert})}(q^2). \quad (58)$$

Table 8.

The masses (in GeV) of the bound ( $\bar{b}c$ ) states below the threshold of the decay into the  $BD$  meson pair (\* is the present paper)

State	*	[53]	[54]
$1^1S_0$	6.253	6.264	6.314
$1^1S_1$	6.317	6.337	6.355
$2^1S_0$	6.867	6.856	6.889
$2^1S_1$	6.902	6.899	6.917
$2^1P_0$	6.683	6.700	6.728
$2P\ 1^+$	6.717	6.730	6.760
$2P\ 1'^+$	6.729	6.736	–
$2^3P_2$	6.743	6.747	6.773
$3^1P_0$	7.088	7.108	7.134
$3P\ 1^+$	7.113	7.135	7.159
$3P\ 1'^+$	7.124	7.142	–
$3^3P_2$	7.134	7.153	7.166
$3D\ 2^-$	7.001	7.009	–
$3^5D_3$	7.007	7.005	–
$3^3D_1$	7.008	7.012	–
$3D\ 2'^-$	7.016	7.012	–

where  $f_V$  is the leptonic constant of the vector ( $\bar{b}c$ ) state with the mass  $M_V$ ,

$$if_V M_V \epsilon_\mu^\lambda \exp(ipx) = \langle 0 | J_\mu(x) | V(p, \lambda) \rangle, \quad (59)$$

$$J_\mu(x) = \bar{c}(x) \gamma_\mu b(x), \quad (60)$$

where  $\lambda, p$  are the  $B_c^*$  polarization and momentum, respectively, and

$$\int d^4x \exp(iqx) \langle 0 | T J_\mu(x) J_\nu(0) | 0 \rangle = \left( -g_{\mu\nu} + \frac{q_\mu q_\nu}{q^2} \right) \Pi_V^{\text{QCD}} + q_\mu q_\nu \Pi_S^{\text{QCD}}, \quad (61)$$

$$\Pi_V^{\text{QCD}}(q^2) = \Pi_V^{\text{QCD}(\text{pert})} + \Pi_V^{\text{QCD}(\text{nonpert})}(q^2), \quad (62)$$

$$\Pi_V^{\text{QCD}(\text{nonpert})}(q^2) = \sum C_i(q^2) O^i, \quad (63)$$

where  $O^i$  are the vacuum expectation values of the composite operators such as  $\langle m \bar{\psi} \psi \rangle$ ,  $\langle \alpha_S G_{\mu\nu}^2 \rangle$ , etc. The Wilson coefficients are calculable in the perturbation theory of QCD.  $s_i = (m_c + m_b)^2$  is the kinematical threshold of the perturbative contribution,  $M_V^2 > s_i$ ,  $s_{th}$  is the threshold of the nonresonant hadronic contribution, which is considered to be equal to the perturbative contribution at  $s > s_{th}$ .

Considering the respective correlators, one can write down the sum rules, analogous to eq.(58), for the scalar and pseudoscalar states.

One believes that the sum rule (58) must rather accurately be valid at  $q^2 < 0$ .

For the  $n$ -th derivative of eq.(58) at  $q^2 = 0$  one gets

$$f_V^2 (M_V^2)^{-n} = \frac{1}{\pi} \int_{s_i}^{s_{th}} \frac{\Im m \Pi_V^{\text{QCD}(\text{pert})}(s)}{s^{n+1}} ds + \frac{(-1)^n}{n!} \frac{d^n}{d(q^2)^n} \Pi_V^{\text{QCD}(\text{nonpert})}(q^2), \quad (64)$$

so, considering the ratio of the  $n$ -th derivative to the  $n + 1$ -th one, one can obtain the value of the vector  $B_c^*$  meson mass. The calculation result depends on the  $n$  number in the sum rules (64), because of taking into the account both the finite number of terms in the perturbation theory expansion and the restricted set of composite operators.

The analogous procedure can be performed in the sum rule scheme with the Borel transform, leading to the dependence of the results on the transformation parameter.

As one can see from eq.(64), the result, obtained in the framework of the QCD sum rules, depends on the choice of the values for the hadronic continuum threshold energy and the current masses of quarks. Then, this dependence causes large errors in the estimates of the masses for the lightest pseudoscalar, vector and scalar ( $\bar{b}c$ ) states.

Thus, the QCD sum rules give the estimates of the quark binding energy in the quarkonium, and the estimates are in agreement with the results of the potential models, but sum rules involve a considerable parametric uncertainty.

## 2.2. Radiative transitions in the $B_c$ family

The  $B_c$  mesons have no annihilation channels for the decays due to QCD and electromagnetic interactions. Therefore, the mesons, lying below the threshold for the  $B$  and  $D$  mesons production, will, in a cascade way, decay into the  $0^-(1S)$  state by emission of  $\gamma$  quanta and  $\pi$  mesons. Theoretical estimates of the transitions between the levels with the emission of the  $\pi$  mesons have uncertainties, and the electromagnetic transitions are quite accurately calculable.

### 2.2.1. Electromagnetic transitions

The formulae for the radiative E1-transitions have form [17,68]

$$\begin{aligned}
\Gamma(\bar{n}P_J \rightarrow n^1S_1 + \gamma) &= \frac{4}{9} \alpha_{\text{em}} Q_{\text{eff}}^2 \omega^3 I^2(\bar{n}P; nS) w_J(\bar{n}P) , \\
\Gamma(\bar{n}P_J \rightarrow n^1S_0 + \gamma) &= \frac{4}{9} \alpha_{\text{em}} Q_{\text{eff}}^2 \omega^3 I^2(\bar{n}P; nS) (1 - w_J(\bar{n}P)) , \\
\Gamma(n^1S_1 \rightarrow \bar{n}P_J + \gamma) &= \frac{4}{27} \alpha_{\text{em}} Q_{\text{eff}}^2 \omega^3 I^2(nS; \bar{n}P) (2J + 1) w_J(\bar{n}P) , \\
\Gamma(n^1S_0 \rightarrow \bar{n}P_J + \gamma) &= \frac{4}{9} \alpha_{\text{em}} Q_{\text{eff}}^2 \omega^3 I^2(nS; \bar{n}P) (2J + 1) (1 - w_J(\bar{n}P)) , \\
\Gamma(\bar{n}P_J \rightarrow nD_{J'} + \gamma) &= \frac{4}{27} \alpha_{\text{em}} Q_{\text{eff}}^2 \omega^3 I^2(nD; \bar{n}P) (2J' + 1) w_J(\bar{n}P) w_{J'}(nD) S_{JJ'} , \\
\Gamma(nD_J \rightarrow \bar{n}P_{J'} + \gamma) &= \frac{4}{27} \alpha_{\text{em}} Q_{\text{eff}}^2 \omega^3 I^2(nD; \bar{n}P) (2J' + 1) w_{J'}(\bar{n}P) w_J(nD) S_{J'J} ,
\end{aligned} \tag{65}$$

where  $\omega$  is the photon energy,  $\alpha_{\text{em}}$  is the electromagnetic fine structure constant.

In eq.(65) one uses

$$Q_{\text{eff}} = \frac{m_c Q_{\bar{b}} - m_b Q_c}{m_c + m_b} , \tag{66}$$

where  $Q_{c,b}$  are the electric charges of the quarks. For the  $B_c$  meson with the parameters from the Martin potential, one gets  $Q_{\text{eff}} = 0.41$ .

$w_J(nL)$  is the probability that the spin  $S = 1$  in the  $nL$  state, so that  $w_0(nP) = w_2(nP) = 1$ ,  $w_1(nD) = w_3(nD) = 1$ , and the  $w_1(nP)$ ,  $w_2(nD)$  values have been presented in the previous section (see eqs.(50), (53), (56) ).

The statistical factor  $S_{JJ'}$  takes values [68]

$J$	$J'$	$S_{JJ'}$
0	1	2
1	1	1/2
1	2	9/10
2	1	1/50
2	2	9/50
2	3	18/25.

The  $I(\bar{n}L; nL')$  value is expressed through the radial wave functions,

$$I(\bar{n}L; nL') = \left| \int R_{\bar{n}L}(r)R_{nL'}(r)r^3 dr \right|. \quad (67)$$

For the set of the transitions one obtains

$$\begin{aligned} I(1S, 2P) &= 1.568 \text{ GeV}^{-1}, & I(1S, 3P) &= 0.255 \text{ GeV}^{-1}, \\ I(2S, 2P) &= 2.019 \text{ GeV}^{-1}, & I(2S, 3P) &= 2.704 \text{ GeV}^{-1}, \\ I(3D, 2P) &= 2.536 \text{ GeV}^{-1}, & I(3D, 3P) &= 2.416 \text{ GeV}^{-1}. \end{aligned} \quad (68)$$

For the dipole magnetic transitions one has [5,17,68]

$$\Gamma(\bar{n}^1S_i \rightarrow n^1S_f + \gamma) = \frac{16}{3} \mu_{\text{eff}}^2 \omega^3 (2f + 1) A_{if}^2, \quad (69)$$

where

$$A_{if} = \int R_{\bar{n}S}(r)R_{nS}(r)j_0(\omega r/2)r^2 dr,$$

and

$$\mu_{\text{eff}} = \frac{1}{2} \frac{\sqrt{\alpha_{\text{em}}}}{2m_c m_b} (Q_c m_b - Q_{\bar{b}} m_c). \quad (70)$$

Note, in contrast to the  $\psi$  and  $\Upsilon$  particles, the total width of the  $B_c^*$  meson is equal to the width of its radiative decay into the  $B_c(0^-)$  state.

The electromagnetic widths, calculated with accordance of eqs.(65),(69), and the frequencies of the emitted photons are presented in Tables 9, 10, 11.

Note, E0-transitions with the conversion of virtual  $\gamma$ -quantum into the lepton pair can take place. Moreover, due to the tensor forces, the states with  $J > 0$  and  $S = 1$  can, in addition to the  $L$ -wave, have the admixture of  $|L \pm 2|$ -waves, giving the quadrupole moment to the corresponding states and causing the E2-transitions. However, the mentioned transitions are suppressed by the additional factor  $\alpha_{\text{em}}$  in the first case, and by the small value of amplitude, determining, say, the probability of the admixture appearance of the  $D$ -wave in the  $1^-(nS)$  state.

Thus, the registration of the cascade electromagnetic transitions in the  $(\bar{b}c)$  family can be used for the observation of the higher  $(\bar{b}c)$  excitations, having no annihilation channels of the decays.

**Table 9.**

The energies (in MeV) and widths (in keV) of the electromagnetic E1-transitions in the ( $\bar{b}c$ ) family (\* is the present paper)

Transition	$\omega$	$\Gamma[*]$	$\Gamma[53]$
$2P_2 \rightarrow 1S_1 + \gamma$	426	102.9	112.6
$2P_0 \rightarrow 1S_1 + \gamma$	366	65.3	79.2
$2P 1'^+ \rightarrow 1S_1 + \gamma$	412	8.1	0.1
$2P 1^+ \rightarrow 1S_1 + \gamma$	400	77.8	99.5
$2P 1'^+ \rightarrow 1S_0 + \gamma$	476	131.1	56.4
$2P 1^+ \rightarrow 1S_0 + \gamma$	464	11.6	0.0
$3P_2 \rightarrow 1S_1 + \gamma$	817	19.2	25.8
$3P_0 \rightarrow 1S_1 + \gamma$	771	16.1	21.9
$3P 1'^+ \rightarrow 1S_1 + \gamma$	807	2.5	2.1
$3P 1^+ \rightarrow 1S_1 + \gamma$	796	15.3	22.1
$3P 1'^+ \rightarrow 1S_0 + \gamma$	871	20.1	–
$3P 1^+ \rightarrow 1S_0 + \gamma$	860	3.1	–
$3P_2 \rightarrow 2S_1 + \gamma$	232	49.4	73.8
$3P_0 \rightarrow 2S_1 + \gamma$	186	25.5	41.2
$3P 1'^+ \rightarrow 2S_1 + \gamma$	222	5.9	5.4
$3P 1^+ \rightarrow 2S_1 + \gamma$	211	32.1	54.3
$3P 1'^+ \rightarrow 2S_0 + \gamma$	257	58.0	–
$3P 1^+ \rightarrow 2S_0 + \gamma$	246	8.1	–
$2S_1 \rightarrow 2P_2 + \gamma$	159	14.8	17.7
$2S_1 \rightarrow 2P_0 + \gamma$	219	7.7	7.8
$2S_1 \rightarrow 2P 1'^+ + \gamma$	173	1.0	0.0
$2S_1 \rightarrow 2P 1^+ + \gamma$	185	12.8	14.5
$2S_0 \rightarrow 2P 1'^+ + \gamma$	138	15.9	5.2
$2S_0 \rightarrow 2P 1^+ + \gamma$	150	1.9	0.0

### 2.2.2. Hadronic transitions

In the framework of QCD the consideration of the hadronic transitions between the states of the heavy quarkonium family is built on the basis of the multipole expansion for the gluon emission by the heavy nonrelativistic quarks [23], with forthcoming hadronization of gluons, independently of the heavy quark motion.

In the leading approximation over the velocity of the heavy quark motion, the action, corresponding to the heavy quark coupling to the external gluon field,

$$S_{\text{int}} = -g \int d^4x A_\mu^a(x) \cdot j_\mu^a(x), \quad (71)$$

can be expressed in the form

$$S_{\text{int}} = g \int dt r^k E_k^a(t, \mathbf{x}) \frac{\lambda_a^{ij}}{2} \Psi_n(\mathbf{r}) \Psi_f^{ji}(\mathbf{r}) K(s_n, f) d^3\mathbf{r}, \quad (72)$$

Table 10.

The energies (in MeV) and widths (in keV) of the electromagnetic E1-transitions in the ( $\bar{b}c$ ) family (\* is the present paper)

Transition	$\omega$	$\Gamma[*]$	$\Gamma[53]$
$3P_2 \rightarrow 3D_1 + \gamma$	126	0.1	0.2
$3P_2 \rightarrow 3D 2'^- + \gamma$	118	0.5	–
$3P_2 \rightarrow 3D 2^- + \gamma$	133	1.5	3.2
$3P_2 \rightarrow 3D_3 + \gamma$	127	10.9	17.8
$3P_0 \rightarrow 3D_1 + \gamma$	80	3.2	6.9
$3P 1'^+ \rightarrow 3D_1 + \gamma$	116	0.3	0.4
$3P 1^+ \rightarrow 3D_1 + \gamma$	105	1.6	0.3
$3P 1'^+ \rightarrow 3D 2'^- + \gamma$	108	3.5	–
$3P 1^+ \rightarrow 3D 2^- + \gamma$	112	3.9	9.8
$3P 1'^+ \rightarrow 3D 2^- + \gamma$	123	2.5	11.5
$3P 1^+ \rightarrow 3D 2'^- + \gamma$	97	1.2	–
$3D_3 \rightarrow 2P_2 + \gamma$	264	76.9	98.7
$3D_1 \rightarrow 2P_0 + \gamma$	325	79.7	88.6
$3D_1 \rightarrow 2P 1'^+ + \gamma$	279	3.3	0.0
$3D_1 \rightarrow 2P 1^+ + \gamma$	291	39.2	49.3
$3D_1 \rightarrow 2P_2 + \gamma$	265	2.2	2.7
$3D 2'^- \rightarrow 2P_2 + \gamma$	273	6.8	–
$3D 2'^- \rightarrow 2P_2 + \gamma$	258	12.2	24.7
$3D 2'^- \rightarrow 2P 1'^+ + \gamma$	287	46.0	92.5
$3D 2'^- \rightarrow 2P 1^+ + \gamma$	301	25.0	–
$3D 2^- \rightarrow 2P 1'^+ + \gamma$	272	18.4	0.1
$3D 2^- \rightarrow 2P 1^+ + \gamma$	284	44.6	88.8

where  $\Psi_n(\mathbf{r})$  is the wave function of the quarkonium, emitting gluon,  $\Psi_f^{ij}(\mathbf{r})$  is the wave function of the colour-octet state of the quarkonium,  $K(s_n, f)$  corresponds to the spin factor (in the leading approximation, the heavy quark spin is decoupled from the interaction with the gluons).

Then the matrix element for the E1-E1 transition of the quarkonium  $nL_J \rightarrow n'L'_{J'} + gg$  can be written in the form

$$M(nL_J \rightarrow n'L'_{J'} + gg) = 4\pi\alpha_S E_k^a E_m^b \cdot \int d^3r d^3r' r_k r'_m G_{s_n, s_n}^{ab}(r, r') \Psi_{nL_J}(r) \Psi_{n'L'_{J'}}(r'), \quad (73)$$

where  $G_{s_n, s_n}^{ab}(r, r')$  corresponds to the propagator of the colour-octet state of the heavy quarkonium

$$G = \frac{1}{\epsilon - H_{Q\bar{Q}}^c}, \quad (74)$$

where  $H_{Q\bar{Q}}^c$  is the hamiltonian of the coloured state.

Table 11.

The energies (in MeV) and widths (in keV) of the electromagnetic M1-transitions in the ( $\bar{b}c$ ) family (\* is the present paper)

Transition	$\omega$	$\Gamma[*]$	$\Gamma[53]$
$2S_1 \rightarrow 1S_0 + \gamma$	649	0.098	0.123
$2S_0 \rightarrow 1S_1 + \gamma$	550	0.096	0.093
$1S_1 \rightarrow 1S_0 + \gamma$	64	0.060	0.135
$2S_1 \rightarrow 2S_0 + \gamma$	35	0.010	0.029

One can see from eq.(73), that the determination of the transition matrix element depends on both the wave function of the quarkonium and the hamiltonian  $H_{Q\bar{Q}}^c$ . Thus, the theoretical consideration of the hadronic transitions in the quarkonium family is model dependent.

In a number of papers of ref.[24], for the calculation of the values such as (73), the potential approach has been developed.

In papers of ref.[25] it is shown that nonperturbative conversion of the gluons into the  $\pi$  meson pair allows one to give a consideration in the framework of the low-energy theorems in QCD, so that this consideration agrees with the papers, performed in the framework of PCAC and soft pion technique [26].

However, as it follows from eq.(73) and the Wigner-Eckart theorem, the differential width for the E1-E1 transition allows the representation in the form [24]

$$\frac{d\Gamma}{dm^2}(nL_J \rightarrow n'L'_{J'} + h) = (2J' + 1) \sum_{k=0}^2 \left\{ \begin{matrix} k & L & L' \\ s & J' & J \end{matrix} \right\}^2 A_k(L, L'), \quad (75)$$

where  $m^2$  is the invariant mass of the light hadron system  $h$ ,  $\{ \}$  are 6j-symbols,  $A_k(L, L')$  is the contribution by the irreducible tensor of the rang, equal to  $k < 3$ ,  $s$  is the total quark spin inside the quarkonium.

In the limit of soft pions, one has  $A_1(L, L') = 0$ .

From eqs.(73), (75) it follows, that, with the accuracy up to the difference in the phase spaces, the widths of the hadronic transitions in the ( $Q\bar{Q}$ ) and ( $Q\bar{Q}'$ ) quarkonia are related to the following expression [23,24]

$$\frac{\Gamma(Q\bar{Q}')}{\Gamma(Q\bar{Q})} = \frac{\langle r^2(Q\bar{Q}') \rangle^2}{\langle r^2(Q\bar{Q}) \rangle^2}. \quad (76)$$

Then the experimental data on the transitions of  $\psi' \rightarrow J/\psi + \pi\pi$ ,  $\Upsilon' \rightarrow \Upsilon + \pi\pi$ ,  $\psi(3770) \rightarrow J/\psi + \pi\pi$  [27] allow one to extract the values of  $A_k(L, L')$  for the transitions  $2S \rightarrow 1S + \pi\pi$  and  $3D \rightarrow 1S + \pi\pi$  [53].

The invariant mass spectrum of the  $\pi$  meson pair has the universal form [25,26]

$$\frac{1}{\Gamma} \frac{d\Gamma}{dm} = B \frac{|\mathbf{k}_{\pi\pi}|}{M^2} (2x^2 - 1) \sqrt{x^2 - 1}, \quad (77)$$

where  $x = m/2m_\pi$ ,  $|\mathbf{k}_{\pi\pi}|$  is the  $\pi\pi$  pair momentum.



The estimates for the widths of the hadronic transitions in the  $(\bar{b}c)$  family have been made in ref.[53]. The hadronic transition widths, having the values comparable with the electromagnetic transition width values, are presented in Table 12.

The transitions in the  $(\bar{b}c)$  family with the emission of  $\eta$  mesons are suppressed by the low value of the phase space.

Thus, the registration of the hadronic transitions in the  $(\bar{b}c)$  family with the emission of the  $\pi$  meson pairs can be used to observe the higher 2S- and 3D-excitations of the basic state.

### 2.3. Leptonic constant of $B_c$ meson

As we have seen in Section 2.1, the value of the leptonic constant of the  $B_c$  meson determines the splitting of the basic 1S-state of the  $(\bar{b}c)$  system. Moreover, the higher excitations in the  $(\bar{b}c)$  system transform, in a cascade way, into the lightest  $0^-$  state of  $B_c$ , whose widths of the decays are essentially determined by the value of  $f_{B_c}$ , too. In the quark models [69–71], used to calculate the weak decay widths of mesons, the leptonic constant, as the parameter, determines the quark wave package inside the meson (generally, the wave function is chosen in the oscillator form), therefore, the practical problem for the extraction of the value for the weak charged current mixing matrix element  $|V_{bc}|$  from the data on the weak  $B_c$  decays can be only solved at the known value of  $f_{B_c}$ .

Thus, the leptonic constant  $f_{B_c}$  is the most important quantity, characterizing the bound state of the  $(\bar{b}c)$  system.

In the present Section we calculate the value of  $f_{B_c}$  in different ways.

To describe the bound states of the quarks, the use of the nonperturbative approaches is required. The bound states of the heavy quarks allow one to consider simplifications, connected to both large values of the quark masses  $\Lambda_{QCD}/m_Q \ll 1$  and the nonrelativistic quark motion  $v \rightarrow 0$ . Therefore the value of  $f_{B_c}$  can be quite reliably determined in the framework of the potential models and the QCD sum rules [11].

Table 12. The widths (in keV) of the radiative hadronic transitions in the  $(\bar{b}c)$  family

Transition	$\Gamma$ [53]
$2S_0 \rightarrow 1S_0 + \pi\pi$	50
$2S_1 \rightarrow 1S_1 + \pi\pi$	50
$3D_1 \rightarrow 1S_1 + \pi\pi$	31
$3D_2 \rightarrow 1S_1 + \pi\pi$	32
$3D_3 \rightarrow 1S_1 + \pi\pi$	31
$3D_2 \rightarrow 1S_0 + \pi\pi$	32

Table 13.

The leptonic  $B_c$  meson constant (in MeV), calculated in the different potential models (the accuracy  $\sim 15\%$ )

Model	Martin	Coulomb	[6]	[53]	[72]	[73,74]	[75]
$f_{B_c}$	510	460	570	495	410	600	500

### 2.3.1. $f_{B_c}$ from potential models

In the framework of the nonrelativistic potential models, the leptonic constants of the pseudoscalar and vector mesons (see eqs.(59), (60))

$$\langle 0|\bar{c}(x)\gamma_\mu b(x)|B_c^*(p, \epsilon)\rangle = if_V M_V \epsilon_\mu \exp(ipx), \quad (78)$$

$$\langle 0|\bar{c}(x)\gamma_5\gamma_\mu b(x)|B_c(p)\rangle = if_P p_\mu \exp(ipx), \quad (79)$$

are determined by expression (28)

$$f_V = f_P = \sqrt{\frac{3}{\pi M_{B_c(1S)}}} R_{1S}(0), \quad (80)$$

where  $R_{1S}(0)$  is the radial wave function of the  $1S$  state of the  $(\bar{b}c)$  system, at the origin. The wave function is calculated by solving the Schrödinger equation with different potentials [5–8,10,54], in the quasipotential approach [72] or by solving the Bethe-Salpeter equation with instant potential and in the expansion up to the second order over the quark motion velocity  $v/c$  [73,74].

The values of the leptonic  $B_c$  meson constant, calculated in different potential models and effective Coulomb potential with the "running"  $\alpha_S$  constant, determined in Section 2.1, are presented in Table 13.

Thus, in the approach accuracy, the potential quark models give the  $f_{B_c}$  values, which are in a good agreement with each other, so that

$$f_{B_c}^{\text{pot}} = 500 \pm 80 \text{ MeV}. \quad (81)$$

### 2.3.2. $f_{B_c}$ from QCD sum rules

In the framework of the QCD sum rules [11], expressions (58)-(64) have been derived for the vector states. The expressions are considered at  $q^2 < 0$  in the schemes of the spectral density moments (64) or with the application of the Borel transform [11]. As one can see from eqs.(58) - (64), the result of the QCD sum rule calculations is determined not only by physical parameters such as the quark and meson masses, but also by the unphysical parameters of the sum rule scheme such as the number of the spectral density moment or the Borel transformation parameter. In the QCD sum rules, this unphysical dependence of the  $f_{B_c}$  value is due to the consideration being performed with the finite number of terms in the expansion of the QCD perturbation theory for the Wilson coefficients of the unit and composite operators. In the calculations, the set of the composite operators is also restricted.

Table 14.

The leptonic  $B_c$  constant (in MeV), calculated in the QCD sum rules (SR – the scaling relation)

Model	[76]	[35]	[36]	[67]	[77]	[78]	[79]	SR[21]
$f_{B_c}$	375	400	360	300	160	300	450	460

Thus, the ambiguity in the choice of the hadronic continuum threshold and the parameter of the sum rule scheme essentially reduces the reliability of the QCD sum rule predictions for the leptonic constants of the vector and pseudoscalar  $B_c$  states.

Moreover, the nonrelativistic quark motion inside the heavy quarkonium  $v \rightarrow 0$  leads to the  $\alpha_S/v$ -corrections, becoming the most important, to the perturbative part of the quark current correlators, where  $\alpha_S$  is the effective Coulomb coupling constant in the heavy quarkonium. As it is noted in refs.[11,21,76], the Coulomb  $\alpha_S/v$ -corrections can be summed up and represented in the form of the factor, corresponding to the Coulomb wave function of the heavy quarks, so that

$$F(v) = \frac{4\pi\alpha_S}{3v} [1 - \exp(-4\pi\alpha_S/3v)]^{-1}, \quad (82)$$

where  $2v$  is the relative velocity of the heavy quarks inside the quarkonium. The expansion of the factor (82) in the first order over  $\alpha_S/v$

$$F(v) \approx 1 + \frac{2\pi\alpha_S}{3v}, \quad (83)$$

gives the expression, obtained in the first order of the QCD perturbation theory [11].

Note, the  $\alpha_S$  parameter in eq.(82) should be at the scale of the characteristic quark virtualities in the quarkonium (see Section 2.1), but at the scale of the quark or quarkonium masses, as sometimes one makes it thereby decreasing the value of factor (82).

The choice of the  $\alpha_S$  parameter essentially determines the spread of the sum rule predictions for the  $f_{B_c}$  value (see Table 14)

$$f_{B_c}^{SR} = 160 \div 570 \text{ MeV}. \quad (84)$$

As one can see from eq.(84), the ambiguity in the choice of the QCD sum rule parameters leads to the essential deviations in the results from the  $f_{B_c}$  estimates (81) in the potential models.

However, as it has been noted in Section 2.1,

- 1) the large value of the heavy quark masses  $\Lambda_{QCD}/m_Q \ll 1$ ,
- 2) the nonrelativistic heavy quark motion inside the heavy quarkonium  $v \rightarrow 0$ , and
- 3) the universal scaling properties of the potential in the heavy quarkonium, when the kinetic energy of the quarks and the quarkonium state density do not depend on the heavy quark flavours (see eqs.(10) - (15)),

allow one to state the scaling relation (17) for the leptonic constants of the S-wave quarkonia

$$\frac{f^2}{M} \left( \frac{M}{4\mu} \right)^2 = \text{const}.$$

Indeed, at  $\Lambda_{QCD}/m_Q \ll 1$  one can neglect the quark-gluon condensate contribution, having the order of magnitude  $O(1/m_b m_c)$  (the contribution into the  $\psi$  and  $\Upsilon$  leptonic constants is less than 15%). At  $v \rightarrow 0$  one has to take into account the Coulomb-like  $\alpha_S/v$ -corrections in the form of factor (82), so that the imaginary part of the correlators for the vector and axial quark currents has the form

$$\Im m \Pi_V(q^2) \approx \Im m \Pi_P(q^2) = \frac{\alpha_S}{2} q^2 \left( \frac{M}{4\mu} \right)^2, \quad (85)$$

where

$$v^2 = 1 - \frac{4m_b m_c}{q^2 - (m_b - m_c)^2}, \quad v \rightarrow 0.$$

Moreover, condition (15) can be used in the specific QCD sum rule scheme, so that this scheme excludes the dependence of the results on the parameters such as the number of the spectral density moment or the Borel parameter.

Indeed, for example, the resonance contribution into the hadronic part of the vector current correlator, having the form

$$\Pi_V^{(\text{res})}(q^2) = \int \frac{ds}{s - q^2} \sum_n f_{Vn}^2 M_{Vn}^2 \delta(s - M_{Vn}^2), \quad (86)$$

can be rewritten as

$$\Pi_V^{(\text{res})}(q^2) = \int \frac{ds}{s - q^2} s f_{Vn(s)}^2 \frac{dn(s)}{ds} \frac{d}{dn} \sum_k \theta(n - k). \quad (87)$$

where  $n(s)$  is the number of the vector S-state versus the mass, so that

$$n(m_k^2) = k. \quad (88)$$

Taking the average value for the derivative of the step-like function, one gets

$$\Pi_V^{(\text{res})}(q^2) = \left\langle \frac{d}{dn} \sum_k \theta(n - k) \right\rangle \int \frac{ds}{s - q^2} s f_{Vn(s)}^2 \frac{dn(s)}{ds}, \quad (89)$$

and, supposing

$$\left\langle \frac{d}{dn} \sum_k \theta(n - k) \right\rangle \approx 1, \quad (90)$$

one can, in average, write down

$$\Im m \langle \Pi^{(\text{hadr})}(q^2) \rangle = \Im m \Pi^{(\text{QCD})}(q^2), \quad (91)$$

so, taking into the account the Coulomb factor and neglecting power corrections over  $1/m_Q$ , at the physical points  $s_n = M_n^2$  one obtains

$$\frac{f_n^2}{M_n} \left( \frac{M}{4\mu} \right)^2 = \frac{\alpha_S}{\pi} \frac{dM_n}{dn}, \quad (92)$$

where one has supposed that

$$m_b + m_c \approx M_{B_c} , \quad (93)$$

$$f_{V_n} \approx f_{P_n} = f_n . \quad (94)$$

Further, as it has been shown in Section 2.1, in the heavy quarkonium the value of  $dn/dM_n$  does not depend on the quark masses (see eq.(15)), and, with the accuracy up to the logarithmic corrections,  $\alpha_S$  is the constant value (the last fact is also manifested in the flavour independence of the Coulomb part of the potential in the Cornell model). Therefore, one can draw the conclusion that, in the leading approximation, the right hand side of eq.(92) is the constant value, and there is the scaling relation (17) [21]. This relation is valid in the resonant region, where one can neglect the contribution by the hadronic continuum.

Note, scaling relation (17) is in a good agreement with the experimental data on the leptonic decay constants of the  $\psi$  and  $\Upsilon$  particles (see Table 6), for which one has  $4\mu/M = 1$  [21].

The value of the constant in the right hand side of eq.(17) is in agreement with the estimate, when we suppose

$$\left\langle \frac{dM_\Upsilon}{dn} \right\rangle \approx \frac{1}{2} [(M_{\Upsilon'} - M_\Upsilon) + (M_{\Upsilon''} - M_{\Upsilon'})] , \quad (95)$$

and  $\alpha_S = 0.36$ , as it is in the Cornell model.

Further, in the limit case of  $B$  and  $D$  mesons, when the heavy quark mass is much greater than the light quark mass  $m_Q \gg m_q$ , one has

$$\mu \approx m_q$$

and

$$f^2 \cdot M = \frac{16\alpha_S}{\pi} \frac{dM}{dn} \mu^2 . \quad (96)$$

Then it is evident that at one and the same  $\mu$  one gets

$$f^2 M = \text{const} . \quad (97)$$

Scaling law (97) is very well known in EHQT [14] for mesons with a single heavy quark ( $Q\bar{q}$ ), and it follows, for example, from the identity of the  $B$  and  $D$  meson wave functions within the limit, when an infinitely heavy quark can be considered as a static source of gluon field (then eq.(97) follows from eq.(80)).

In our derivation of eqs.(96) and (97) we have neglected power corrections over the inverse heavy quark mass. Moreover, we have used the notion about the light constituent quark with the mass equal to

$$m_q \approx 330 \text{ MeV} , \quad (98)$$

so that this quark has to be considered as nonrelativistic one  $v \rightarrow 0$ , and the following conditions take place

$$m_Q + m_q \approx M_{(Q\bar{q})}^{(*)} , \quad m_q \ll m_Q , \quad (99)$$

$$f_V \approx f_P = f . \quad (100)$$

In agreement with eqs.(96) and (98), one finds the estimates<sup>1</sup>

$$f_{B^{(*)}} = 120 \pm 20 \text{ MeV} , \quad (101)$$

$$f_{D^{(*)}} = 220 \pm 30 \text{ MeV} , \quad (102)$$

that is in an agreement with the estimates in the other schemes of the QCD sum rules [11,12].

Thus, in the limits of  $4\mu/M = 1$  and  $\mu/M \ll 1$ , scaling relation (17) is consistent.

The  $f_{B_c}$  estimate from eq.(17) contains the uncertainty, connected to the choice of the ratio for the  $b$ - and  $c$ -quark masses, so that (see Table 14)

$$f_{B_c} = 460 \pm 60 \text{ MeV} . \quad (103)$$

In ref.[76] the sum rule scheme with the double Borel transform was used. So, it allows one to study effects, related to the power corrections from the gluon condensate, corrections due to nonzero quark velocity and nonzero binding energy of the quarks in the quarkonium.

Indeed, for the set of narrow pseudoscalar states, one has the sum rules

$$\sum_{k=1}^{\infty} \frac{M_k^4 f_{P_k}^2}{(m_b + m_c)^2 (M_k^2 - q^2)} = \frac{1}{\pi} \int \frac{ds}{s - q^2} \Im m \Pi_P(s) + C_G(q^2) \langle \frac{\alpha_S}{\pi} G^2 \rangle , \quad (104)$$

where

$$C_G(q^2) = \frac{1}{192 m_b m_c} \frac{q^2}{\bar{q}^2} \left( \frac{3(3v^2 + 1)(1 - v^2)^2}{2v^5} \ln \frac{v + 1}{v - 1} - \frac{9v^4 + 4v^2 + 3}{v^4} \right) , \quad (105)$$

and

$$\bar{q}^2 = q^2 - (m_b - m_c)^2 , \quad v^2 = 1 - \frac{4m_b m_c}{\bar{q}^2} . \quad (106)$$

Acting by the Borel operator  $L_\tau(-q^2)$  on eq.(104), one gets

$$\sum_{k=1}^{\infty} \frac{M_k^4 f_{P_k}^2}{(m_b + m_c)^2} \exp(-M_k^2 \tau) = \frac{1}{\pi} \int ds \Im m \Pi_P(s) \exp(-s\tau) + C'_G(\tau) \langle \frac{\alpha_S}{\pi} G^2 \rangle , \quad (107)$$

where

$$L_\tau(x) = \lim_{n, x \rightarrow \infty} \frac{x^{n+1}}{n!} \left( -\frac{d}{dx} \right)^n , \quad \frac{n}{x} = \tau , \quad (108)$$

$$C'_G(\tau) = L_\tau(-q^2) C_G(q^2) . \quad (109)$$

For the exponential set in the left hand side of eq.(107), one uses the Euler-MacLaurin formula

$$\begin{aligned} \sum_{k=1}^{\infty} \frac{M_k^4 f_{P_k}^2}{(m_b + m_c)^2} \exp(-M_k^2 \tau) &= \int_{m_n}^{\infty} dM_k \frac{dM_k}{dM_k} M_k^4 f_{P_k}^2 \exp(-M_k^2 \tau) + \\ &\sum_{k=0}^{n-1} M_k^4 f_{P_k}^2 \exp(-M_k^2 \tau) + \dots . \end{aligned} \quad (110)$$

---

<sup>1</sup>In ref.[21] the dependence of the S-wave state density  $dn/dM_n$  on the reduced mass of the system with the Martin potential has been found by the Bohr-Sommerfeld quantization, so that at the step from  $(\bar{b}b)$  to  $(\bar{b}q)$ , the density changes less than about 15%.

Making the second Borel transform  $L_{M_k^2}(\tau)$  on eq. (107) with account of eq.(110), one finds the expression for the leptonic constants of the pseudoscalar ( $\bar{b}c$ ) states, so that

$$f_{Pk}^2 = \frac{2(m_b + m_c)^2}{M_k^3} \frac{dM_k}{dk} \left\{ \frac{1}{\pi} \Im m \Pi_P(M_k^2) + C_G''(M_k^2) \left\langle \frac{\alpha_S}{\pi} G^2 \right\rangle \right\}, \quad (111)$$

where we have used the following property of the Borel operator

$$L_\tau(x) x^n \exp(-bx) \rightarrow \delta_+^{(n)}(\tau - b). \quad (112)$$

Explicit form for the spectral density and Wilson coefficients can be found in ref.[76].

Expression (111) is in the agreement with the above performed derivation of scaling relation (17).

The numerical effect from the mentioned corrections is considered to be not large (the power corrections are of the order of 10%), and the uncertainty, connected to the choice of the quark masses, dominates in the error of the  $f_{B_c}$  value determination (see eq.(103)).

Thus, we have shown that, in the framework of the QCD sum rules, the most reliable estimate of the  $f_{B_c}$  value (103) is coming from the use of the scaling relation (17) for the leptonic decay constants of the quarkonia, and this relation agrees very well with the results of the potential models.

### 3. Decays of $B_c$ mesons

#### 3.1. Life time of $B_c$ mesons

The processes of the  $B_c$  meson decay can be subdivided into three classes a) the  $\bar{b}$ -quark decay with the spectator  $c$ -quark, b) the  $c$ -quark decay with the spectator  $\bar{b}$ -quark, c) the annihilation channel  $B_c^+ \rightarrow l^+ \nu_l (c\bar{s}, u\bar{s})$ ,  $l = e, \mu, \tau$ .

The total width is summed from three partial widths

$$\Gamma(B_c \rightarrow X) = \Gamma(b \rightarrow X) + \Gamma(c \rightarrow X) + \Gamma(\text{ann}). \quad (113)$$

The simplest estimates with no account for the quark binding inside the  $B_c$  meson and in the framework of the spectator mechanism of the decay for the first and second cases, lead to the expressions

$$\begin{aligned} \Gamma(b \rightarrow X) &= \frac{G_F^2 |V_{bc}|^2 m_b^5}{192\pi^3} \cdot 9, \\ \Gamma(c \rightarrow X) &= \frac{G_F^2 |V_{cs}|^2 m_c^5}{192\pi^3} \cdot 5, \end{aligned} \quad (114)$$

So, that  $m_b$  and  $m_c$  are chosen for to represent correctly the spectator parts of the total widths for the  $B$  and  $D$  mesons.

The width of the annihilation channel equals

$$\Gamma(\text{ann}) = \sum_i \frac{G_F^2}{8\pi} |V_{bc}|^2 f_{B_c}^2 M_{bc} m_i^2 \left(1 - \frac{m_i^2}{m_{B_c}^2}\right)^2 \cdot C_i, \quad (115)$$

Fig. 2. The diagrams of the  $B_c$  meson decays: (a) the  $c$ -spectator decay; (b) the  $b$ -spectator decay; (c) the annihilation

where  $C_i = 1$  for the  $\tau\nu_\tau$  channel and  $C_i = 3|V_{cs}|^2$  for the  $\bar{c}s$  channel, and  $m_i$  is the mass of the most heavy fermion ( $\tau$  or  $c$ ).

Note that in the case of the nonleptonic decays, an account of the strong interaction results in the multiplicative factor of enhancement to formulae (114)-(115) (see section 3.2).

The mentioned widths, calculated with the use of the know values of parameters  $m_q$ ,  $|V_{bc}| = 0.046$ ,  $|V_{cs}| = 0.96$  etc., are presented in Table 15.

Thus, the rough estimate of the life time leads to  $\tau_{B_c} \approx (2-5) \cdot 10^{-13}$  s. So, the fraction of the  $c$ -quark decay is approximately 50 %, the  $b$ -quark one is 45 %, and the annihilation

Table 15. The widths ( $10^{-6}$  eV) of the inclusive decays of  $b$ - and  $c$ -quarks in free and bound states (in the  $B_c$  meson) and the branching ratios ( $BR$  in %) of inclusive  $B_c$  decays

Decay mode	free quarks	$B_c^+$	$BR$	Decay mode	free quarks	$B_c^+$	$BR$
$b \rightarrow \bar{c} + e^+ \nu_e$	62	62	4.7	$c \rightarrow s + e^+ + \nu_e$	124	74	5.6
$\bar{b} \rightarrow \bar{c} + \mu^+ \nu_\mu$	62	62	4.7	$c \rightarrow s + \mu^+ + \nu_\mu$	124	74	5.6
$\bar{b} \rightarrow \bar{c} + \tau^+ \nu_\tau$	14	14	1.0	$c \rightarrow s + u + \bar{d}$	675	405	30.5
$\bar{b} \rightarrow \bar{c} + \bar{d} + u$	248	248	18.7	$c \rightarrow s + u + \bar{s}$	33	20	1.5
$\bar{b} \rightarrow \bar{c} + \bar{s} + u$	13	13	1.0	$c \rightarrow d + e^+ \nu$	7	4	0.3
$\bar{b} \rightarrow \bar{c} + \bar{s} + c$	87	87	6.5	$c \rightarrow d + \mu^+ + \nu_\mu$	7	4	0.3
$\bar{b} \rightarrow \bar{c} + \bar{d} + c$	5	5	0.4	$c \rightarrow d + u + \bar{d}$	39	23	1.7
$B_c^+ \rightarrow \tau^+ + \nu_\tau$	–	63	4.7	$B_c^+ \rightarrow c + \bar{s}$	–	162	12.2
$B_c^+ \rightarrow c + \bar{d}$	–	8	0.6	$B_c^+ \rightarrow$ all	–	1328	100



channel is 5 %. However, these estimates do not take into account a quite strong binding of the quarks inside the  $B_c$  meson: corresponding corrections to the estimates can reach about 40 %.

Let us consider this effect in the semileptonic modes of decays with the spectator  $\bar{b}$ -quark. The final state of such decays generally contains the  $B_s^{(*)}$  mesons with the more small phase space of the lepton pair.

The effect of the phase space decrease is shown on Figure 3, where the kinematical borders of Dalitz plot for the  $B_c^+ \rightarrow B_s e^+ \nu$  decay are compared with the borders for the  $c$ -quark and calculated at different values of the  $c$ -quark mass. As one can see from Figure 3, the end-point of the leptonic spectrum is approximately one and the same in the different decays

$$E^{\max} = \frac{M_{B_c}^2 - M_{B_s}^2}{2M_{B_c}}. \quad (116)$$

However, the maximum values of the leptonic pair masses  $q_{max}^2$  are different.

One can easily find that the spectator model better describes the semileptonic decay  $D \rightarrow K$ . In the case of the  $B_c$  meson decay, the admissible kinematical region is strongly reduced. With the account for the phase space reduction in the spectator model, one can get [34]:

$$\Gamma(B_c^+ \rightarrow X_b e^+ \nu) \approx 0.71 \Gamma(D^+ \rightarrow X_s e^+ \nu). \quad (117)$$

The effect of the phase space reduction does not sizably appear in the case of decays with the spectator  $c$ -quark. For such decays, as one can see from Figure 4, the spectator model well describes the  $B$  meson decays as well as the  $B_c$  meson decays, and one can believe that

$$\Gamma(B_c^+ \rightarrow X_c e^+ \nu) \approx \Gamma(B^+ \rightarrow X_c e^+ \nu). \quad (118)$$

Another possible way of the estimate is related with the summation of the exclusive decays into the channels  $B_s e^+ \nu$  and  $B_s^* e^+ \nu$ . In agreement with the same kinematical arguments, their sum is the main fraction of the semileptonic decays [82]. If one neglects the decaying quark momentum inside the  $B_c$  meson, the admissible region of masses in the inclusive semileptonic decay  $Q \rightarrow Q' e \nu$  is varied within the limits

$$(m_{q'} + m_{\text{sp}})^2 < (M_x^2) < m_{q'}^2 + m_{\text{sp}}^2 + m_{\text{sp}} \frac{m_{q'}^2}{m_q}. \quad (119)$$

From approximate formula (119) with the use of the constituent quark masses, one can see, that the admissible  $M_x$  region in the decay  $B_c \rightarrow X_c$  is varied in the limit of 200 MeV and, hence, the final state is saturated by the lowest states. For the considered case ( $m_q = m_c = 1.7$  GeV,  $m_{q'} = m_s = 0.55$  GeV and  $m_{\text{sp}} = m_b = 5.1$  GeV), this region has the widths, equal to 340 MeV, that is less than the expected difference of masses between the basic state and the first orbital excitation of the  $(\bar{b}s)$  system.

Thus, one can consider that

$$\Gamma(B_c^+ \rightarrow X_b e^+ \nu) \approx \Gamma(B_c \rightarrow B_s + e \nu) + \Gamma(B_c \rightarrow B_s^* + e \nu). \quad (120)$$

Fig. 3. The Dalitz diagrams for the semileptonic decays: (1)  $B_c \rightarrow B_s^* l \nu$ , (2)  $B_c \rightarrow B_s l \nu$ , (3)  $D \rightarrow K^* l \nu$ , (4)  $D \rightarrow K l \nu$ , (5)  $c \rightarrow s l \nu$  ( $m_c = 1.7$  GeV,  $m_s = 0.55$  GeV), (6)  $c \rightarrow s l \nu$  ( $m_c = 1.5$  GeV,  $m_s = 0.15$  GeV);  $E$  is the lepton energy,  $q^2$  is the square of the lepton pair mass

The results of different quark models for the semileptonic  $B_c$  decays (see section 3.2)

Fig. 4. The Dalitz diagrams for the semileptonic decays: (1)  $B_c \rightarrow \psi l \nu$ , (2)  $B_c \rightarrow \eta_c l \nu$ , (3)  $B \rightarrow D l \nu$ , (4)  $B \rightarrow D^* l \nu$ , 5)  $b \rightarrow c l \nu$ ,  $E$  is the lepton energy,  $q^2$  is the square of the lepton pair mass

lead to the following sum of the widths of decays into  $B_s$  and  $B_s^*$

$$\Gamma(B_c \rightarrow B_s + e\nu) + \Gamma(B_c \rightarrow B_s^* + e\nu) \approx (60 \pm 7) 10^{-15} \text{ GeV} \approx 0.5 \Gamma(D^+ \rightarrow X_s e^+ \nu) . \quad (121)$$

Accounting for the current theoretical uncertainties, one can calculate

$$\Gamma(B_c \rightarrow X_{\bar{b}} + e^+ \nu) = (0.6 \pm 0.2) \Gamma(D^+ \rightarrow X_s e^+ \nu) . \quad (122)$$

For the  $c$ -spectator decays, the calculations in quark models and QCD sum rules show, that the semileptonic decays are saturated by the transitions into the lowest  $\eta_c$  and  $J/\psi$  states, i.e.

$$\Gamma(B_c^+ \rightarrow X_c e^+ \nu) \approx \Gamma(B_c^+ \rightarrow (\eta_c + J/\psi) e^+ \nu) \approx \Gamma(B^+ \rightarrow X_c e^+ \nu) . \quad (123)$$

With the account for these factors, the probabilities of inclusive decays are presented in Table 15. The widths of the hadronic inclusive decays, which are in details discussed in Section 3.3, are also shown.

The compact sizes of  $B_c$  meson lead to the large value of the weak decay constant ( $f_{B_c} \approx 500 \text{ MeV}$ ), that enforces the role of the annihilation channel into the massive fermions  $c, \tau$ . The decays of  $B_c$  meson into the light fermions are suppressed due to the forbidding over the spirality. Although the use of the effective masses for the  $u$ - and  $d$ -quarks instead of the current masses can increase the width of the annihilation channel into  $u\bar{d}$ , the latter will yet be much less than the width into the heavy massive fermions. In agreement with eq. (115), the conservative estimates of the annihilation decay probabilities are presented in Table 15.

Thus, the consideration of three types of processes for the  $B_c$  meson decay leads to the life time estimate

$$\tau_{B_c} \sim 5 \cdot 10^{-13} \text{ s}$$

with the following approximate sharing of branching fractions: 37 %, 45 % and 18 % correspond to the  $c$ -spectator mechanism,  $\bar{b}$ -spectator one and the annihilation, respectively.

The uncertainty in the estimation of the  $B_c$  meson life time is generally related to the choice of quark masses. The mass of  $b$ -quark  $m_b = 4.9 \text{ GeV}$  is chosen so that one can describe the  $B$  meson life time in the framework of the spectator mechanism. Note, that the differences of the life times for the charged and neutral  $B$  mesons are unessential and, hence, the given choice of the mass is quite certain. For the  $D$  mesons, this is not the case, since the life times of  $D^+$  and  $D^0$  mesons differ twice.

Nevertheless, there is another way, that is more reliable for the extraction of the  $c$ -quark mass, this is the consideration of the semileptonic decays of  $D$  mesons. Indeed, the value  $m_c = 1.5 \text{ GeV}$  in the spectator mechanism well describes the decays  $D^+ \rightarrow \bar{K}^0 e^+ \nu$  and  $D^0 \rightarrow \bar{K}^- e^+ \nu$ , whose widths approximately are equal to each other. Note, at any other reasonable choice of  $m_c$  (from the total widths, say), the error in the  $B_c$  meson life time will be not large, since the summed branching ratio of the  $B_c$  meson decays due to the  $c$ -quark decays is about 40 %.

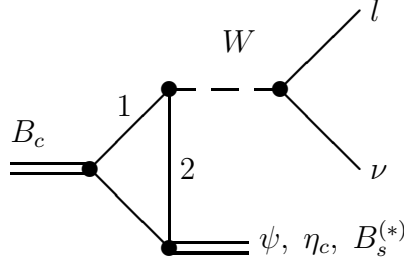


Fig. 5. The diagram of the semileptonic decay of  $B_c$  meson

## 3.2. Semileptonic decays of $B_c$ mesons

### 3.2.1. Quark models

In the framework of quark models, the semileptonic decays of  $B_c$  mesons are considered in refs.[30,32,34]. The detailed study of the  $B_c$  meson decays in the quark model of the relativistic oscillator WSB [71] has been first made in ref.[32] and further in ref.[34], where the quark model ISGW [70] has also been used. The covariant description approach, early offered for the composed quarkonium model, is developed in ref.[30].

Consider the amplitude of the  $B_c^+ \rightarrow M_X e^+ \nu_e$  transition with the weak decay of the quark 1 into the quark 2 (Figure 5)

$$A = \frac{G_F}{\sqrt{2}} V_{12} l_\mu H^\mu, \quad (124)$$

where  $G_F$  is the Fermi constant,  $V_{12}$  is the element of the Kobayashi–Maskawa matrix. The lepton current  $l_\mu$  is determined by the expression

$$l_\mu = \bar{e}(q_1)\gamma_\mu(1 - \gamma_5)\nu(q_2), \quad (125)$$

where  $q_1$  and  $q_2$  are the lepton and neutrino momenta, respectively,  $(q_1 + q_2)^2 = t$ .

The  $H_\mu$  quantity in eq.(124) is the matrix element of the hadronic current  $J_\mu$

$$J_\mu = V_\mu - A_\mu = \bar{Q}_1\gamma_\mu(1 - \gamma_5)Q_2. \quad (126)$$

The matrix element for the  $B_c$  meson decay into the pseudoscalar state  $P$  can be written down in the form

$$\langle B_c(p)|A_\mu|P(k)\rangle = F_+(t)(p+k)_\mu + F_-(t)(p-k)_\mu, \quad (127)$$

and for the transition into the vector meson  $V$  with the mass  $M_V$  and the polarization  $\lambda$ , one has

$$\begin{aligned} \langle B_c(p)|J_\mu|V(k, \lambda)\rangle &= -(M + M_V)A_1(t) \epsilon_\mu^{(\lambda)} \\ &+ \frac{A_2(t)}{M + M_V} (\epsilon^{(\lambda)}p)_\mu (p + k)_\mu \end{aligned}$$

$$\begin{aligned}
& + \frac{A_3(t)}{M + M_V} (\epsilon^{(\lambda)} p)_\mu (p - k)_\mu \\
& + i \frac{2V(t)}{M + M_V} \epsilon_{\mu\nu\alpha\beta} \epsilon_{(\lambda)}^\nu p^\alpha k^\beta.
\end{aligned} \tag{128}$$

Relations (127), (128) define the form factors of the  $B_c^+ \rightarrow M_X e^+ \nu_e$  transitions, so, for the massless leptons,  $F_-$  and  $A_3$  do not give contributions into matrix element (124).

In the Covariant model of the quarkonium (see Appendix I), one can easily find

$$F_+(t) = \frac{1}{2} (m_1 + m_2) \sqrt{\frac{M_P}{M}} \frac{1}{m_2} \xi_P(t), \tag{129}$$

$$F_-(t) = -\frac{1}{2} (m_1 - m_2 + 2m_{\text{sp}}) \sqrt{\frac{M_P}{M}} \frac{1}{m_2} \xi_P(t), \tag{130}$$

Here  $m_{\text{sp}}$  is the mass of the spectator quark (see Figure 5), and the function  $\xi(t)$  has the form

$$\begin{aligned}
\xi_X(t) = & \left( \frac{2\omega\omega_X}{\omega^2 + \omega_X^2} \right)^{3/2} \exp \left\{ -\frac{m_{\text{sp}}^2}{\omega^2 + \omega_X^2} \frac{t_{\text{max}} - t}{MM_X} \right. \\
& \left. \left( 1 + \frac{\omega^2}{\omega_X^2} \left( 1 - \frac{t_{\text{max}} - t}{4MM_X} \right) \right) \right\},
\end{aligned} \tag{131}$$

where  $M_X$  is the recoil meson mass,  $\omega_X$  is the wave function parameter (I.6)-(I.8) for the recoil meson.

$$t_{\text{max}} = (M - M_X)^2, \tag{132}$$

$t_{\text{max}}$  is the maximal square of the lepton pair mass.

For the vector state one has  $M_V = M_X$ , and we obtain

$$V(t) = \frac{1}{2} (M + M_V) \sqrt{\frac{M_V}{M}} \frac{1}{m_2} \xi_V(t), \tag{133}$$

$$A_1(t) = \frac{1}{2} \frac{M^2 + M_V^2 - t + 2M(m_2 - m_{\text{sp}})}{M + M_V} \sqrt{\frac{M_V}{M}} \frac{1}{m_2} \xi_V(t), \tag{134}$$

$$A_2(t) = \frac{1}{2} (M + M_V) \left( 1 - \frac{2m_{\text{sp}}}{M} \right) \sqrt{\frac{M_V}{M}} \frac{1}{m_2} \xi_V(t), \tag{135}$$

$$A_3(t) = -\frac{1}{2} (M + M_V) \left( 1 + \frac{2m_{\text{sp}}}{M} \right) \sqrt{\frac{M_V}{M}} \frac{1}{m_2} \xi_V(t). \tag{136}$$

It is interesting to note, that the exponential form of the form factor dependence on  $t$  (131) can be quite accurately represented, in the admissible kinematical region, by the form, corresponding to the model of the meson dominance

$$\xi_k(t) = \xi_k(0) \frac{1}{1 - t/m_k^2}, \tag{137}$$

where  $m_k$  are presented in Table 16. One can see from eqs.(130)–(136), that the form factors (excepting  $A_1(t)$ ) are also representable in form (137), and the degeneration takes place

$$m_V = m_{A_2} = m_{A_3} \approx m_+, \tag{138}$$

Table 16. The  $m_k$  parameters (in GeV) for the  $\xi(t)$  representation in eq.(137)

	$B_c^+ \rightarrow \psi e^+ \nu_e$	$B_c^+ \rightarrow \eta_c e^+ \nu_e$	$B_c^+ \rightarrow B_s e^+ \nu_e$	$B_c^+ \rightarrow B_s^* e^+ \nu_e$
$m_k$ , GeV	6.3	6.45	1.9	1.95

if  $\omega_P \approx \omega_V$ ,  $M_P \approx M_V$ .

As for the  $A_1(t)$  form factor, it can be represented in the form

$$A_1(t) = \varphi(t) \frac{1}{1 - t/m_{A_1}^2} = a_1 + \frac{A_1'(0)}{1 - t/m_{A_1}^2}, \quad (139)$$

where

$$m_{A_1} = m_V, \quad (140)$$

$$A_1'(0) = \frac{1}{2} \frac{M^2 + M_V^2 - m_{A_1}^2 + 2M(m_2 - m_{\text{sp}})}{M + M_V} \sqrt{\frac{M_V}{M}} \frac{1}{m_2} \xi_V(0), \quad (141)$$

$$a_1 = A_1(0) - A_1'(0). \quad (142)$$

The values of the transition form factors at zero mass of the lepton pair are shown in Table 17. The numerical calculations in ref.[30] have been performed for the mass values

$$m_b = 4.9 \text{ GeV}, \quad m_c = 1.6 \text{ GeV}, \quad m_s = 0.5 - 0.55 \text{ GeV}. \quad (143)$$

The element of the Kobayashi–Maskawa matrix has been taken equal to  $V_{bc} = 0.046$ .

The  $f_{B_c}$  constant in ref.[30] has been varied in the limits

$$f_{B_c} = 360 - 570 \text{ MeV}, \quad (144)$$

where the upper limit corresponds to the values, obtained in the nonrelativistic potential model [34,52], in the parton model [75], and in the QCD sum rules [36,76]. The lower limit corresponds to the value, obtained in the Borel sum rules of QCD [36,76]. Note, that for the  $B_c^+ \rightarrow \psi e^+ \nu_e$  decay, the result weakly depends on the  $f_{B_c}$  choice (3 %).

One has also supposed

$$f_{\eta_c} = f_{\psi}, \quad (145)$$

Table 17. The form factors of the semileptonic  $B_c$  decays

mode	$F_+(0)$	$A_1(0)$	$A_1'(0)$	$A_2(0)$	$V(0)$
$B_c^+ \rightarrow \psi e^+ \nu_e$	–	0.73	0.14	0.67	1.31
$B_c^+ \rightarrow \eta_c e^+ \nu_e$	0.89	–	–	–	–
$B_c^+ \rightarrow B_s e^+ \nu_e$	0.61	–	–	–	–
$B_c^+ \rightarrow B_s^* e^+ \nu_e$	–	0.52	–	–2.79	5.03

and one has varied the values

$$f_{B_S} = 100 - 110 \text{ MeV} , \quad (146)$$

$$f_{B_S^*} = 160 - 180 \text{ MeV} , \quad (147)$$

that does not contradict the estimates, made in the QCD sum rules [12].

Note, that for the semileptonic  $B_c$  meson decays  $B_c^+ \rightarrow M_X e^+ \nu_e$ , where  $M_X$  is the recoil meson, the explicit covariance of the model allows one to take into account corrections on the velocity of the  $M_X$  meson. As for corrections due to the quark motion inside the meson, they are taken into account due to the difference between the constituent and current masses of the quark.

In the ISGW model for the meson state vector, one uses the following nonrelativistic expression

$$\begin{aligned} |X(\mathbf{p}_X; s_x)\rangle &= \sqrt{2m_x} \int d^3p \sum C_{m_L m_S}^{s_x L S} \phi_X(\mathbf{p})_{L m_L} \chi_{s\bar{s}}^{S m_S} \\ &|q\left(\frac{m_q}{m_x} \mathbf{p}_X + \mathbf{p}, s\right) \bar{q}\left(\frac{m_{\bar{q}}}{m_x} \mathbf{p}_X - \mathbf{p}, \bar{s}\right)\rangle. \end{aligned} \quad (148)$$

where  $\chi_{s\bar{s}}^{S m_S}$  is the spin wave function of the quark-antiquark pair in the state with the total spin  $S$  and the spin projection  $m_S$ ,  $C_{m_L m_S}^{s_x L S}$  is the coupling between the orbital momentum  $L$  and the total spin  $S$  of the system with the total momentum  $s_x$ ;  $\phi_X(\mathbf{p})_{L m_L}$  is the corresponding nonrelativistic wave function,  $\mathbf{p}_X$  is the meson momentum,  $\mathbf{p}$  is the relative momentum of quarks. In the considered model, the meson mass is equal to the sum of quark masses in the approximation of infinitely narrow wave package, only.

As the probe functions, the nonrelativistic oscillator wave functions have been chosen

$$\begin{aligned} \Psi^{1S} &= \frac{\beta_s^{3/2}}{\pi^{3/4}} \exp\left(-\frac{\beta_s^2 r^2}{2}\right), \\ \Psi_{11}^{1P} &= -\frac{\beta_P^{5/2}}{\pi^{3/4}} r \exp\left(-\frac{\beta_P^2 r^2}{2}\right), \\ \Psi^{2S} &= \left(\frac{2}{3}\right)^{1/2} \frac{\beta_S^{7/2}}{\pi^{3/4}} \left(r^2 - \frac{3}{2}\beta_S^{-2}\right) \exp\left(-\frac{\beta_S^2 r^2}{2}\right). \end{aligned}$$

The  $\beta$  parameters have been determined by the variational principle and the Cornell potential [5].

In the WSB model, the mesons are considered as a relativistic bound state of a quark  $q_1$  and an antiquark  $\bar{q}_2$  in the system of infinitely large momentum [71]:

$$\begin{aligned} |P, m, j, j_z\rangle &= \sqrt{2}(2\pi)^{3/2} \sum_{s_1, s_2} \int d^3p_1 d^3p_2 \delta^3(\mathbf{p} - \mathbf{p}_1 - \mathbf{p}_2) \\ &L_m^{j, j_z}(\mathbf{p}_{1t}, x, s_1, s_2) a_1^{s_1+}(\mathbf{p}_1) b_2^{s_2+}(\mathbf{p}_2) |0\rangle, \end{aligned}$$

where  $P_\mu = (P_0, 0, 0, P)$ , and at  $P \rightarrow \infty$ ,  $x = p_{1z}/p$  corresponds to the momentum fraction, carried out by the nonspectator quark,  $p_{1t}$  is the transverse momentum.

For the orbital part of wave function, the solution of the relativistic oscillator is used

$$L_m(\mathbf{p}_t, x) = N_m \sqrt{x(1-x)} \exp\left(-\frac{\mathbf{p}_t^2}{2\omega^2}\right) \exp\left[-\frac{m^2}{2\omega^2}\left(x - \frac{1}{2} - \frac{m_{q_1}^2 - m_{q_2}^2}{2m^2}\right)^2\right]. \quad (149)$$

In the both models, the calculation of hadronic matrix elements  $\langle B_c(p) | J_\mu | X(k) \rangle$  comes to the calculation of the matrix elements of the quark currents between the quark states and the overlapping the corresponding wave functions.

In the potential models, the bound state of two particles is described by the wave function with the argument, being the relative momentum of the particle motion in the meson system of the mass centre. However, in the case of the decays with large recoil momenta, one can not chose the system, where the both mesons (the initial one and the decay product) would be at rest, so that one has a kinematical uncertainty in the form factor values.

For instance, in the ISGW model the form factor dependence on the invariant mass of lepton pair  $t$  is determined by the function  $\xi(t)$ :

$$\xi_{\text{ISGW}}(t) = \left(\frac{2\beta\beta_1}{\beta^2 + \beta_1^2}\right)^{3/2} \exp\left(-\frac{m_{\text{sp}}^2}{2\tilde{M}\tilde{M}_1} \frac{t_{\text{max}} - t}{k^2(\beta^2 + \beta_1^2)}\right); \quad (150)$$

where  $\beta$  and  $\beta_1$  are the parameters of wave functions for the initial and final mesons,  $m_{\text{sp}}$  is the spectator quark mass,  $\tilde{M}$  and  $\tilde{M}_1$  are the model parameters (the masses of the initial and final "mock"-mesons) [70]. The  $k$  parameter in eq.(150) is introduced synthetically for the correct description of the electromagnetic form factor of  $\pi$  meson ( $k = 0.7$ ). So, the authors of ref.[70] related this factor with possible relativistic corrections at large recoil momenta.

Recently in ref.[83], the model for the description of the heavy quarkonium decays has been offered. In this model, the required behaviour of form factors (at  $k = 0.7$ ) is automatical with no introduction of additional parameters. In contrast to the above mentioned approaches (the Covariant quark model and ISGW model), the nonrelativistic approximation is performed for the hadronic matrix element as a whole, but it is not performed separately for the wave functions of the initial and final states, only. At small recoil momenta, this formalism practically repeats the ISGW model, but at large momenta, there are some differences in the structure of the spin part of the wave function and the argument of the wave function of the final meson. So, the latter change is the most important and it leads to the difference in the form factor dependence on  $t$  [84].

The transition form factors in the ISGW model depend on  $\beta_{B_c}$  and  $\beta_{B_S}$ . For its values,  $\beta_{B_c} = 0.82$  and  $\beta_{B_S} = 0.51$  are obtained from the variational principle. Since the considered model is the nonrelativistic approximation, the form factors are the most accurately predicted at  $q^2 = q_{\text{max}}^2 = (M_{B_c} - M_X)^2$  (at the maximal value of the lepton pair invariant mass).

One can calculate the form factors in the region of low  $q^2$  values in two different ways: by the use of the exponential dependence on  $q^2$  as in ISGW or in the pole model of meson dominance. The results for the decay widths, calculated in these ways, are presented in Table 21. The additional parameter in the ISGW model is  $k = 1$  (150).



The results, obtained in ref.[83], is also presented in the same Table. In the constituent quark model, the exponential dependence of the form factors can be represented in the pole form. As one can see from Table 21, in the ISGW model for the decays, where the  $c$ -quark is the spectator, the exponential dependence and the pole model give the different results.

In the WSB model, the form factor values at  $q^2 = 0$  are predicted dependently of the  $\omega$  parameter (see eq.(149)), that corresponds to the average transverse momentum of quarks inside the meson. In ref.[34] the  $\omega$  values were equal to the average  $p_t^2$  values, estimated in the ISGW model ( $\omega_X \approx \beta_X$ ). Note, that the  $\omega$  parameter is external for the WSB model.

The results of the mentioned approaches are presented in Table 21.

Note, that the relative yield of the pseudoscalar states in respect to the vector states is much greater in ref. [83], where  $\Gamma^*/\Gamma \approx 2$  in comparison with  $\Gamma^*/\Gamma \approx 3-4$  in the ISGW model. This leads to that, for example, the exclusive decay modes  $B_c^+ \rightarrow \psi(\eta_c)e^+\nu_e$  practically saturate the  $b \rightarrow ce\nu$  transition. This feature is analogous to the consideration of the  $B \rightarrow D^{(*)}e\nu$  decay, that also saturates free  $b$ -quark decay. The decays into the excited states and manyparticle modes are suppressed.

As one can see, these three models for the decays with the spectator  $b$ -quark, give the close values

$$\Gamma(B_c \rightarrow B_s + e + \nu) + \Gamma(B_c \rightarrow B_s^* + e + \nu) = (60 \pm 7) \cdot 10^{-6} \text{ eV}.$$

Note also, that in the case of the heavy quarkonium  $B_c$ , the application of the non-relativistic wave function instead of the wave function of the relativistic oscillator in the meson of the WSB model, seems to be more acceptable. This circumstance and uncertainty in  $\omega$ , maybe, explain, why the WSB model gives the underestimated value for the width of the  $B_c^+ \rightarrow J/\psi + e + \nu$  decay.

### 3.2.2. $B_c^+ \rightarrow J/\Psi(\eta_c)e^+\nu$ decay in QCD sum rules

The most suitable for the registration modes of the  $B_c$  decays are the semileptonic or hadronic transitions with the  $J/\psi$  particle in the final state. But in the QCD sum rules (SR) [30,36,35] and in the quark models, one found different results for both the widths of the corresponding decays and the form factors of the transitions, although in the framework of the separate approach, the calculations, performed in different ways, coincided with each other. Recently in ref. [31], one has shown that the existing discrepancy can be cancelled by means of account for the higher QCD corrections in SR.

The widths of the semileptonic  $B_c$  decays are defined, in general, by the form factors  $F_+$ ,  $V$ ,  $A_1$  and  $A_2$  (see eqs.(127), (128)). Following the notation of ref.[31], redefine the form factors (127), (128) in the way

$$f_+ = F_+, \quad F_0^A = (M_{B_c} + M_V)A_1, \\ F_+^A = -\frac{A_2}{M_{B_c} + M_V}, \quad F_V = \frac{V}{M_{B_c} + M_V}.$$

For the calculation of these form factors in the QCD SR, let us consider the three-point functions

$$\begin{aligned}\Pi_\mu(p_1, p_2, q^2) &= i^2 \int dx dy \exp\{i(p_2x - p_1y)\} \\ &\quad \langle 0|T\{\bar{c}(x)\gamma_5 c(x), V_\mu(0), \bar{b}(y)\gamma_5 c(y)\}|0\rangle, \end{aligned} \quad (151)$$

$$\begin{aligned}\Pi_{\mu\nu}^{V,A}(p_1, p_2, q^2) &= i^2 \int dx dy \exp\{i(p_2x - p_1y)\} \\ &\quad \langle 0|T\{\bar{c}(x)\gamma_\nu c(x), J_\mu^{V,A}(0), \bar{b}(y)\gamma_5 c(y)\}|0\rangle, \end{aligned} \quad (152)$$

Introduce the Lorentz structures in the correlators

$$\Pi_\mu = \Pi_+(p_1 + p_2)_\mu + \Pi_- q_\mu, \quad (153)$$

$$\Pi_{\mu\nu}^V = i\Pi_V \epsilon_{\mu\nu\alpha\beta} p_2^\alpha p_1^\beta, \quad (154)$$

$$\Pi_{\mu\nu}^A = i\Pi_0^A g_{\mu\nu} + \Pi_1^A p_2^\mu p_1^\nu + \Pi_2^A p_1^\mu p_2^\nu + \Pi_3^A p_2^\mu p_2^\nu + \Pi_4^A p_1^\mu p_2^\nu. \quad (155)$$

The form factors  $f_+$ ,  $F_V$ ,  $F_0^A$  and  $F_+^A$  are determined by the amplitudes  $\Pi_+$ ,  $\Pi_V$ ,  $\Pi_0^A$  and  $\Pi_+^A = \frac{1}{2}(\Pi_1 + \Pi_2)$ , respectively. For the amplitudes, one can write down the double dispersion relation

$$\Pi_i(p_1^2, p_2^2, q^2) = -\frac{1}{(2\pi)^2} \int \frac{\rho_i(s_1, s_2, Q^2)}{(s_1 - p_1^2)(s_2 - p_2^2)} ds_1 ds_2, \quad (156)$$

where  $Q^2 = -q^2 > 0$ .

The integration region in eq.(156) is determined by the condition

$$-1 < \frac{2s_1 s_2 + (s_1 + s_2 - q^2)(m_b^2 - m_c^2 - s_1)}{\lambda^{1/2}(s_1, s_2, q^2)\lambda^{1/2}(m_c^2, s_1, m_b^2)} < 1, \quad (157)$$

where  $\lambda(x_1, x_2, x_3) = (x_1 + x_2 - x_3)^2 - 4x_1 x_2$ .

In accordance with the general ideology of the QCD sum rules [11], the right hand, theoretical, side of eq.(156) can be calculated at large euclidian  $p_1^2$  and  $p_2^2$  values by the use of the operator product expansion (OPE). The perturbative parts of the corresponding spectral densities (the unit operator in OPE) to the one loop approximation are presented in Appendix II. Since we consider the systems, composed of the heavy quarks, one can neglect the power corrections [36].

Consider the physical part of SR. As has been already mentioned in the consideration of the axial constant of  $B_c$ , there are two approaches. In the first one, one assumes that the physical part includes the contribution of the lowest mesons and the continuum, that is approximated by the perturbative part of the spectral function from some threshold values  $s_0^1$  and  $s_0^2$  [35,36]. The contribution of the higher excitations and the continuum is suppressed due to the Borel transformations over two variables ( $-p_1^2$ ) and ( $-p_2^2$ ). The numerical results, obtained in such way of ref.[35,36], are presented below.

In the second way, one saturates the spectral density by infinite number of narrow resonances [30], so that

$$\begin{aligned}
\rho_+(s_1, s_2, Q^2) &= (2\pi)^2 \sum_{i,j=1}^{\infty} f_{B_c}^i \frac{M_{B_c}^{i^2}}{m_b + m_c} f_{\eta_c}^j \frac{M_{\eta_c}^{j^2}}{2m_c} f_+^{ij}(Q^2) \\
&\quad \delta(s_1 - M_{B_c}^{i^2}) \delta(s_2 - M_{\eta_c}^{j^2}) \\
\rho_V(s_1, s_2, Q^2) &= 2(2\pi)^2 \sum_{i,j=1}^{\infty} f_{B_c}^i \frac{M_{B_c}^{i^2}}{m_b + m_c} \frac{M_{\psi}^{j^2}}{g_{\psi}} F_V^{ij}(Q^2) \\
&\quad \delta(s_1 - M_{B_c}^{i^2}) \delta(s_2 - M_{\psi}^{j^2}) \\
\rho_{0,+}^A(s_1, s_2, Q^2) &= (2\pi)^2 \sum_{i,j=1}^{\infty} f_{B_c}^i \frac{M_{B_c}^{i^2}}{m_b + m_c} \frac{M_{\psi}^{j^2}}{g_{\psi}} F_{0,+}^{ij}(Q^2) \\
&\quad \delta(s_1 - M_{B_c}^{i^2}) \delta(s_2 - M_{\psi}^{j^2}) \tag{158}
\end{aligned}$$

Substituting the expressions for the spectral densities (158)–(158) in the dispersion relations for correlators (156) to the one hand, and their perturbative values to the other hand, one gets the corresponding sum rules.

Applying the procedure, described in Appendix III, for the both sums over the resonances, one obtains for the form factors under consideration

$$f_+^{kl}(Q^2) = \frac{8m_c(m_b + m_c)}{M_{B_c}^k M_{\eta_c}^l f_{B_c}^k f_{\eta_c}^l} \frac{dM_{B_c}^k}{dk} \frac{dM_{\eta_c}^l}{dl} \frac{1}{(2\pi)^2} \rho_+(M_{B_c}^{k^2}, M_{\eta_c}^{l^2}, Q^2), \tag{159}$$

$$\begin{aligned}
F_V^{kl}(Q^2) &= \frac{2(m_b + m_c)g_{\psi}^l}{M_{B_c}^k M_{\psi}^l f_{B_c}^k} \frac{dM_{B_c}^k}{dk} \frac{dM_{\psi}^l}{dl} \frac{1}{(2\pi)^2} \rho_V(M_{B_c}^{k^2}, M_{\psi}^{l^2}, Q^2), \\
F_{0,+}^{kl}(Q^2) &= \frac{4(m_b + m_c)g_{\psi}^l}{M_{B_c}^k M_{\psi}^l f_{B_c}^k} \frac{dM_{B_c}^k}{dk} \frac{dM_{\psi}^l}{dl} \frac{1}{(2\pi)^2} \rho_{0,+}(M_{B_c}^{k^2}, M_{\psi}^{l^2}, Q^2). \tag{160}
\end{aligned}$$

Choosing the  $k$  and  $l$  values, one can extract the transitions between the given resonances. At  $k = l = 1$ , one gets the required form factors for the  $B_c^+ \rightarrow J/\psi(\eta_c)e^+ \nu$  decays.

Thus, we use the phenomenological parameters  $dM_k/dk$  instead of the additional parameters such as the continuum thresholds. As has been mentioned, the former is, in a sense, the density of the quarkonium states with the given quantum numbers. One can quite accurately calculate these factors. The masses of the radial excitations of  $\psi$  are known experimentally [15], and for the  $B_c$  and  $\eta_c$  systems, composed of the heavy quarks, one can use the predictions of the potential models [5–10,52,57–66].

The  $dM_k/dk$  values at  $k = 1$  for the systems under the consideration, are presented in Table 18.

Let us chose the following values of parameters  $f_{B_c} = 360$  MeV,  $f_{\eta_c} = 330$  MeV, [36,76],  $m_b = 4.6 \pm 0.1$  GeV,  $m_c = 1.4 \pm 0.05$  GeV,  $g_{J/\psi} = 8.1$  (from the data on  $\Gamma(J/\psi \rightarrow e^+ e^-)$ ). For the axial constant, we chose 360 MeV [30] instead of 460, to compare the form factor values with the results of ref.[36]. The  $B_c$  meson mass will be varied from 6.245 to 6.284 GeV (the data of the different potential models). Note, that at such choice of

Table 18. The derivatives  $dM_k/dk$  (in GeV) for the lowest states

Quarkonium	$B_c$	$J/\psi$	$\eta_c$
$dM_k/dk _{k=1}$	0.75	0.75	0.76

the parameters, we do not go out from the integration region (157). In ref.[36] one used  $M_{B_c} = 6.35$  GeV. The form factors values, obtained in ref.[30,36,35] at  $Q^2 = 0$ , are show in Table 19. The deviation from the central values in Table 19 corresponds to the variation of the quark and  $B_c$  meson masses within the limits, mentioned above (for [30]). As in the case of the potential models, the SR predictions agree with each other.

In ref.[30], the form factors have the following pole behaviour

$$F_i(Q^2) = \frac{F_i(0)}{1 + Q^2/m_{\text{pole}}^2} \phi_i(Q^2), \quad (161)$$

where  $m_{\text{pole}} = 6.3\text{--}6.4$  GeV, and  $\phi_i(Q^2) = 1 + a_i Q^2$ . The representation of  $f_+$ ,  $F_V$ ,  $F_0^A$  and  $F_+^A$  by the form (159)–(160) gives the following  $a_i$  values, which are quite low and equal to  $-0.025$ ,  $-0.007$ ,  $-0.012$ ,  $-0.02$  respectively. The behaviour, considered above, does not practically differ from the ordinary pole behaviour [30], where  $a_i = 0$ . The results for the transition widths are presented in Table 20.

As one can see from Tables 19 and 20, the results of the Borel SR are, in general, in a good agreement with the results of the considered approach, within the model errors. The widths, obtained in ref.[35], are greater, than in ref.[30,36], since in ref.[35], the  $q^2$ -dependence of the transition form factors strongly differs from the behaviour, expected in the meson dominance model.

The deviation from the quark models is related, from our point of view, with that in the calculations of the transition form factors in the QCD sum rules, one has to account

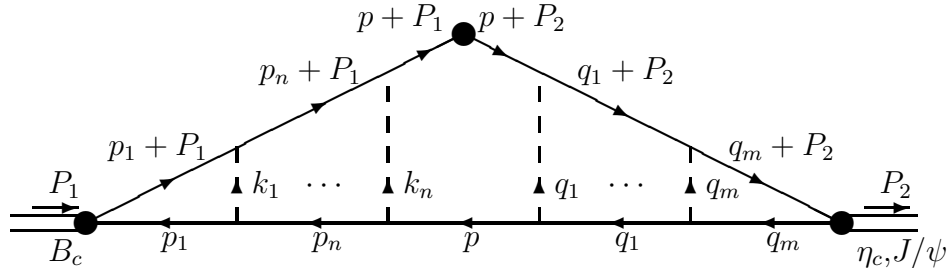


Fig. 6. The Coulomb corrections in the semileptonic  $B_c$  meson decay

Table 19. The form factors of the  $B_c \rightarrow J/\psi(\eta_c)e\nu$  transitions at  $Q^2 = 0$

$f_+(0)$	$F_V(0)$ GeV <sup>-1</sup>	$F_+^A(0)$ GeV <sup>-1</sup>	$F_0^A(0)$ GeV	Reference
$0.23 \pm 0.01$	$0.035 \pm 0.03$	$-0.024 \pm 0.002$	$2 \pm 0.2$	[30]
$0.2 \pm 0.02$	$0.04 \pm 0.01$	$-0.03 \pm 0.01$	$2.5 \pm 0.3$	[36]
$0.55 \pm 0.1$	$0.048 \pm 0.007$	$-0.030 \pm 0.003$	$3.0 \pm 0.5$	[35]

for  $\alpha_S/v$ -corrections, where  $v$  is the relative velocity of the quarks inside the meson. For the heavy quarkonia, where the velocity of the quark motion is small, such corrections, corresponding to the Coulomb-like interactions (Figure 6), can play an essential role [31].

Indeed, the spectral densities  $\rho_i(s_1, s_2, Q^2)$ , determining the  $B_c$  decay form factors, are calculated near the threshold  $s_1 = M_{B_c}^2$ ,  $s_2 = M_{\eta_c, \psi}^2$ . When the recoil meson momentum is small, the calculation of the ladder diagrams in the formalism of the nonrelativistic quantum mechanics (see [17], Figure 6), leads to the finite renormalization of  $\rho$ , so that

$$\bar{\rho}_i(s_1, s_2, Q_{\max}^2) = C \rho_i(s_1, s_2, Q_{\max}^2), \quad (162)$$

where the factor  $C$  has the form

$$C = \left| \frac{\Psi_{B_c}^C(0)\Psi_{\eta_c, \psi}^C(0)}{\Psi_{B_c}^{free}(0)\Psi_{\eta_c, \psi}^{free}(0)} \right|, \quad (163)$$

and  $\Psi^{C, free}(0)$  are the Coulomb and free wave functions of quarks, so that

$$\left| \frac{\Psi^C(0)}{\Psi^{free}(0)} \right|^2 = \frac{4\pi\alpha_S}{3v} [1 - \exp(-\frac{4\pi\alpha_S}{3v})]^{-1}. \quad (164)$$

For the two-point quark correlators, determining the decay constants  $f$  of the heavy quarkonia  $\psi$ ,  $\Upsilon$ ,  $B_c$ , the account for factor (163) led to the essential enhancement of  $f$ , so that one observed the agreement with the experimental data on  $f_\psi$  and  $f_\Upsilon$ . Note, that the expansion in (164) over  $\alpha_S/v \rightarrow 0$  exactly leads to the dominant term, appearing in account for the one-loop  $\alpha_S$ -corrections to the two-point correlator of currents. Moreover, these corrections have been taken into account in the evaluation of  $f$  for the three-point

Table 20.

The widths (in units  $10^{-6}$  eV) of the semileptonic  $B_c$  decays in the QCD sum rules with no account of  $\alpha_S/v$ -corrections

mode	[30]	[36]	[35]
$B_c^+ \rightarrow J/\psi e^+ \nu$	4.6	7	10.5
$B_c^+ \rightarrow \eta_c e^+ \nu$	1.4	1	9.

correlators, but one did not take into account the loop corrections in the determination of the three-point spectral densities.

One would, in a logics, not to account for the  $\alpha_S$ -corrections in the  $f$  evaluation as well as in the  $\rho$  determination, or one would take into account these corrections in both cases. As one can see, for example, from (159), one can write down

$$f_+^{kl}(Q^2) = \frac{8m_c(m_b + m_c)C}{M_{B_c}M_{\eta_c}f_{B_c}^{(0)}f_{\eta_c}^{(0)}C_{B_c}^{1/2}C_{\eta_c}^{1/2}} \frac{dM_{B_c}^k}{dk} \frac{dM_{\eta_c}^l}{dl} \frac{1}{(2\pi)^2} \rho_+^{(0)}(M_{B_c}^k, M_{\eta_c}^l, Q^2), \quad (165)$$

where the  $f^{(0)}$  and  $\rho^{(0)}$  values are calculated with no account for the  $\alpha_S$ -corrections, and the factors  $C$  appear due to the Coulomb-like corrections and defined in eqs.(163), (164). It is evident, that

$$\frac{C}{C_{B_c}^{1/2}C_{\eta_c}^{1/2}} = 1. \quad (166)$$

Thus, in the determination of the transition form factors, we can use the "bare"  $f$  and  $\rho$  quantities, calculated in zero approximation over  $\alpha_S$  [85], instead of that, say, was done in ref. [36], where  $\rho^{(0)}$  was used without the  $C$  factor and the  $f$  constants with the account for the  $\alpha_S$ -corrections, i.e. with the factors  $C_{B_c}$  and  $C_{\eta_c, \psi}$ , were instantaneously used.

As the result, one gets the following values for the form factors  $f_+$  and  $F_0^A$  [31]

$$f_+(0) = 0.85 \pm 0.15, \quad F_0^A = 6.5 \pm 1 \text{ GeV}.$$

For the corresponding widths, one has found [31]

$$\Gamma(B_c^+ \rightarrow \psi e^+ \nu) \approx 44 \cdot 10^{-6} \text{ eV}, \quad \Gamma(B_c^+ \rightarrow \eta_c e^+ \nu) \approx 15 \cdot 10^{-6} \text{ eV}.$$

Note, that we have neglected the contributions of the form factors  $F_V$  and  $F_+^A$  in the decay  $B_c \rightarrow J/\psi e \nu$ . This can result in the overestimation of the widths values up to 10–20 %. One can make the agreement between the obtained values of the widths and the results of the quark models (see Table 21) within the limits of the theoretical uncertainties of the used methods.

Comparing the results of the QCD SR and the quark models, one can accept as a central value of the  $B_c \rightarrow J/\psi e \nu$  decay width (with the accuracy about 40 %)

$$\Gamma(B_c \rightarrow J/\psi e \nu) \approx 40 \cdot 10^{-6} \text{ eV},$$

that corresponds to the branching fraction, equal to 3 %. Then the relative probability of the three lepton yield in the  $B_c$  decays, when two of them reconstruct  $J/\psi$ , equals

$$Br(B_c^+ \rightarrow (l^+ l^-)_{J/\psi} l'^+ \nu) \approx 8 \cdot 10^{-3},$$

where  $l, l'$  denotes  $e$  or  $\mu$ .

### 3.2.3. Approximate spin symmetry

In the bound state, the heavy quark virtualities are much less than their masses, i.e. the following kinematical expansion for the quark momentum  $p_Q$  is accessible

$$p_Q^\mu = m_Q \cdot v^\mu + k^\mu, \quad (167)$$

Table 21.

The partial widths (in  $10^{-6}$  eV) of the semileptonic  $B_c$  decays (ISGW1 and ISGW2 are the results of the ISGW model with the exponential dependence of the form factors and the pole model, respectively)

mode	ISGW1 [34]	ISGW2 [34]	WSB [34]	[30]	[83]
$B_c^+ \rightarrow \psi e^+ \nu_e$	38.5	53.1	21.8	37.3	34.4
$B_c^+ \rightarrow \eta_c e^+ \nu_e$	10.6	16.1	16.5	20.4	14.2
$B_c^+ \rightarrow D^0 e^+ \nu_e$	0.033	0.12	0.002	–	0.094
$B_c^+ \rightarrow D^{0*} e^+ \nu_e$	0.13	0.32	0.011	–	0.268
$B_c^+ \rightarrow \psi(2S) e^+ \nu_e$	–	–	–	–	1.45
$B_c^+ \rightarrow \eta'_c e^+ \nu_e$	–	–	–	–	0.727
$B_c^+ \rightarrow B_s e^+ \nu_e$	16.4	17.9	11.1	$16 \pm 4$	26.6
$B_c^+ \rightarrow B_s^* e^+ \nu_e$	40.9	46.3	43.7	$41 \pm 6$	44.0
$B_c^+ \rightarrow B_d e^+ \nu_e$	1.0	1.1	0.5	–	2.30
$B_c^+ \rightarrow B_d^* e^+ \nu_e$	2.5	3.0	2.9	–	3.32

so that

$$v \cdot k \approx 0, \quad |k^2| \ll m_Q^2. \quad (168)$$

Then in the system, where  $v = (1, \mathbf{0})$ , the heavy quark hamiltonian in a gluon field of an external source has the form

$$H = m_Q + V(\mathbf{r}) + \frac{\mathbf{k}^2}{2m_Q} + g \frac{\boldsymbol{\sigma} \cdot \mathbf{B}}{2m_Q} + O\left(\frac{1}{m_Q^2}\right), \quad (169)$$

so that in the limit  $\Lambda_{QCD} \ll m_Q$ , the spin-flavour symmetry EHQT [14] takes place for hadrons with a single heavy quark.

For the heavy quarkonium, one has purely phenomenologically, that the kinetic energy does practically not depend on their flavours, however, the value of the potential energy term  $V(\mathbf{r})$  is determined by the average distance between the heavy quarks. This distance depends on the quark masses, i.e. the flavours. Therefore, there is no flavour symmetry of the wave functions in the heavy quarkonium. However, the magnetic field of the heavy quark is determined by its motion velocity (as well as magnetic moment). The quark motion is nonrelativistic in the heavy quarkonium, so that

$$\mathbf{B} \sim O(\mathbf{v}) \sim O\left(\frac{1}{m_Q}\right). \quad (170)$$

From eqs.(169), (170) it follows, that the spin-dependent potential in the heavy quarkonium appears in the second order over the inverse heavy quark masses (see Section 2)

$$V_{SD} \sim O\left(\frac{1}{m_Q^2}\right). \quad (171)$$

Thus, in the leading approximation for the heavy quarkonium, one can neglect the spin-dependent forces in comparison with the kinetic energy and the nonrelativistic potential.

This means, that in this approximation, the quark spin is decoupled from the interaction with the gluons of low virtualities, therefore the masses of the  $nL_J$  quarkonium states are degenerated over  $J$ , and these states have the identical wave functions.

Thus, there is the approximate spin symmetry for the heavy quarks in the heavy quarkonium.

Further, let us consider the matrix element

$$M = \langle n^S L_J(Q\bar{Q}') | \Gamma | h \rangle, \quad (172)$$

where  $\Gamma$  is the operator of quark currents,  $h$  is a state. Then the spin symmetry means that the action of spin operators of the heavy quark is factorized, and the matrix element  $\bar{M}$ , obtained by the action of the quark  $Q$  spin (or by the antiquark  $\bar{Q}'$  spin)

$$S_\mu^Q = \frac{1}{4} \epsilon_{\mu\nu\alpha\beta} v_Q^\nu \sigma^{\alpha\beta}, \quad \sigma^{\alpha\beta} = \frac{i}{2} [\gamma^\alpha; \gamma^\beta], \quad (173)$$

is related with the matrix element  $M$  by the equation

$$\bar{M} = \langle n^S L_J(Q\bar{Q}') | S_\mu^Q \Gamma | h \rangle = \sum C_{SS'}^{JJ'} \langle n^{S'} L_{J'}(Q\bar{Q}') | \Gamma | h \rangle, \quad (174)$$

where  $\bar{M}$  is the sum of the matrix elements with  $J'$ , and  $C_{SS'}^{JJ'}$  are defined by the rules for the spin operator action.

For the semileptonic  $B_c^+ \rightarrow \eta_c(\psi) l^+ \nu$  decays, the spin symmetry is valid in the point of zero recoil of  $\eta_c(\psi)$ . Indeed, in this case the spectator  $c$ -quark and the  $\bar{c}$ -quark, produced in the weak decay of the  $\bar{b}$ -quark, are practically at rest in respect to each other, so binding into the state, they interact with low virtualities, characteristic for the heavy quarkonium. At a nonzero velocity of the  $\bar{c}$ -quark, it must exchange with the  $c$ -quark by a momentum, comparable with its mass, for to make the bound state, where their velocities are close. Thus, at the nonzero meson recoil, the gluons with high virtualities can shift the heavy quark spin, and the spin symmetry does already not take place.

At the zero recoil of the charmonium  $v_{B_c} = v_{\eta_c(\psi)}$ , in the covariant amplitude of the weak current, the nonzero contributions are given by  $A_1(t)$ ,  $F_\pm(t)$  at  $t = t_{max}$ , and the heavy quark spin symmetry means, that

$$(M_{B_c} + M_{\eta_c}) F_+ + (M_{B_c} - M_{\eta_c}) F_- = (M_{B_c} + M_\psi) A_1, \quad t = t_{max}, \quad M_{\eta_c} = M_\psi. \quad (175)$$

Thus, in the approximation of zero spin-dependent splitting of the heavy quarkonium, one derives the specific relation for the form factors of the semileptonic exclusive  $B_c$  decays into the charmonium.

Note now, that the covariant model, considered above, gives the semileptonic form factor values for the  $B_c$  decay into the charmonium, so that these quantities satisfy the symmetry relation (175). In contrast to the decays of the heavy hadrons with a single heavy quark, where the form factor normalization at zero recoil is fixed due to the flavour symmetry, the normalization of form factors for the weak semileptonic transitions between the heavy quarkonia is determined by the overlapping of their wave functions, which depend on the quarkonium model. For the oscillator wave functions in the considered potential model, we get

$$(M_{B_c} + M_\psi) A_1(t_{max}) = \sqrt{2M_{B_c} 2M_\psi} \xi(t_{max}), \quad (176)$$



where

$$\xi(t_{\max}) = \left( \frac{2\omega_{B_c}\omega_\psi}{\omega_{B_c}^2 + \omega_\psi^2} \right)^{3/2}. \quad (177)$$

In ref.[37] the factor  $\xi(t_{\max})$  was determined in the quarkonium model with the Coulomb potential, that is quite rough approximation.

Note further, that in the semileptonic  $B_c$  decay, the lepton pair kinematically has, in average, large invariant masses  $m(l^+\nu) \approx 1.9$  GeV, so that the  $A_1$  form factor contribution dominates, and in accordance with the meson dominance of the  $t$ -dependence of the form factors, relation (175), giving  $A_1(t_{\max})$ , determines, in a sense, the matrix element of the semileptonic  $B_c^+ \rightarrow \psi(\eta_c)l^+\nu$  decay. This feature can be used for the determination of the  $B_c$  meson mass from the  $\psi l^+$  mass spectrum as well as the element  $|V_{bc}|$  of the Kobayashi–Maskawa matrix.

### 3.3. Hadronic decays of $B_c$ mesons

Although the semileptonic  $B_c^+ \rightarrow J/\psi\mu^+(e^+)\nu_\mu(\nu_e)$  decays can serve as a good trigger for the  $B_c$  registration, the complete  $B_c$  reconstruction needs a large statistics because of the neutrino presence in the decay products. The direct measurement of the  $B_c$  meson mass is possible only in the hadronic exclusive decays. The preliminary estimates of some nonleptonic decay widths with the  $J/\psi$  particle in the final state were made in refs. [29,33,81] in the framework of the potential models. The hadronic decays were in details considered in refs.[32,34,83]. In ref.[34] for the calculations of the transition form factors, one used the WSB and ISGW models, mentioned above. In the calculations of the decay widths, the phase space reduction was accounted for the  $c$ -spectator decays (see Section 3.1), in contrast to some other calculations [33,81]. In the forthcoming consideration of the hadronic decays of the  $B_c$  meson, we will follow the results of the latter paper.

The effective four-fermion hamiltonian for the nonleptonic decays of the  $c$ - and  $b$ -quarks has the form [86]

$$\mathcal{H}_{\text{eff}}^c = \frac{G}{2\sqrt{2}} V_{uq_1} V_{cq_1}^* [C_+(\mu)O_+^c + C_-(\mu)O_-^c] + h.c. , \quad (178)$$

$$\mathcal{H}_{\text{eff}}^b = \frac{G}{2\sqrt{2}} V_{q_1b} V_{q_2q_3}^* [C_+(\mu)O_+^b + C_-(\mu)O_-^b] + h.c. , \quad (179)$$

where

$$O_\pm^c = (\bar{q}_{1\alpha}\gamma_\nu(1-\gamma_5)c_\beta)(\bar{u}_\gamma\gamma^\nu(1-\gamma_5)q_{2\delta})(\delta_{\alpha\beta}\delta_{\gamma\delta} \pm \delta_{\alpha\delta}\delta_{\gamma\beta}),$$

$$O_\pm^b = (\bar{q}_{1\alpha}\gamma_\nu(1-\gamma_5)b_\beta)(\bar{q}_{3\gamma}\gamma^\nu(1-\gamma_5)q_{2\delta})(\delta_{\alpha\beta}\delta_{\gamma\delta} \pm \delta_{\alpha\delta}\delta_{\gamma\beta}).$$

The factors  $C_\pm^{c,b}(\mu)$  account for the strong corrections to the corresponding four-fermion operators because of hard gluons [34,86].

The transition amplitudes must not depend on the subtraction point  $\mu$ , if one consistently calculates them in the perturbation theory, i.e. one constructs the corresponding functions of the initial and final hadronic states in the perturbation theory, in accordance to the operators.

The problem is complicated, when one deals with the factorization approximation, used for the calculation of the matrix elements. In this approximation, one assumes

that the current is proportional to a single stable or quasistable hadronic field, and one calculates its matrix element between the vacuum and the corresponding asymptotic hadronic state, so this procedure gives a value, proportional to the decay constant of hadron. After that, the amplitude of the weak decay is factorized and it is completely determined by the hadronic matrix element of an other current, that can be calculated by use of a model, as in the case of the semileptonic decays. In this approximation, the interaction in the final state is neglected.

Note, that the exact factorization takes place in the leading order of the  $1/N_c$  expansion [87]. In this approximation, one has to be careful in the choice of the subtraction point, since the matrix elements depend on  $\mu$ . (The dependence of coefficients for the four-fermion operators of effective hamiltonian on the subtraction point does not compensated by the functions of the initial and final states.) The most suitable choice is  $\mu \approx m_c$ , since the radius of the  $B_c$  meson is determined by the  $c$ -quark mass, and the transferred momenta in the decays are about  $m_c$  [34].

The anomalous dimensions of the  $O_+^c$  and  $O_-^c$  operators at  $\mu = m_c$  have the form

$$\gamma_{\pm} = -\frac{\alpha_S}{2\pi} \frac{3}{N_c} (1 \mp N_c) \quad (180)$$

In the leading logarithm approximation at  $\mu > m_c$ , one has [88]

$$\begin{aligned} C_+^c(\mu) &= \left( \frac{\alpha_S(M_W^2)}{\alpha_S(m_b^2)} \right)^{6/23} \left( \frac{\alpha_S(m_b^2)}{\alpha_S(\mu^2)} \right)^{6/25}, \\ C_-^c(\mu) &= [C_+^c(\mu)]^{-2}. \end{aligned} \quad (181)$$

at  $\alpha_S(m_c^2) = 0.27$ ,  $\alpha_S(m_b^2) = 0.19$ ,  $\alpha_S(M_W^2) = 0.11$ , one has the values  $C_+^c(m_c) = 0.80$  and  $C_-^c(m_c) = 1.57$ .

At  $\mu > m_b$ , the anomalous dimensions of the  $C_{\pm}^b$  operators are determined by eq.(180), but at  $m_c < \mu < m_b$  one finds

$$\gamma_{\pm} = -\frac{\alpha_S}{2\pi} \left[ 3 \frac{N_c^2 - 1}{4N_c} + \frac{3}{2N_c} (1 \mp N_c) \right], \quad (182)$$

$$C_+^b(\mu) = \left( \frac{\alpha_S(M_W^2)}{\alpha_S(m_b^2)} \right)^{6/23} \left( \frac{\alpha_S(m_b^2)}{\alpha_S(\mu^2)} \right)^{-3/25}, \quad (183)$$

$$C_-^b(\mu) = \left( \frac{\alpha_S(M_W^2)}{\alpha_S(m_b^2)} \right)^{-12/23} \left( \frac{\alpha_S(m_b^2)}{\alpha_S(\mu^2)} \right)^{-12/25}. \quad (184)$$

The numerical values are  $C_+^b(m_c) = 0.90$  and  $C_-^b(m_c) = 1.57$ .

For the nonleptonic inclusive spectator decays of  $B_c$  meson, the enhancement factor due to the "dressing" of the four-fermion operators by hard gluons, is equal to

$$3 \left[ C_+^2 \frac{N_c + 1}{2N_c} + C_-^2 \frac{N_c - 1}{2N_c} \right], \quad (185)$$

where 3 is the colour factor. For the annihilation decays, the corresponding factor equals

$$3 \left[ C_+ \frac{N_c + 1}{2N_c} + C_- \frac{N_c - 1}{2N_c} \right]^2. \quad (186)$$

The widths of the annihilation and inclusive spectator decays are presented in Table 15. As has been mentioned, the quark masses have the following values  $m_c = 1.5$  GeV,  $m_b = 4.9$  GeV and  $m_s = 0.15$  GeV, i.e. one takes the choice for the good description of both the semileptonic decays of  $B$  and  $D$  mesons and the total  $B$  meson width. The enhancement factors (185), (186) are calculated in the large  $N_c$  limit (this approximation gives a good description of  $B$  and  $D$  meson decays [71,89]). For the  $b$ -spectator decays, one accounts for the phase space reduction, in contrast to calculations in ref.[32].

The results of calculations for the widths of exclusive decays (here we consider the two-particle states) were performed in the models of WSB, ISGW and [83] and are presented in Tables 22 and 23. The Cabibbo nonsuppressed widths of  $b$ -spectator decays are shown in Table 22.

The  $a_1$  and  $a_2$  coefficients, accounting for the renormalization of the four-fermion operators, are defined in the following way

$$a_1 = C_+ \frac{N_c + 1}{2N_c} + C_- \frac{N_c - 1}{2N_c}, \quad (187)$$

$$a_2 = C_+ \frac{N_c + 1}{2N_c} - C_- \frac{N_c - 1}{2N_c}. \quad (188)$$

In the limit  $N_c \rightarrow \infty$  one has

$$\begin{aligned} a_1 &\approx 0.5 \cdot (C_+ + C_-), \\ a_2 &\approx 0.5 \cdot (C_+ - C_-). \end{aligned} \quad (189)$$

The  $a_1$  and  $a_2$  values, used in refs.[34,83], differ from each other because of a different choices for the quark masses and the  $\Lambda_{QCD}$  parameter.

Note, that for the decays with the  $B$  mesons in the final state, the contribution of the annihilation and "penguin" diagrams is suppressed as  $O(\sin^{10} \theta_c)$ . As one can see from Table 22, the WSB results agree with the ISGW model, and the sum of the two-particle decay widths is equal to the total inclusive width of the  $b$ -spectator decay (see Table 15).

The widths in the model of ref.[83] are slightly greater. The reason for the deviation from the results of two other models can be the fact, that for the  $b$ -spectator decays, there are  $B$  and  $B_s$  mesons in the final state, so that these mesons are relativistic systems because of the light quark presence and, hence, the nonrelativistic approximation can poorly work.

Among the  $c$ -spectator decays, the widths, presented in Table 23, are given for the decays, where the WSB and ISGW models result in close values and one can neglect contributions of the annihilation and "penguin" diagrams. As one can see from Table 23, the data of ISGW model well agree with the results of model [83].

The total inclusive nonleptonic width of the  $B_c$  meson decay with the  $J/\psi$  particle in the final state can be obtained from the corresponding width of the semileptonic decay

$$\Gamma(B_c \rightarrow J/\psi X_{u\bar{d}(\bar{s})}) = 3 \cdot a_1^2 \Gamma(B_c \rightarrow J/\psi e\nu) |V_{ud(s)}|^2. \quad (190)$$

In the large  $N_c$  limit, one has  $3 \cdot a_1^2 = 4.6$  ( $a_1 = 1.18$ ) and

$$\Gamma(B_c \rightarrow J/\psi X_{u\bar{d}(\bar{s})}) \approx 190 \cdot 10^{-6} \text{ eV}.$$

Table 22.

The widths (in units  $10^{-6}$  eV) of two-particle hadronic  $\bar{b}$ -spectator decays ( $M_{B_c} = 6.27$  GeV,  $M_{B_s} = 5.39$  GeV,  $M_{B_s^*} = 5.45$  GeV)

Decay mode	WSB	$a_1 = 1.23$ $a_2 = 0.33$	ISGW	$a_1 = 1.23$ $a_2 = 0.33$	[83]	$a_1 = 1.12$ $a_2 = -0.26$
$B_c^+ \rightarrow B_s + \pi^+$	$a_1^2$ 31.1	47.8	$a_1^2$ 44.0	67.7	$a_1^2$ 58.4	73.3
$B_c^+ \rightarrow B_s + \rho^+$	$a_1^2$ 12.5	19.2	$a_1^2$ 20.2	3.1	$a_1^2$ 44.8	56.1
$B_c^+ \rightarrow B_s^* + \pi^+$	$a_1^2$ 25.6	39.4	$a_1^2$ 34.7	53.4	$a_1^2$ 51.6	64.7
$B_c^+ \rightarrow B_s^* + \rho^+$	$a_1^2$ 115.6	177.8	$a_1^2$ 152.1	234	$a_1^2$ 150	188
$B_c^+ \rightarrow B^+ + \bar{K}^0$	$a_2^2$ 28.2	3.1	$a_2^2$ 61.4	6.7	$a_2^2$ 96.5	4.25
$B_c^+ \rightarrow B^+ + \bar{K}^{*0}$	$a_2^2$ 10.0	1.1	$a_2^2$ 24.1	2.6	$a_2^2$ 68.2	3.01
$B_c^+ \rightarrow B^{*+} + \bar{K}^0$	$a_2^2$ 31.0	3.4	$a_2^2$ 28.3	3.1	$a_2^2$ 73.3	3.23
$B_c^+ \rightarrow B^{*+} + \bar{K}^{*0}$	$a_2^2$ 147.1	16	$a_2^2$ 163.8	18	$a_2^2$ 141	6.23
$B_c^+ \rightarrow B^0 + \pi^+$	$a_1^2$ 0.97	1.49	$a_1^2$ 1.89	2.9	$a_1^2$ 3.30	4.14
$B_c^+ \rightarrow B^0 + \rho^+$	$a_1^2$ 0.94	1.45	$a_1^2$ 2.14	3.3	$a_1^2$ 5.97	7.48
$B_c^+ \rightarrow B^{*0} + \pi^+$	$a_1^2$ 1.58	2.42	$a_1^2$ 1.28	2.0	$a_1^2$ 2.90	3.64
$B_c^+ \rightarrow B^{*0} + \rho^+$	$a_1^2$ 8.82	13.6	$a_1^2$ 8.86	12.	$a_1^2$ 11.9	15.0
$B_c^+ \rightarrow B^+ + \pi^0$	$a_2^2$ 0.48	0.05	$a_2^2$ 0.95	0.1	$a_2^2$ 1.65	0.074
$B_c^+ \rightarrow B^+ + \rho^0$	$a_2^2$ 0.47	0.05	$a_2^2$ 1.07	0.12	$a_2^2$ 2.98	0.132
$B_c^+ \rightarrow B^+ + \omega$	$a_2^2$ 0.38	0.04	$a_2^2$ 0.87	0.09	–	–
$B_c^+ \rightarrow B^{*+} + \pi^0$	$a_2^2$ 0.79	0.09	$a_2^2$ 0.64	0.07	$a_2^2$ 1.45	0.064
$B_c^+ \rightarrow B^{*+} + \rho^0$	$a_2^2$ 4.41	0.48	$a_2^2$ 4.43	0.48	$a_2^2$ 5.96	0.263
$B_c^+ \rightarrow B^{*+} + \omega$	$a_2^2$ 3.60	0.39	$a_2^2$ 3.53	0.38	–	–
$B_c^+ \rightarrow B_s + K^+$	$a_1^2$ 2.18	3.35	$a_1^2$ 3.28	5.	$a_1^2$ 4.2	5.27
$B_c^+ \rightarrow B_s^* + K^+$	$a_1^2$ 1.71	2.6	$a_1^2$ 2.52	3.9	$a_1^2$ 2.96	3.72
$B_c \rightarrow B^0 + K^+$	–	–	–	–	$a_1^2$ 0.255	0.32
$B_c \rightarrow B^0 + K^{*+}$	–	–	–	–	$a_1^2$ 0.180	0.226
$B_c \rightarrow B^{*0} + K^+$	–	–	–	–	$a_1^2$ 0.195	0.244
$B_c \rightarrow B^{*0} + K^{*+}$	–	–	–	–	$a_1^2$ 0.374	0.47

The branching ratio of the  $B_c$  decay with the  $J/\psi$  particle in the final state equals

$$BR(B_c \rightarrow J/\psi + X) \approx 0.2 .$$

The WSB and ISGW models give close results for the two-particle  $B_c$  meson decays with the  $B$  mesons in the final state. Unfortunately, it is complex to detect the  $B_c$  mesons in such decay modes, since one has to reconstruct the  $B$  mesons from the products of their weak decays. For the  $B_c$  meson observation and its mass determination, the  $B_c^+ \rightarrow J/\psi\pi^+$  decay is more preferable [34]. Its branching ratio is equal to

$$BR(B_c^+ \rightarrow J/\psi\pi^+) \approx 2 \cdot 10^{-3} .$$

Table 23. The widths (in units  $10^{-6}$  eV) of two-particle hadronic  $c$ -spectator decays

Decay mode	ISGW	$a_1 = 1.18$	[83]	$a_1 = 1.26$
$B_c^+ \rightarrow \eta_c + \pi^+$	$a_1^2$ 1.71	2.63	$a_1^2$ 2.07	3.29
$B_c^+ \rightarrow \eta_c + \rho^+$	$a_1^2$ 4.04	6.2	$a_1^2$ 5.48	8.70
$B_c^+ \rightarrow J/\psi + \pi^+$	$a_1^2$ 1.79	2.75	$a_1^2$ 1.97	3.14
$B_c^+ \rightarrow J/\psi + \rho^+$	$a_1^2$ 5.07	7.8	$a_1^2$ 5.95	9.45
$B_c^+ \rightarrow \eta_c + K^+$	$a_1^2$ 0.127	0.195	$a_1^2$ 0.161	0.256
$B_c^+ \rightarrow \eta_c + K^{*+}$	$a_1^2$ 0.203	0.31	$a_1^2$ 0.286	0.453
$B_c^+ \rightarrow J/\psi + K^+$	$a_1^2$ 0.130	0.2	$a_1^2$ 0.152	0.242
$B_c^+ \rightarrow J/\psi + K^{*+}$	$a_1^2$ 0.263	0.4	$a_1^2$ 0.324	0.514
$B_c \rightarrow \psi(2S) + \pi^+$	–	–	$a_1^2$ 0.251	0.398
$B_c \rightarrow \psi(2S) + \rho^+$	–	–	$a_1^2$ 0.71	1.13
$B_c \rightarrow \psi(2S) + K^+$	–	–	$a_1^2$ 0.018	0.029
$B_c \rightarrow \psi(2S) + K^{*+}$	–	–	$a_1^2$ 0.038	0.060

The  $B_c$  meson decays, where the  $CP$  violation can be observed,  $B_c^\pm \rightarrow (c\bar{c})D^\pm$ ,  $B_c \rightarrow D\rho(\pi)$  and  $B_c \rightarrow D^0D_s$  are of a special interest.

The approximate estimates for the decay branching fractions and the asymmetry parameter of  $CP$  violation, are obtained in ref.[80]. The corresponding results are presented in Table 24. The asymmetry parameter  $A$  is defined in the following way

$$A = \frac{\Gamma(B_c^- \rightarrow \bar{X}) - \Gamma(B_c^+ \rightarrow X)}{\Gamma(B_c^- \rightarrow \bar{X}) + \Gamma(B_c^+ \rightarrow X)}. \quad (191)$$

A large value of the asymmetry is expected in the  $B_c \rightarrow D_s^*D^0$  decays with the  $D^0$  meson, decaying into the eigen  $CP$  invariance state. However, the branching ratio of such event is too low

$$BR(B_c^+ \rightarrow D_s^{*+}D^0) \approx 10^{-6}.$$

The  $D_s^{*+}$  meson identification is also complicated. As one can see from Table 24, the best mode for the  $CP$  violation observation in the  $B_c$  meson decay can be  $B_c^\pm \rightarrow (c\bar{c})D^\pm$ . However, even at the expected statistics of the  $B_c$  meson yield at the future colliders (about  $10^9$ – $10^{11}$  events), it is difficult to observe such events, if one takes into account the branching fractions of the  $(c\bar{c})$  states and  $D$  meson decays.

It is difficult to estimate the decay widths, but it is worth to mention about the  $B_c$  meson decay modes such as  $B_c \rightarrow 3DX$  or  $B_c \rightarrow D_s\phi$  and  $B_c \rightarrow \bar{D}K$ . The  $B_c \rightarrow \psi(3S)D$  decay can be of a great interest, when  $\psi(3S)$  has the decay into the  $D$  meson pair. However, it is probable, that this decay width, as the width of the decay into three  $D$  mesons, is small because of a smallness of the phase space, yet. The  $B_c \rightarrow D_s\phi$  decay width can be roughly estimated of the order of 2 % [52], but it will be very difficult to observe the  $B_c$  meson in such mode because of the complex reconstruction of the  $D_s$  meson.

## 4. Production of $B_c$ mesons

The electromagnetic and hadronic production of  $B_c$  as the particle with the mixed flavour supposes the joint production of the heavy quarks  $\bar{b}$  and  $c$ . This explains the low value of the  $B_c$  production cross section in comparison with the production cross sections of the particles from the  $\psi$  and  $\Upsilon$  families. On the other hand, the absence of the  $B_c$  decays channels into light hadrons due to the strong interactions leads to that all bound ( $\bar{b}c$ ) states basically transformed into the lowest state with the probability close to unit, due to the radiative transitions (see Section 2).

From the theoretical point of view, the production of  $B_c$  meson, having the small sizes, takes place with the virtualities of the order of the heavy quark mass sum. This fact makes sure the perturbation theory to be applicable to the processes of the  $B_c$  production. The nonperturbative part, related with the account for the  $B_c$  wave function, is quite reliably calculated in this case.

### 4.1. Production of $B_c$ mesons in $e^+e^-$ -annihilation

The simplest example of the  $B_c$  production in  $e^+e^-$ -annihilation (in the region of  $Z$  peak) is described by the diagrams on Figure 7.

The matrix element of the ( $\bar{b}c$ ) quarkonium production is transformed from the corresponding matrix element  $T(p_b, p_c)$  for four heavy quark production by the integration over the relative momentum of the  $\bar{b}$ - and  $c$ -quarks with the weight of the quarkonium wave function

$$T_j = \int \frac{d^3\mathbf{q}}{(2\pi)^3} \Psi(\mathbf{q}) T(p_{\bar{b}}, p_c)_{\alpha\beta}^{ab} (-\hat{p}_{\bar{b}} + m_b)^{\alpha'\alpha} (-\hat{p}_c + m_c)^{\beta'\beta} \Gamma_j^{\alpha'\beta'} \frac{\sqrt{2M}}{\sqrt{2m_b 2m_c}} \frac{\delta^{ab}}{\sqrt{3}}, \quad (192)$$

where  $M$  is the meson mass and

$$\Gamma^{\alpha\beta} = \frac{1}{\sqrt{2}} \gamma_5^{\alpha\beta}, \quad \Gamma_\lambda^{\alpha\beta} = \frac{1}{\sqrt{2}} \gamma_\mu^{\alpha\beta} \epsilon_\lambda^\mu \quad (193)$$

**Table 24.** The branching ratios ( $BR$ ) and asymmetries ( $A$ ) for the  $CP$  violating  $B_c$  decays

$X$	$BR(B_c^+ \rightarrow X)$	$A$
$\eta_c D^{*+}$	$1.0 \cdot 10^{-4}$	$1.5 \cdot 10^{-2}$
$\eta_c D^+$	$1.2 \cdot 10^{-4}$	$-0.3 \cdot 10^{-2}$
$J/\psi D^+$	$0.5 \cdot 10^{-4}$	$0.6 \cdot 10^{-2}$
$D^0 \rho^+$	$2.8 \cdot 10^{-5}$	$1.9 \cdot 10^{-3}$
$D^+ \rho^0$	$1.6 \cdot 10^{-5}$	$3.0 \cdot 10^{-3}$
$D^{*0} \pi^+$	$3.3 \cdot 10^{-5}$	$1.3 \cdot 10^{-3}$
$D^{*+} \pi^0$	$1.8 \cdot 10^{-5}$	$2.0 \cdot 10^{-3}$
$D^0 \pi^+$	$1.6 \cdot 10^{-6}$	$-8.9 \cdot 10^{-3}$
$D^+ \pi^0$	$0.4 \cdot 10^{-6}$	$-13.8 \cdot 10^{-3}$

Fig. 7. The diagrams of the single  $B_c$  meson production in  $e^+e^-$ -annihilation

for the pseudoscalar state and the vector one ( $B_c, B_c^*$ ), respectively. The quark momenta are determined by the relations

$$p_{\bar{b}} = \frac{m_b}{M}p + q, \quad p_c = \frac{m_c}{M}p - q, \quad (194)$$

$$p \cdot q = 0. \quad (195)$$

For the heavy quarkonium one has  $|\mathbf{q}| \ll m_b, m_c$  and eq.(192) can be simplified by the substitution for  $T_{\alpha\beta}^{ab}(p_{\bar{b}}, p_c)$  by its value at  $\mathbf{q} = \mathbf{0}$ . Then

$$\int \frac{d^3\mathbf{q}}{(2\pi)^3} \Psi(\mathbf{q}) = \Psi(\mathbf{x})|_{\mathbf{x}=\mathbf{0}} \quad (196)$$

In papers of refs.[41–44] the total cross sections of the  $B_c$  and  $B_c^*$  mesons and its distributions over the variable  $z = 2E_{B_c}/\sqrt{s}$  have been obtained. The result of the precise numerical calculations in the technique of spiral amplitudes with the Monte Carlo integration over the phase space is presented on Figure 8. One can see that this distribution is rather hard with the maximum at  $z_{\max} = M/(M + m_c) \approx 0.8$ . At this value of  $z_{\max}$  the  $B_c$  meson and  $\bar{c}$ -quark have zero relative velocity. If one remembers, in the considered approximation the relative motion of the  $c$ - and  $\bar{b}$ -quarks inside the  $B_c$  meson is absent, then one clearly finds, that the maximum in the distribution corresponds to the configuration, when all quarks move as a whole with one and the same velocity. In this case the minimal virtualities of the initial  $\bar{b}$ -quark  $p^2 = (m_b + 2m_c)^2$  and the gluon  $k^2 \approx 4m_c^2$  are realized. At any other  $z$  values, these virtualities increase. Note, these speculations are correct only for the last two diagrams on Figure 7, when one can neglect the contribution of the first and second diagrams, suppressed up to two orders of magnitude in respect to the former. In the asymptotic limit  $s \rightarrow \infty$ , when one can neglect terms of the order of  $M^2/s$  and the higher powers of this ratio, choosing the special gauge condition (the axial gauge with the four-vector  $n = (1, 0, 0, -1)$  along the direction of the  $b$ -quark motion),

one can show that the contribution of the last diagram on Figure 7 survives only. In this case the expression for  $\sigma^{-1}d\sigma/dz$  acquires the sense of the fragmentation function of the  $\bar{b}$ -quark into the  $B_c$  meson, if one chooses the  $b$ -quark production cross section  $\sigma$  as the normalization factor at the same energy.

The function of the  $\bar{b} \rightarrow B_c$  fragmentation, where  $B_c$  is the pseudoscalar state, has the following form

$$\begin{aligned} \dot{D}(z)_{\bar{b} \rightarrow B_c} = & \frac{8\alpha_s^2 |\Psi(0)|^2}{81m_c^3} \frac{rz(1-z)^2}{(1-(1-r)z)^6} (6 - 18(1-2r)z + \\ & (21 - 74r + 68r^2)z^2 - 2(1-r)(6 - 19r + 18r^2)z^3 \\ & + 3(1-r)^2(1-2r+2r^2)z^4), \end{aligned} \quad (197)$$

and for the fragmentation into the vector state one has

$$\begin{aligned} D(z)_{\bar{b} \rightarrow B_c^*} = & \frac{8\alpha_s^2 |\Psi(0)|^2}{27m_c^3} \frac{rz(1-z)^2}{(1-(1-r)z)^6} (2 - 2(3-2r)z + \\ & 3(3-2r+4r^2)z^2 - 2(1-r)(4-r+2r^2)z^3 + \\ & (1-r)^2(3-2r+2r^2)z^4), \end{aligned} \quad (198)$$

where  $r = m_c/(m_b + m_c)$ . As one can see from Figure 8,  $D_{\bar{b} \rightarrow B_c}(z)$  and  $D_{\bar{b} \rightarrow B_c^*}(z)$  are in a good agreement with the results of precise calculations. The  $\bar{b} \rightarrow B_c^*$  process has slightly more hard distribution in comparison with the  $\bar{b} \rightarrow B_c$  one. At  $\alpha_s = 0.22$ ,  $|\Psi(0)|^2 = f_{B_c}^2 M_{B_c}/12$ ,  $f_{B_c} = 560$  MeV and  $m_c = 1.5$  GeV, the corresponding integral probabilities are equal to  $3.8 \cdot 10^{-4}$  for  $\bar{b} \rightarrow B_c$  and  $5.4 \cdot 10^{-4}$  for  $\bar{b} \rightarrow B_c^*$ . The probabilities of the  $c$ -quark fragmentation into  $B_c$  are suppressed by two orders of magnitude in respect to the values, given above. As the fraction of the  $b\bar{b}$  production, the total number of the produced  $B_c(\bar{B}_c)$  mesons with the account of the  $B_c^*(\bar{B}_c^*)$  states and the first radial excitations is equal to (at  $\alpha_s = 0.22$ )

$$R_{B_c} = \frac{\sigma(e^+e^- \rightarrow B_c^+ + x) + \sigma(e^+e^- \rightarrow B_c^- + x)}{\sigma(e^+e^- \rightarrow b\bar{b})} = 2 \cdot 10^{-3} \quad (199)$$

Due to the quark-hadron duality, there is the independent way of estimation for this ratio. To reach this goal, one has to compare the obtained cross section of the bound  $\bar{b}c$  state production with the cross section for the production of the colour-singlet ( $\bar{b}c$ ) pair in the process  $e^+e^- \rightarrow b\bar{b}c\bar{c}$  with the low values of invariant mass  $M_{\bar{b}c}$

$$\int_{m_0^2}^{M_{\text{th}}^2} \frac{d\sigma(e^+e^- \rightarrow b\bar{b}c\bar{c})_{\bar{b}c\text{-singl}}}{dM_{\bar{b}c}^2} dM_{\bar{b}c}^2, \quad (200)$$

where  $m_0 = m_b + m_c \leq M_{\bar{b}c} \leq M_B + M_D + \Delta M = M_{\text{th}}$  and  $\Delta M \approx 0.5 \div 1$  GeV. Supposing  $m_0 = 6.1$  GeV and  $M_{\text{th}} = 8$  GeV as the threshold value, one gets the  $\bar{b}c$  system production cross section of the order of 7 pb. On the other hand, the sum of the cross sections for the production of  $B_c$  and its first excitations equals 9.3 pb, as is seen from Table 25.



Table 25.

The cross sections (in pb) for the production of the  $S$ -wave states of  $B_c$  mesons in the  $Z$  boson peak

State	$1^1S_0$	$1^1S_1$	$2^1S_0$	$2^1S_1$
$\sigma(\alpha_S = 0.22)$	3.14	4.37	0.805	1.078

The comparison of these two independent estimates states, on the one hand, about a good agreement. On the other hand, it means that the contribution of the higher excitations is not large, and the total cross section is saturated by the  $S$ -wave levels.

Recent direct calculations of the cross sections for the  $P$  level production [91] confirm this conclusion. According to the estimates of this paper, the sum over the cross sections for the  $P$ -wave levels production is less than 10 % from the sum of the  $S$ -wave level contributions.

In ref.[48] the functions of the heavy quark fragmentation into the heavy polarized vector quarkonium have been studied, so, for the longitudinally polarized quarkonium, one has found the expression

$$D(z)_{\bar{b} \rightarrow B_c^*}^L = \frac{8\alpha_s^2 |\Psi(0)|^2}{81m_c^3} \frac{rz(1-z)^2}{(1-(1-r)z)^6} (2 - 2(3-2r)z + (9-10r+16r^2)z^2 - 2(1-r)(4-5r+6r^2)z^3 + (1-r)^2(3-6r+6r^2)z^4), \quad (201)$$

that does not depend on the polarization of the fragmentating quark. At  $r = 1/2$ , expression (201) coincides with the result, obtained for the heavy quarkonium with the hidden flavour ( $\Upsilon, \psi$ ) [48].

Fig. 8. The functions of the  $\bar{b}$ -quark fragmentation into the  $B_c$  and  $B_c^*$  mesons

Fragmentation function (201) agrees with the consideration of the heavy quark fragmentation into the heavy meson ( $Q\bar{q}$ ), where in the limit of infinitely heavy quark, EHQT leads to the equal probability production of the vector quarkonium with the arbitrary orientation of its spin, i.e. to the absence of the spin alinement and to the ratio of the vector and pseudoscalar state yields, equal to  $V/P = 3$  [94].

For the heavy quarkonium, the relative yield of the vector and pseudoscalar mesons is close to unit, and the spin alinement of the vector state has a notable value. For the  $B_c^*$  meson, this can be observed in the angle distribution of the  $B_c^* \rightarrow B_c\gamma$  decay, which composes the total  $B_c^*$  width. This distribution has the form

$$\frac{d\Gamma}{d\cos\theta} \sim 1 - \left(\frac{3\xi - 2}{2 - \xi}\right) \cos^2\theta, \quad (202)$$

where  $\theta$  is the angle between the photon and the  $B_c^*$  polarization axis in the system of  $B_c^*$  rest, and the asymmetry parameter  $\xi$  determines the relative yield of the transversally polarized  $B_c^*$  state

$$\xi = \frac{T}{L + T}. \quad (203)$$

For the integral asymmetry at the small mass of the generated quark, entering the meson,  $r \ll 1$ , one has

$$\xi = \frac{2}{3} + \frac{5}{16}r + O(r^2). \quad (204)$$

The anisotropy in the  $B_c^* \rightarrow B_c\gamma$  decay is numerically equal to 6 %.

In ref.[48] the vector quarkonium spin alinement has been studied versus the transverse momentum in respect to the fragmentation axis. One has derived quite bulky analytical expressions for the fragmentation functions  $D_{b \rightarrow B_c^*}^{L,T}(p_t)$ , that linearly tend to zero at  $p_t \rightarrow 0$  and decrease as  $1/p_t^3$  at  $p_t \rightarrow \infty$ . It is interesting, that the average transverse momentum at the fragmentation into the longitudinally polarized vector  $B_c$  quarkonium is twice greater than the average transverse momentum at the fragmentation into the transversally polarized  $B_c^*$  meson,  $\langle p_t \rangle \approx 7$  GeV.

The event with the  $B_c$  meson has the characteristic signature. The hadron jet from the  $b$ -quark must be produced in the direction, opposite to the  $B_c$  motion. The  $B_c$  meson must be accompanied by the  $\bar{D}$  meson with the average ratio of the momenta  $\langle z_D \rangle / \langle z_{B_c} \rangle \approx 0.3$  and the average angle between the momenta about  $20^\circ$  [44].

The single  $B_c$  meson production in  $e^+e^-$ -annihilation has been also considered in refs.[41,52].

In ref.[39] the exclusive production of the  $B_c^{(*)+}B_c^{(*)-}$  pairs in  $e^+e^-$ -annihilation has been calculated at low energies, where one can neglect the  $Z$  boson contribution. The total cross sections of the vector and pseudoscalar states have the form

$$\begin{aligned} \sigma(e^+e^- \rightarrow (Q_1\bar{Q}_2)_P(\bar{Q}_1Q_2)_P) &= \frac{\pi^3\alpha_S^2(4m_2^2)\alpha_{\text{em}}^2}{3^7 4m_2^6} \frac{m_1^2}{M^2} f_P^4(1-v^2)^3 v^3 \times \\ &\left(3e_1\left(\frac{2m_2}{m_1} - 1 + v^2\right) - 3e_2\left(2 - (1-v^2)\frac{m_2}{m_1}\right) \frac{m_2^3\alpha_S(4m_1^2)}{m_1^3\alpha_S(4m_2^2)}\right)^2, \quad (205) \\ \sigma(e^+e^- \rightarrow (Q_1\bar{Q}_2)_P(\bar{Q}_1Q_2)_V) &= \frac{\pi^3\alpha_S^2(4m_2^2)\alpha_{\text{em}}^2}{3^7 2m_2^6} f_P^2 f_V^2 (1-v^2)^4 v^3 \times \end{aligned}$$

$$\left(3e_1 - 3e_2 \frac{m_2^3 \alpha_S(4m_1^2)}{m_1^3 \alpha_S(4m_2^2)}\right)^2, \quad (206)$$

$$\begin{aligned} \sigma(e^+e^- \rightarrow (Q_1\bar{Q}_2)_V(\bar{Q}_1Q_2)_V) &= \frac{\pi^3 \alpha_S^2(4m_2^2) \alpha_{\text{em}}^2}{3^7 2m_2^6} f_V^4 (1-v^2)^3 v^3 \times \\ &\left(3e_1 - 3e_2 \frac{m_2^3 \alpha_S(4m_1^2)}{m_1^3 \alpha_S(4m_2^2)}\right)^2 [3(1-v^2) + (1+v^2)(1-a)^2 + \\ &\frac{a^2}{2}(1-v^2)(1-3v^2)], \end{aligned} \quad (207)$$

where  $v = \sqrt{1 - 4M^2/s}$ ,  $M = m_1 + m_2$ ,

$$a = \frac{m_1}{M} \left(1 - \frac{e_2 m_2^4 \alpha_S(4m_1^2)}{e_1 m_1^4 \alpha_S(4m_2^2)}\right) / \left(1 - \frac{e_2 m_2^3 \alpha_S(4m_1^2)}{e_1 m_1^3 \alpha_S(4m_2^2)}\right). \quad (208)$$

The relative yield of the  $B_c$  meson pairs  $R = \sigma(B_c^+ B_c^-) / \sigma(b\bar{b})$  reaches its maximum at the energy  $\sqrt{s} = 14$  GeV, where it is equal to  $R \approx 10^{-4}$ . This ratio rapidly decreases with the energy growth, where the single  $B_c$  production becomes to dominate.

As one can see, the study of the  $B_c$  meson production in  $e^+e^-$ -annihilation allows one to make the analytical researches of the heavy quark dynamics.

Thus, in the  $Z^0$  boson pole, where the  $b$ -quark production cross section is large, one has to expect of the order of 2 events with the  $B_c$  production per each thousand  $b\bar{b}$  pairs. As it is planned, in the experiments at the LEP accelerator, the number about  $2 \cdot 10^7$   $Z^0$  bosons will be detected. This means, that the total number of  $B_c(\bar{B}_c)$  events has to be of the order of  $10^4$ . Certainly, the real number of reconstructed events will be less, if one takes into account the particular modes of the decay.

## 4.2. Hadronic production of $B_c$ mesons

As has been mentioned, the process of the  $B_c$  meson production in  $e^+e^-$ -annihilation at large energies can be reformulated as the process of the  $\bar{b} \rightarrow B_c(B_c^*)$  fragmentation, appearing with the probability about  $10^{-3}$ .

The hadronic  $B_c$  production turns out to be more complex. First, at hadronic production the region of low partonic energies dominates, so that the asymptotic regime with the cross section factorization

$$\frac{d\sigma}{dz} \sim \sigma_{b\bar{b}} D_{\bar{b} \rightarrow B_c}(z) \quad (209)$$

is not yet realized. Second, in the hadron interactions a new type of diagrams appears, so we will further label the latter as the recombinational diagrams, for which the factorization does not take place.

The contribution of such diagrams, dominating at low masses of the  $B_c^- \bar{b} c$  system, decreases with the growth of this mass, however, it remains essential even at large masses and large transverse momenta. The contribution of such type diagrams into the  $B_c^{(*)}$  production has been first calculated for the exclusive  $B_c^{(*)}$  pair production in the quark-antiquark annihilation at low energies [38].

The typical set of the QCD diagrams in the fourth order over  $\alpha_S$  is shown on Figure 9. Here, as in the case of the  $B_c$  production in  $e^+e^-$ -annihilation, the matrix element of the

Fig. 9. The diagrams of the single  $B_c$  meson production in the gluon and quark subprocesses

( $\bar{b}c$ ) quarkonium production is obtained from the corresponding matrix element of four quarks production by the integration over the relative momentum of the  $c$ - and  $\bar{b}$ -quarks with the weight, determined by the quarkonium wave function.

At high energies, where the  $B_c$  production cross sections are accessible for the meson observation, the gluon-gluon contribution into the production dominates.

The energetic spectra of the  $B_c$  and  $B_c^*$  mesons in the system of mass centre for two colliding gluons are shown on Figure 10 at the different values of the total energy  $\sqrt{s} = 20, 40$  and  $100$  GeV.

The  $\sigma(gg \rightarrow B_c(B_c^*)\bar{c}b)$  values are presented on Figure 11 at the several energies of the interacting gluons for  $m_b = 5.1$  GeV,  $m_c = 1.5$  GeV and  $\alpha_S = 0.2$ . The ratio of the cross sections  $\sigma_{B_c^*}/\sigma_{B_c}$  is about 3 at the energies 20, 40 and 100 GeV and it is about 2 at the energy 1 TeV, when in  $e^+e^-$ -annihilation, where the  $\bar{b} \rightarrow B_c$  fragmentation dominates, this ratio is  $\sigma_{B_c^*}/\sigma_{B_c} \approx 1.3$ .

The variation of the  $\sigma_{B_c^*}/\sigma_{B_c}$  ratio is the consequence of the change in the production mechanism. The fragmentational component gives the low contribution in comparison with the contribution of the recombination diagrams. This can be noted from Figure 10, where the differential cross sections for the  $B_c$  and  $B_c^*$  meson production, calculated by the Monte Carlo integration of the exact expression for the matrix element squared, are presented in comparison with the cross section, calculated under the fragmentation

Fig. 10. The differential  $d\sigma/dz$  cross sections for the single production of the  $B_c$  mesons (a) and  $B_c^*$  mesons (b) in the gluon annihilation at different values of the total energy

formulae (197), (198).

The total cross section of the  $B_c(B_c^*)$  mesons is obtained from the partonic one  $\sigma_{ij}(\hat{s})$

Fig. 11. The total cross sections for the single production of  $B_c$  mesons (empty triangles) and  $B_c^*$  mesons (solid triangles) in the gluon annihilation in comparison with the production cross section (multiplied by the factor  $2 \cdot 10^{-3}$ ) of the  $\bar{b}b$  quark pairs (solid line)

by the convolution with the functions of the parton distributions in the initial hadrons

$$\sigma_{\text{tot}}(s) = \int_{4(m_b+m_c)^2}^s \frac{d\hat{s}}{s} \int_{-1+\hat{s}/s}^{1-\hat{s}/s} \frac{dx}{x^*} \sum_{ij} f_a^i(x_1) f_b^j(x_2) \hat{\sigma}_{ij}(\hat{s}), \quad x^* = \left(x^2 + \frac{4\hat{s}}{s}\right)^{1/2}. \quad (210)$$

The cross sections, calculated with the account of the known parameterizations for  $f_{a,b}^{i,j}(x)$  [92], are presented in Table 26.

The energy 40 GeV is close to the c.m.s. energy for the carrying out the fixed target experiments at the HERA accelerator. At  $\sqrt{s} = 1.8$  TeV we present the cross section of the  $B_c$  production in  $p\bar{p}$ -collisions at Tevatron, and, finally, the energy  $\sqrt{s} = 16$  TeV corresponds to the conditions of the  $pp$ -experiment at the future LHC collider. The energetic dependence of the cross section, summed over the particle and antiparticle  $\bar{B}_c$  production, is shown on Figure 12.

From the values, presented in Table 26, it follows that at  $\sqrt{s} = 40$  GeV, the summed cross section  $\sigma_{\text{sum}}$  for the meson production is about  $10^{-4}$  of the total cross section of the  $b\bar{b}$  production, so this makes the  $B_c$  study practically to be impossible in this experiment. One has to note, that in this case we can not restrict ourselves by the  $gg \rightarrow B_c \bar{c}b$  contribution and we have taken into account the contribution of the  $q\bar{q} \rightarrow B_c \bar{c}b$  process.

The experiments at Tevatron and LHC, where  $\sigma_{\text{sum}}/\sigma_{b\bar{b}}$  is about  $10^{-2}$ , will give the real possibility for the observation of hadronic  $B_c$  production. Therefore, at the energies of these two facilities, we present the most interesting distributions of the cross sections for the  $1^1S_0$  and  $1^3S_1$  states production (note, that as our calculations show, the cross section at the energies under consideration is completely determined by the gluon-gluon interaction, since the quark-quark contribution is suppressed by two orders of magnitude,  $10^{-2}$ ).

The distributions for the  $1^1S_0$  pseudoscalar and  $1^3S_1$  vector mesons are shown on Figures 13 and 14 at the energy of the interacting hadrons 1.8 TeV.

The distributions  $d\sigma/dx$  (see Figure 14b) show, that we deal with the central  $B_c$  production, where the complete cross section is collected in the interval from  $-0.3$  to  $0.3$ . The average transverse momentum of  $B_c$  is about 6 GeV, and from the distribution over the angle between the directions of the  $B_c$  and  $\bar{c}$ -quark motions, one can conclude that  $\bar{c}$ -quark generally moves in the direction close to the  $B_c$  one [46].

One has to note, that the considered diagrams of the QCD perturbation theory are the diagrams of the fourth order over  $\alpha_S$ . This results in the strong dependence of the

Table 26.

The cross sections (in nb) of hadronic production of the  $B_c(B_c^*)$  mesons (the standard deviation in the last digit is shown in the brackets)

$n^{2S+1}L_j$	$1^1S_0$	$1^3S_1$	$2^1S_0$	$2^3S_1$
$\sigma_{\text{tot}}(40 \text{ GeV}) \cdot 10^5$	1.63(2)	9.5(2)	0.13(1)	0.75(2)
$\sigma_{\text{tot}}(100 \text{ GeV}) \cdot 10^3$	7.8(2)	36(1)	1.1(2)	5.2(2)
$\sigma_{\text{tot}}(1.8 \text{ TeV})$	13.3(8)	53(3)	2.7(2)	10.4(5)
$\sigma_{\text{tot}}(16 \text{ TeV}) \cdot 10^{-2}$	1.96(8)	7.6(2)	0.43(2)	1.66(8)

Fig. 12.

The total cross sections (in nb) for the single production of  $B_c$  mesons (empty circles) in  $p\bar{p}$ -interactions at different energies and the cross sections (in mkb) for the beauty particle production (solid circles)

cross section on the particular  $\alpha_S$  choice. The latter must be determined by the typical virtuality in the production process. The analysis shows, that this virtuality is large in the contributions, decreasing faster than  $1/\hat{s}$ , only. In the remaining contributions, including the fragmentational one, it is not large and about  $4m_c m_b$ . Under this reason the  $\alpha_S = 0.2$  value, chosen as the strong coupling constant, is the most reasonable at this scale. The use of the running coupling constant  $\alpha_S(\hat{s})$ , for example, leads to the decrease of the  $B_c(B_c^*)$  production cross section by about 7 times. The pessimistic estimates of the  $B_c(B_c^*)$  production are presented in ref.[93], where, as one can see, the  $\alpha_S(\hat{s})$  value has been used.

At low energies of hadron collisions, the quark-antiquark annihilation with the  $B_c$  production dominates in respect to the gluonic one, since, in this case, the latter has a much lower luminosity, that decreases also with the growth of the total energy of the partonic subprocess. At the low energies of the quark-antiquark annihilation, the exclusive  $B_c^+ B_c^-$  pair production can be essential. The total cross sections of the vector and pseudoscalar  $B_c$  meson production due to the quark-antiquark annihilation have the form

$$\sigma(1^-, 1^-) = \frac{\alpha_S^4 \pi^3}{8 \cdot 3^8} \frac{f_V^4}{\mu^6} \lambda^3 \sqrt{1-\lambda} (1.3 + 1.4\lambda + 0.3\lambda^2), \quad (211)$$

$$\sigma(1^-, 0^-) = \frac{\alpha_S^4 \pi^3}{16 \cdot 3^8} \frac{f_V^2 f_P^2}{\mu^6} \frac{(m_b - m_c)^2}{M^2} \lambda^3 \sqrt{1-\lambda} (1 + 2\lambda), \quad (212)$$

$$\sigma(0^-, 0^-) = \frac{\alpha_S^4 \pi^3}{16 \cdot 3^8} \frac{f_P^4}{\mu^6} \lambda^3 \sqrt{1-\lambda} (1 - \lambda)^2, \quad (213)$$

wherefrom one can see, that the vector state production dominates. In eqs.(211)–(213)

Fig. 13. The differential  $d\sigma/dp_t$  cross sections for the single production of  $B_c$  and  $B_c^*$  mesons in  $p\bar{p}$  interactions at the energy 1.8 TeV

we have introduced the notations

$$\begin{aligned}\lambda &= 4M^2/s, \\ \mu &= \frac{m_b m_c}{m_b + m_c}.\end{aligned}$$

Fig. 14. The differential cross sections for the single production of  $B_c$  and  $B_c^*$  mesons in  $p\bar{p}$ -interactions at the energy 1.8 TeV; (a)  $d\sigma/dy$ , where  $y$  is the particle rapidity, (b)  $d\sigma/dx$ , where  $x = 2E/s^{1/2}$



Table 27.

The total cross sections (in units  $10^{-2}$  pb) for the pair production of  $B_c$  mesons due to the quark-antiquark annihilation in  $p\bar{p}(pp)$  interactions at low energies

$\sqrt{s}$ , GeV	$\sigma(1^-, 1^-)$	$\sigma(1^-, 0^-)$	$\sigma(0^-, 0^-)$
30	0.9 (0.08)	0.24 (0.022)	0.006 (0.0004)
40	5.8 (0.94)	1.6 (0.25)	0.054 (0.007)
50	15.8 (3.5)	4.3 (0.95)	0.18 (0.034)

The numerical estimates of the total cross sections for the  $B_c$  production in  $p\bar{p}$  interactions are presented in Table 27.

Summing up the consideration of the hadronic production, one can draw the conclusions.

1. The mechanism of the hadronic  $B_c(B_c^*)$  production strongly differs from the production in  $e^+e^-$ -annihilation.
2. The relative fraction of the fragmentation contribution is low even in the region of large transverse momenta.
3. The vector state production is enforced in respect to  $e^+e^-$ -annihilation.

Thus, the hadronic  $B_c$  production requires the analysis for the large number of diagrams and its detailed study opens the possibility for the investigation of effects of the heavy quark dynamics in the higher orders of the QCD perturbation theory. As for the  $B_c$  yield at the real physical facilities, it is quite high, but the registration of the  $B_c$  events is essentially determined by the detector acceptance (cuts of the transverse momenta of particles, characteristics of the vertex detector and so on).

### 4.3. $B_c$ meson production in $\nu N$ -, $ep$ - and $\gamma\gamma$ - collisions

In the previous sections we have considered the  $B_c$  meson production in the processes, where one has the maximal current statistics for the production of hadrons with heavy quarks, i.e. at Fermilab and LEP colliders. In the present section we consider the estimates for the  $B_c$  meson production in the processes of the deep inelastic scattering of neutrino and electrons by nucleons and in  $\gamma\gamma$ -interactions at future facilities.

#### 4.3.1. $B_c$ production in $\nu N$ -interactions

The diagrams of the neutrino-production of the  $B_c$  mesons on quarks and gluons are shown on Figure 15.

Note, that for the  $B_c$  production in the neutrino collisions with gluons, the suppression of the partonic subprocess cross section by the factor  $|V_{bc}|^2$  in comparison with the partonic subprocess of the  $B_c$  neutrino-production on light quarks, is compensated by the more high luminosity of the gluonic subprocess in comparison with the quark one, so that the both mechanisms of the  $B_c$  production in the neutrino-nucleon scattering give the comparable contributions, and  $\sigma(\nu N \rightarrow B_c X) \approx 10^{-43}$  cm<sup>2</sup> at the neutrino energy  $E_\nu \approx 500$ –1000 GeV in the laboratory system.

Fig. 15. The diagrams of the  $B_c$  meson production in the processes of the neutrino scattering on gluons (a) and quarks (b)

After the integration over the valent parton  $d$  distribution, the  $c$ -quark production in the  $W^{*+}d \rightarrow c$  process, suppressed as  $\sin^2 \theta_c$ , has the value, comparable with the  $c$ -quark production in the  $W^{*+}s \rightarrow c$  process, since the strange quark "sea" is suppressed in respect to both the valent quark distribution and the "sea" of the more light  $d$ -quark.

The estimates of the  $B_c$  meson production cross sections, calculated on the basis of the diagrams on Figure 15, agree with the estimates, obtained in the model of the vector meson dominance (Figure 16) and in the model of the soft gluon emission of the  $(\bar{b}c)$  pair, that in the colour-singlet state and with the low invariant mass  $M(\bar{b}c) < M_B + M_D$ , transforms, in accordance with the quark-hadron duality, into the  $(\bar{b}c)$  bound state, which radiatively decays into the basic  $1S_0$  state in a cascade way with the probability, equal to 1.

As a result, one can reliably state that the total cross section for the  $B_c$  meson production in  $\nu N$ -collisions is of the order of  $10^{-6}$  from the total cross section of the  $\nu N$ -scattering, so that, at a characteristic statistics about  $10^6$  events in neutrino experiments, one can expect only several events with the  $B_c$  meson production.

#### 4.3.2. Production of $B_c$ mesons in $ep$ -scattering

In contrast to  $\nu N$ -scattering, in  $ep$ -collisions in addition to the processes of the weak charged current exchange, the main contribution into the  $B_c$  meson production will give the processes with the virtual  $\gamma$ -quanta exchange (Figure 17).

The exact calculation of the diagrams on Figure 17 is not yet performed at present. However, one can think that the estimate, made in the Monte Carlo simulation system for hadron production HERWIG [49], is quite reliable, since the HERWIG parameters have

Fig. 16. The diagrams of the  $B_c^*$  meson production in the model of vector meson dominance

been chosen to get correct values for total hadronic cross sections of the charmed and beauty particles production, being in an agreement with the experimental values. Moreover, the HERWIG estimates of the  $B_c$  production cross sections in  $e^+e^-$  and hadronic interactions agree with the values, obtained in the exact calculation of the diagrams in the QCD perturbation theory.

Thus, in accordance with the estimates in the HERWIG system, one can expect about  $10^3$  events per year with the  $B_c$  production at the HERA facilities. This  $B_c$  yield is comparably close to that of at LEP. However, the extraction of  $B_c$  events at HERA is complicated by the presence of a hadronic background, that is essentially lower at LEP.

### 4.3.3. Photonic production of $B_c$ mesons

At present, the future  $\gamma\gamma$ -colliders with the high luminosity ( $\sim 10^{34} \text{ cm}^{-2}\text{s}^{-1}$ ) are intensively discussed. In this section we calculate the cross section of single  $B_c$  production at energies  $\sqrt{s}$  about 30 GeV in accordance with the diagrams, shown on Figure 18. The calculation technique coincides with that of described in the section on the hadronic production of  $B_c$ .

The total cross sections of the  $B_c$  and  $B_c^*$  production are presented in Table 28, where one takes  $\alpha_S \approx 0.2$ . One can see that near threshold the pseudoscalar state production is suppressed in comparison with the production of the vector one, so at  $\sqrt{s} = 15$  GeV one has  $\sigma_{B_c^*}/\sigma_{B_c} \sim 55$ . Such behavior of the  $\sigma_{B_c^*}/\sigma_{B_c}$  ratio has been noted in [6], where the strong suppression of the pseudoscalar meson pair production in respect to the vector one takes place in the quark-antiquark annihilation. At large energies of the initial photons this ratio decreases and becomes  $\sigma_{B_c^*}/\sigma_{B_c} \sim 4$ . The inclusive cross sections  $\sigma_{B_c}$  and  $\sigma_{B_c^*}$  have the maximum at  $\sqrt{s} = 20 - 30$  GeV and with the  $s$  growth they fall like the total cross section for the heavy quarks  $\sigma_{b\bar{b}}$  production.

The distributions  $\sigma^{-1}d\sigma/dz$  over the variable  $z = 2|\mathbf{p}|/\sqrt{s}$ , with  $\mathbf{p}$  being the meson momentum, are shown on Figures 19 and 20 for the  $B_c$  and  $B_c^*$  mesons. As follows from these figures the scaling in these distributions is broken: with the energy growth the shift onto the low  $z$  values takes place. Note, the analogous picture has been observed in the gluonic production of  $B_c$  mesons.

Note, that the detailed consideration shows, that in the matrix element of the  $\gamma\gamma \rightarrow b\bar{b}c\bar{c}$  process and hence in the  $\gamma\gamma \rightarrow B_c\bar{b}c$  matrix element one can distinguish three groups of contributions, which are separately gauge invariant under both the gluon field transformation and the photon one. The first group of contributions is composed of the diagrams when the quark production is independent (we will label these diagrams

Fig. 17. The diagrams of the  $B_c$  meson production in parton process of  $\gamma^*g$ -scattering

Fig. 18. The types of diagrams in the photonic production of  $B_c$  mesons

as the recombination diagrams), the second group consist of the diagrams, where the  $(c\bar{c})$  pair is produced from the  $b$ -quark line (we will mark these diagrams as the  $b$ -quark fragmentation diagrams, their contribution will be denoted as  $\sigma^{b-frag}$ ), the third group contains the diagrams with the  $(b\bar{b})$  pair production from the  $c$ -quark line, so that they are  $c$ -fragmentation diagrams with the corresponding contributions denoted as  $\sigma^{c-frag}$ .

In refs.[43,91,93] the assumption was offered that the  $b$ -fragmentation contribution has to dominate at large values of the  $B_c$  transverse momentum, independently of the type of the process. So the approximate equation has to be valid:

$$\frac{d\sigma_{B_c}^{q-frag}}{dP_t} = \int_{2P_t/\sqrt{s}}^1 \frac{d\sigma_{q\bar{q}}}{dk_t} \left(\frac{P_t}{z}\right) \cdot \frac{D_{q \rightarrow B_c}(z)}{z} dz, \quad (214)$$

where  $d\sigma_{q\bar{q}}/dk_t$  is the differential cross section for the production of the fragmenting  $q$ -quark in the Born approximation,  $k_t$  is its transversal momentum, and  $D_{q \rightarrow B_c}(z)$  is the function of the  $q \rightarrow B_c + X$  fragmentation.

Remind that in the  $e^+e^-$ -annihilation the  $b$ -quark fragmentation dominates and the  $c$ -quark fragmentation contribution is suppressed by two orders of magnitude. In the  $\gamma\gamma$ -interactions, the  $c$ -quark fragmentation contribution is enlarged due to the quark charge ratio  $(Q_c/Q_b)^4 = 16$  and, therefore we can not neglect it (as one does in  $e^+e^-$ -annihilation). Note further, that the  $c$ -quark fragmentation contribution and the  $b$ -quark fragmentation one are related to each other by the simple permutation of the quark masses and charges ( $m_c \leftrightarrow m_b$  and  $Q_c \leftrightarrow Q_b$ ) (214).

The distributions  $d\sigma/dp_t$ ,  $d\sigma^{c-frag}/dp_t$  and  $d\sigma^{b-frag}/dp_t$  at 100 GeV for the  $B_c$  and  $B_c^*$  meson production are shown on Figures 21 and 22. The distributions, predicted in accordance with eq.(214) for the  $b$ -fragmentation (curve 1) and  $c$ -fragmentation (curve 2) are also shown. One can see that, as in the hadronic production, the contribution of the recombinational type diagram is essential at any reasonable values of the transverse momentum of  $B_c$  meson and it can not be neglected, when one calculates the cross sections

Table 28. The cross section (in pb) of the photonic production of  $B_c$  ( $B_c^*$ )

$\sqrt{s}$ , GeV	15	20	40	100
$\sigma_{B_c}$	$5.1 \cdot 10^{-3}$	$3.8 \cdot 10^{-2}$	$6.7 \cdot 10^{-2}$	$2.5 \cdot 10^{-2}$
$\sigma_{B_c^*}$	$2.8 \cdot 10^{-1}$	$6.0 \cdot 10^{-1}$	$4.0 \cdot 10^{-1}$	$1.1 \cdot 10^{-1}$

Fig. 19. The cross section distributions, normalized to the unit, over  $z$  for the  $B_c$  meson production at different energies

even at the large transverse momenta. One can see from the figure, that for the  $b$ -fragmentation contribution over the  $p_t$ , greater than about 30 GeV, the fragmentational mechanism gives correct predictions. Thus, in its maximum at the energy 20-30 GeV the total cross section, including the  $B_c^*$  and corresponding antiparticle production, is about 1 pb. This corresponds to  $10^5$   $B_c$ , produced at the  $\gamma\gamma$ -collider with luminosity of

Fig. 20. The cross section distributions, normalized to the unit, over  $z$  for the  $B_c^*$  meson production at different energies

Fig. 21.

The  $d\sigma/dp_t$ ,  $d\sigma^{c\text{-frag}}/dp_t$  and  $d\sigma^{b\text{-frag}}/dp_t$  distributions over the transverse momentum for the invariant contributions into the cross section of the  $B_c$  meson production at 100 GeV. The curves 1 and 2 correspond to the prediction of the fragmentational mechanism (217) for the  $b$ -quark (1) and  $c$ -quark (2)

Fig. 22.

The  $d\sigma/dp_t$ ,  $d\sigma^{c\text{-frag}}/dp_t$  and  $d\sigma^{b\text{-frag}}/dp_t$  distributions over the transverse momentum for the invariant contributions into the cross section of the  $B_c^*$  meson production at 100 GeV. The curves 1 and 2 correspond to the prediction of the fragmentational mechanism (217) for the  $b$ -quark (1) and  $c$ -quark (2)

$10^{34} \text{cm}^{-2} \text{s}^{-1}$ . At large energies, the cross section falls like the  $b\bar{b}$  pair production one. The  $B_c$  production mechanism is close to that of in the gluon-gluon interactions, and it does not come to the simple  $b$ -quark fragmentation.

## 5. Conclusion

The discovery and study of the family of  $(\bar{b}c)$  heavy quarkonium with the open charm and beauty will allow one significantly to specify the notion of the dynamics of the heavy quark interactions and the parameters of the Standard Model of elementary particles (such values as the  $b$ - and  $c$ -quark masses, the coupling of the  $b$ - and  $c$ -quarks –  $|V_{bc}|$  etc.). The present review tends to the aim of a creation of a theoretical basis for the object-directed experimental search and study of the  $(\bar{b}c)$  heavy quarkonium family.

Summing the considered problems, one can note the following.

We have shown that below the threshold of the  $(\bar{b}c)$  system decay into the  $BD$  meson pair, there are 16 narrow states of the  $B_c$  meson family, whose masses can be reliably calculated in the framework of the nonrelativistic potential models of the heavy quarkonia. The flavour independence of the QCD-motivated potentials in the region of average distances between the quarks in the  $(\bar{b}b)$ ,  $(\bar{c}c)$  and  $(\bar{b}c)$  systems and their scaling properties allow one to find the regularity of the spectra for the levels, nonsplitted by the spin-dependent forces: in the leading approximation the state density of the system does not depend on the heavy quark flavours, i.e. the distances between the nL-levels of the heavy quarkonium do not depend on the heavy quark flavours.

We have described the spin-dependent splittings of the  $(\bar{b}c)$  system levels, i.e. the splittings, appearing in the second order over the inverse heavy quark masses,  $V_{SD} \approx O(1/m_b m_c)$ , with account of the variation of the effective Coulomb coupling constant of the quarks (the interaction is due to relativistic corrections, coming from the one gluon exchange).

The approaches, developed to describe emission by the heavy quarks, have been applied to the description of the radiative transitions in the  $(\bar{b}c)$  family, whose states have no electromagnetic or gluonic channels of annihilation. The last fact means that, due to the cascade processes with the emission of photons and pion pairs, the higher excitations decay into the lightest pseudoscalar  $B_c$  meson, decaying in the weak way. Therefore, the excited states of the  $(\bar{b}c)$  system have the widths, essentially less (by two orders of magnitude) than those in the charmonium and bottomonium systems.

As for the value of the leptonic decay constant  $f_{B_c}$ , it can be the most reliably estimated from the scaling relation for the leptonic constants of the heavy quarkonia, due to the relation, obtained in the framework of the QCD sum rules in the specific scheme. In the other schemes of the QCD sum rules, it is necessary to do an interpolation of the scheme parameters (the hadronic continuum threshold and the number of the spectral density moment or the Borel parameter) into the region of the  $(\bar{b}c)$  system, so this procedure leads to the essential uncertainties. The  $f_{B_c}$  estimate from the scaling relation agrees with the results of the potential models, whose accuracy for the leptonic constants is notably lower. The value of  $f_{B_c}$  essentially determines the decay widths and the production cross sections of the  $B_c$  mesons.

The theoretical consideration of semileptonic  $B_c$  decays shows, that the results of the potential quark models agree with the predictions of the QCD sum rules, if one accounts for the Coulomb-like  $\alpha_S/v$ -corrections. In this case, the approximate spin symmetry in the sector of heavy quarks allows one to derive the relations for the form factors of semileptonic  $B_c$  decays in the rest point of the recoil meson.

The  $B_c$  meson production allows in some cases the description on the level of analytical expressions, such as the universal functions of the heavy quark fragmentation into the heavy quarkonium. The fragmentational mechanism dominates in the  $B_c$  production in the  $e^+e^-$ -annihilation at high energies (in the peak of  $Z$  boson) and it can be studied at the LEP facilities.

The hadronic production of  $B_c$  is basically determined by the processes of the  $\bar{b}$ - and  $c$ -quark recombination, since the partonic subprocesses have the most large luminosity in the region of low invariant masses of the produced system ( $b\bar{b}c\bar{c}$ ). The  $B_c$  meson yield in respect to the production of the beauty hadrons is of the order<sup>2</sup> of  $10^{-3}$ .

Modes of  $B_c \rightarrow \psi X$  decays with the characteristic signature of the  $J/\psi$  particle have the quite large probability

$$BR(B_c^+ \rightarrow \psi X) \approx 0.2 .$$

Therefore, the  $B_c$  particle search can start from the separation of the events, containing the  $J/\psi$  particle, whose production vertex is beyond the primary intersection point. The selected set of the events will, of course, contain the background from decays of ordinary heavy-light  $B$  mesons ( $\bar{b}u$ ,  $\bar{b}d$ ,  $\bar{b}s$ ), since the probability of the  $B \rightarrow J/\psi K X$  decay is about 1 %, and the heavy-light  $B$  meson yield is three orders of magnitude greater than the  $B_c$  one. The background separation requires the down-cut over the effective mass of the  $J/\psi X$  system, where  $X$  denotes the charged particles, having tracks from the  $J/\psi$  vertex. The most preferable channel for the  $B_c$  extraction is that of the  $B_c^+ \rightarrow \psi l^+ \nu_l$  decay, since  $B_c$  is the only heavy particle with the three lepton vertex of the decay  $\psi l^+ \rightarrow l'^+ l'^- l^+$ . The probability of this channel is equal to

$$BR(B_c^+ \rightarrow \psi l^+ \nu_l) \approx 8 \% , \quad l = e, \mu, \tau .$$

At a quite large statistics<sup>3</sup> the events with the decay  $B_c^+ \rightarrow \psi l^+ \nu$  can give the possibility for the determination of the  $B_c$  mass value under the  $\psi l$  mass spectrum or the missed transverse momentum of neutrino in respect to the direction of the  $B_c$  motion (see Figure 23). The necessary condition for the such measurement is a quite high separation of charged hadrons and leptons.

The straightforward measurement of the  $B_c$  mass can be made in the mode of the  $B_c^+ \rightarrow J/\psi \pi^+$  decay, having the branching ratio, equal to

$$BR(B_c^+ \rightarrow \psi \pi^+) \approx 0.2 \% .$$

---

<sup>2</sup>In the present review we do not consider in details the  $B_c$  production in the neutrino-nucleon interactions, where one can expect only several events with the  $B_c$  production per year, since the coupling constant of the  $b$ - and  $c$ -quarks is low [52], so that these processes have no practical significance for the experimental search of  $B_c$ .

<sup>3</sup>The CDF facility with the vertex detector at the Tevatron FNAL has, in this sense, a preferable position.



Fig. 23.

The distribution over the invariant masses of the  $\psi l$  (a) and  $\psi l \nu_{mis}$  (b) systems in the  $B_c^+ \rightarrow \psi l^+ \nu_l$  decay, where  $\nu_{mis}$  is the neutrino with the momentum, equal to the missed transverse momentum in respect to the direction of the  $B_c$  meson motion

The mode of the  $B_c^\pm \rightarrow J/\psi \pi^\pm \pi^\pm \pi^\mp$  decay, where three  $\pi$  mesons can compose the  $a_1$  meson, also is of the interest. This mode must have a significantly greater probability, than the  $B_c \rightarrow J/\psi \pi$  decay.

Since the  $B_c$  production at the colliding  $e^+e^-$  beams takes, as mentioned, the fragmentational character, in general (see Figure 7), it must be accompanied by the  $D$  meson presence in the same jet, where the  $B_c$  candidate is being observed. Such signature of the event would turn out to give a large advantage for the  $B_c$  meson search at  $e^+e^-$  colliders in respect to the search at hadron colliders, where the recombinational mechanism dominates in the  $B_c$  meson production at the accessible energies in the nearest future (see Figure 9). However, one must take into account the possibility of that the probability of the  $b$ -quark fragmentation production of the free  $c\bar{c}$ -quark pair is one order of magnitude greater than the probability of the fragmentation into the  $B_c$  meson and the single free  $c$ -quark. This means, that with account for the branching ratios for the  $B$  and  $B_c$  decays into  $J/\psi X$ , the events with the  $B_c$  decay and the single  $D$  meson will appear only two times more often, than the decay of the heavy-light  $B$  meson into  $J/\psi X$  with the instantaneous production of two  $D$  mesons in the same jet. It is not clear, whether one can quite effectively separate these two processes at the present of the vertex detectors, i.e. whether one can not lose the vertex of the second  $D$  meson.

It is evident, that the progress in the experimental study of the  $B_c$  meson and general physics of the heavy quarks will be mainly related with the development of the vertex detectors, so that the latter would give the possibility of a reliable observation of several heavy quarks instantaneously (to search the cascade decays, for example). However, since at the present statistics of LEP and Fermilab, several dozens of the  $B_c$  meson production events must be observed, one can think, that the practical registration of  $B_c$  will be

realized in the nearest future.

In the conclusion the authors express their gratitude to O.P.Youshchenko for the discussions and a help in the preparing of the paper. One of the authors (AKL) thanks his collaborators A.V.Berezhnoy and M.V.Shevlyagin.

This work was partially supported by the ISF grant NJQ000.

## 6. Appendices

### I. Covariant quark model

Consider the general statements of the covariant description of the composed quarkonium model.

By definition, the energy fraction, carrying out by the quark  $i$  in the  $(Q\bar{Q}')$  meson, is its constituent mass  $m_i$ , so that

$$M = m + m' , \quad (\text{I.1})$$

where  $M$  is the meson mass,  $m$  and  $m'$  are the fixed values. For the four-momenta, one has

$$\begin{aligned} k &= \frac{m}{M} P + q , \\ k' &= \frac{m'}{M} P - q , \end{aligned} \quad (\text{I.2})$$

where  $P$  is the meson momentum,  $q$  is the relative momentum of quarks inside the meson.

For the quark propagator, one has

$$S(k) = (k_\mu \gamma^\mu + m) D(k) . \quad (\text{I.3})$$

The constituent quark has, in fact, the fixed energy, so that in the  $D(k)$  function, only the imaginary part gives the contribution. In the meson rest frame, one has

$$\Im m D(k) = \frac{\pi}{m} \delta(|k_0| - m) . \quad (\text{I.4})$$

Eq.(I.4) with account for eq.(I.2) can be rewritten in the covariant form

$$\Im m D(k) = \frac{\pi M}{m} \delta(Pq) . \quad (\text{I.5})$$

The quark-meson vertex can be represented as

$$L_{q\bar{q}M} = \bar{v}(k) \Gamma v'(k') D^{-1}(k) D^{-1}(k') \chi(P; q) , \quad (\text{I.6})$$

where  $v$  and  $v'$  are the quark spinors, the  $D(k)$  function is defined in eq.(I.3),  $\Gamma$  is the spinor matrix, determining the quantum numbers of meson.

The nonrelativistic description of the meson means, that the form factor is determined by the expression

$$\chi(P; q) = 2\pi \delta(Pq) \phi(q^2) . \quad (\text{I.7})$$

In the following, we suppose

$$\phi(q^2) = N \exp\left(\frac{q^2}{\omega^2}\right). \quad (\text{I.8})$$

The choice (I.8) reflects the typical form of the  $S$ -wave functions of the charmonium and bottomonium, and it allows one to perform the analytical calculation of the semileptonic decay widths for  $B_c$  meson.

Let us define the decay constants  $f$  for the pseudoscalar and vector mesons

$$\langle 0 | J_{5\mu}(x) | P(q) \rangle = if_P q_\mu \exp\{iqx\}, \quad (\text{I.9})$$

$$\langle 0 | J_\mu(x) | V(q, \lambda) \rangle = if_V M_V \epsilon_\mu^{(\lambda)} \exp\{iqx\}, \quad (\text{I.10})$$

where  $\lambda$  is the vector meson polarization, and the quark currents are

$$J_{5\mu}(x) = \bar{Q}(x) \gamma_5 \gamma_\mu Q'(x), \quad (\text{I.11})$$

$$J_\mu(x) = \bar{Q}(x) \gamma_\mu Q'(x), \quad (\text{I.12})$$

In the nonrelativistic potential model, one has

$$f_P \approx f_V = f, \quad (\text{I.13})$$

so that

$$f = 2\sqrt{\frac{3}{M}} \Psi(\mathbf{0}), \quad (\text{I.14})$$

where  $\Psi(\mathbf{0})$  is the quarkonium wave function at origin. The oscillator function, resulting in eq.(I.8), has the form

$$\Psi(\mathbf{r}) = \left(\frac{\omega^2}{2\pi}\right)^{3/4} \exp\left(-\frac{r^2\omega^2}{4}\right). \quad (\text{I.15})$$

Condition (I.14) means that the normalization constant  $N$  in eq.(I.8) equals

$$N = \frac{M}{m m'} \frac{\sqrt{6}}{f}. \quad (\text{I.16})$$

Thus, for the quark-meson form factor, one finds

$$\chi(P; q) = 2\pi \delta(Pq) \frac{M}{m m'} \frac{\sqrt{6}}{f} \exp\left(\frac{q^2}{\omega^2}\right), \quad (\text{I.17})$$

where  $\omega$  is determined by eqs.(I.14) and (I.15), so that the only free parameter of the model is the constant  $f$ . For the  $\psi$  particle,  $f_\psi$  can be, for example, related with the width of the  $\psi \rightarrow e^+e^-$  decay

$$\Gamma(\psi \rightarrow e^+e^-) = \frac{4\pi}{3} \alpha_{\text{em}}^2 e_c^2 \frac{f_\psi^2}{M_\psi}, \quad (\text{I.18})$$

where  $e_c = 2/3$  is the  $c$ -quark electric charge. From eq.(I.18), the experimental value of the leptonic width [15] gives

$$f_\psi = 410 \pm 15 \text{ MeV}. \quad (\text{I.19})$$

As for the  $f_{B_c}$  and  $f_{B_s}$  values, these constants are determined theoretically in the framework of the QCD sum rules and in the potential models.

Note, that the stated model of composed quarkonium gives, for instance, the exact formula of the nonrelativistic M1-transition for the electromagnetic decay of the vector state into the pseudoscalar one  $V \rightarrow P\gamma$

$$\Gamma(V \rightarrow P\gamma) = \frac{16}{3} \mu^2 \omega_\gamma^3, \quad (\text{I.20})$$

where  $\omega_\gamma$  is the  $\gamma$ -quantum energy, and the magnetic moment  $\mu$  equals

$$\mu = \frac{1}{2} \sqrt{\alpha_{\text{em}}} \left( \frac{e}{2m} + \frac{e'}{2m'} \right), \quad (\text{I.21})$$

where  $e$  and  $e'$  are the quark electric charges in the units of the electron charge.

## II. Spectral densities for three-particle functions

The spectral densities for the three-particle functions are determined in the following way [36]

$$\begin{aligned} \rho_+(s_1, s_2, Q^2) = & \frac{3}{2k^{3/2}} \left\{ \frac{k}{2} (\Delta_1 + \Delta_2) - k[m_3(m_3 - m_1) + \right. \\ & m_3(m_3 - m_2)] - [2(s_1\Delta_2 + s_2\Delta_1) - u(\Delta_1 + \Delta_2)] \\ & \left. \left[ m_3^2 - \frac{u}{2} + m_1m_2 - m_2m_3 - m_1m_3 \right] \right\} \end{aligned} \quad (\text{II.1})$$

$$\begin{aligned} \rho_V(s_1, s_2, Q^2) = & \frac{3}{k^{3/2}} \left\{ (2s_1\Delta_2 - u\Delta_1)(m_3 - m_2) + (2s_2\Delta_1 - u\Delta_2) \right. \\ & \left. (m_3 - m_1) + m_3k \right\} \end{aligned} \quad (\text{II.2})$$

$$\begin{aligned} \rho_0^A(s_1, s_2, Q^2) = & \frac{3}{k^{1/2}} \left\{ (m_1 - m_2) \left[ m_3^2 + \frac{1}{k} (s_1\Delta_2^2 + s_2\Delta_1^2 - u\Delta_1\Delta_2) \right] - \right. \\ & m_2 \left( m_3^2 - \frac{\Delta_1}{2} \right) - m_1 \left( m_3^2 - \frac{\Delta_2}{2} \right) + \\ & \left. m_3 \left[ m_3^2 - \frac{1}{2} (\Delta_1 + \Delta_2 - u) + m_1m_2 \right] \right\} \end{aligned} \quad (\text{II.3})$$

$$\begin{aligned} \rho_+^A(s_1, s_2, Q^2) = & \frac{3}{k^{3/2}} \left\{ m_1 \left[ 2s_2\Delta_1 - u\Delta_2 + 4\Delta_1\Delta_2 + 2\Delta_2^2 \right] + \right. \\ & m_1m_3^2 \left[ 4s_2 - 2u \right] + m_2 \left[ 2s_1\Delta_2 - u\Delta_1 \right] - m_3 \left[ 2(3s_2\Delta_1 + s_1\Delta_2) - \right. \\ & u(3\Delta_2 + \Delta_1) + k + 4\Delta_2\Delta_1 + 2\Delta_2^2 + m_3^2(4s_2 - 2u) \left. \right] + \\ & \frac{6}{k} (m_1 - m_3) \left[ 4s_1s_2\Delta_1\Delta_2 - u(2s_2\Delta_1\Delta_2 + s_1\Delta_2^2 + s_2\Delta_1^2) + \right. \\ & \left. 2s_2(s_1\Delta_2^2 + s_2\Delta_1^2) \right] \left. \right\}. \end{aligned} \quad (\text{II.4})$$

where

$$\begin{aligned}
k &= (s_1 + s_2 + Q^2)^2 - 4s_1s_2, \\
u &= s_1 + s_2 + Q^2, \\
\Delta_1 &= s_1 - m_1^2 + m_3^2, \\
\Delta_2 &= s_2 - m_2^2 + m_3^2.
\end{aligned}$$

In the  $B_c \rightarrow \eta_c(J/\psi)e\nu$  decays, one has  $m_1 = m_b$  and  $m_2 = m_3 = m_c$  for the masses.

### III. QCD sum rule scheme for three-point correlators

Let us consider the sum rules for the  $f_+(Q^2)$  form factor

$$\begin{aligned}
\sum_{i,j=1}^{\infty} f_{B_c}^i \frac{M_{B_c}^{i-2}}{m_b + m_c} f_{\eta_c}^j \frac{M_{\eta_c}^{j-2}}{2m_c} f_+^{ij}(Q^2) \frac{1}{(M_{B_c}^{i-2} - p_1^2)(M_{\eta_c}^{j-2} - p_2^2)} = \\
\frac{1}{(2\pi)^2} \int \frac{\rho_+(s_1, s_2, Q^2)}{(s_1 - p_1^2)(s_2 - p_2^2)} ds_1 ds_2. \quad (\text{III.1})
\end{aligned}$$

Applying the Borel operators  $\hat{L}_{\tau_1}(-p_1^2)$  and  $\hat{L}_{\tau_2}(-p_2^2)$ , defined in Section 2, to eq.(III.1), one derives the following sum rules

$$\begin{aligned}
\sum_{i,j=1}^{\infty} f_{B_c}^i M_{B_c}^{i-2} f_{\eta_c}^j M_{\eta_c}^{j-2} f_+^{ij}(Q^2) \exp(-M_{B_c}^{i-2} \tau_1 - M_{\eta_c}^{j-2} \tau_2) = \\
= \frac{2(m_b + m_c)m_c}{(2\pi)^2} \int ds_1 ds_2 \rho_+(s_1, s_2, Q^2) \exp(-s_1 \tau_1 - s_2 \tau_2) \quad (\text{III.2})
\end{aligned}$$

Introduce the notation

$$S_i = \sum_{j=1}^{\infty} f_{\eta_c}^j M_{\eta_c}^{j-2} f_+^{ij}(Q^2) \exp(-M_{\eta_c}^{j-2} \tau_2) \quad (\text{III.3})$$

and transform the left hand side of eq.(III.2) with the use of the formula by Euler-MacLaurin [90]

$$\begin{aligned}
\sum_{i=1}^{\infty} f_{B_c}^i M_{B_c}^{i-2} S_i \exp(-M_{B_c}^{i-2} \tau_1) = \int_{M_{B_c}^k}^{\infty} dM_{B_c}^n \frac{dn}{dM_{B_c}^n} f_{B_c}^n M_{B_c}^{n-2} S_n \exp(-M_{B_c}^{n-2} \tau_1) \\
+ \sum_{n=0}^{n=k-1} f_{B_c}^n M_{B_c}^{n-2} S_n \exp(-M_{B_c}^{n-2} \tau_1) + \dots \quad (\text{III.4})
\end{aligned}$$

Acting by  $\hat{L}_{\tau'}((M_{B_c}^k)^2)$  to eq.(III.2) and accounting for eq.(III.4), one gets

$$\begin{aligned}
\sum_{j=1}^{\infty} f_{\eta_c}^j M_{\eta_c}^{j-2} f_+^{kj}(Q^2) \exp(-M_{\eta_c}^{j-2} \tau_2) = \\
= \frac{2m_c(m_b + m_c)}{(2\pi)^2} \frac{dM_{B_c}^k}{dk} \frac{2}{M_{B_c}^k f_{B_c}^k} \int \rho(M_{B_c}^{k-2}, s_2, Q^2) \exp(-s_2 \tau_2) \quad (\text{III.5})
\end{aligned}$$

Making the analogous procedure for the sum of the  $\eta_c^i$  resonances, one obtains

$$f_+^{kl}(Q^2) = \frac{8m_c(m_b + m_c)}{M_{B_c}^k M_{\eta_c}^l} \frac{dM_{B_c}^k}{dk} \frac{dM_{\eta_c}^l}{dl} \frac{1}{(2\pi)^2} \rho_+(M_{B_c}^k{}^2, M_{\eta_c}^l{}^2, Q^2) \quad (\text{III.6})$$

Here we have used the property of the Borel operator

$$\hat{L}_\tau(x)(x^n \exp(-bx)) \rightarrow \delta_+^{(n)}(\tau - b) .$$

It is not complex to generalize this procedure for the remaining form factors.

## References

1. Weinberg S *Phys.Rev.Lett.* **19** 1264 (1967);  
Salam A in *Proc. 8-th Nobel Symp. (Stokholm, 1968) p.367*;  
Glashow S L, Iliopoulos J, Maiani I *Phys.Rev.D* **2** 1285 (1970)
2. Higgs P N *Phys.Lett. C* **12** 132 (1964);  
Englert F, Brout R *Phys.Rev.Lett.* **13** 321 (1964);  
Guralnik G S, Hagen C R, Kibble T W *Phys.Rev.Lett.* **13** 385 (1964)
3. Golfand Yu A, Likhtman E P *Pisma Zh.Exp.Teor.Fiz.* **13** 452 (1971);  
Volkov D V, Akulov V P *Pisma Zh.Exp.Teor.Fiz.* **16** 621 (1972);  
Wess J, Zumino B *Nucl.Phys.B* **70** 39 (1974)
4. Fritzsche H, Gell-Mann M, Leutwyler H *Phys.Lett.B* **47** 365 (1973);  
Weinberg S *Phys.Rev.Lett.* **31** 494 (1973)
5. Eichten E et al. *Phys.Rev.D* **17** 3090 (1979), **21** 203 (1980)
6. Godfrey S, Isgur N *Phys.Rev.D* **32** 189 (1985)
7. Richardson J L *Phys.Lett.B* **82** 272 (1979)
8. Martin A *Phys.Lett.B* **93** 338 (1980)
9. Quigg C, Rosner J L *Phys.Lett.B* **71** 153 (1977)
10. Buchmüller W, Tye S-H H *Phys.Rev.D* **24** 132 (1981)
11. Shifman M A, Vainshtein A I, Zakharov V I *Nucl.Phys.B* **147** 345, 448 (1979);  
Reinders L J, Rubinshtein H, Yazaki S *Phys.Rep.* **127** 1 (1985);  
Narison S *Phys.Lett.B* **198** 104 (1987);  
Dominguez C A, Paver N *Phys.Lett.B* **197** 423 (1987), **199** 596 (1987)
12. Shuryak E V *Nucl.Phys.B* **198** 83 (1982);  
Aliev T M, Eletski V L *Yad.Fiz.* **38** 1537 (1983) [*Sov.J.Nucl.Phys.* **38** 936 (1983)];  
Reinders L J *Phys.Rev.D* **38** 947 (1988)
13. Shifman M A *Uspekhi Fiz.Nauk* **151** 193 (1987) [*Sov.Phys.Uspekhi* **30** 91 (1987)]

14. Nussinov S, Wentzel W *Phys.Rev.D* **36** 130 (1987);  
 Voloshin M B, Shifman M A *Sov.J.Nucl.Phys.* **45** 292 (1987), **47** 511 (1988);  
 Lepage G P, Thacker B A *Nucl.Phys.B(Proc.Suppl.)* **4** 199 (1988);  
 Eichten E *Nucl.Phys.B(Proc.Suppl.)* **4** 170 (1988);  
 Politzer H D, Wise M B *Phys.Lett.B* **206** 681 (1988), **208** 504 (1988);  
 Isgur N, Wise M B *Phys.Lett.B* **232** 113 (1989), **237** 527 (1990);  
 Eichten E, Hill B *Phys.Lett.B* **239** 511 (1990);  
 Georgi H *Phys.Lett.B* **240** 447 (1990);  
 Grinstein B *Nucl.Phys.B* **239** 253 (1990), **240** 447 (1990);  
 Bjorken J D *SLAC-PUB-5278 Invited Talk at Recontre de Physique de la Vallee d'Acoste* (La Thuile, Italy, 1990);  
 Bjorken J D, Dunietz I, Taron J *Nucl.Phys.B* **371** 111 (1992);  
 Nuebert M *Nucl.Phys.B* **371** 199 (1992);  
 Isgur N, Wise M B Preprint CEBAF-TH-92-10 (1992); in B Deacays, Ed. S.Stone (Singapore, World Scientific: 1992) p.158;  
 Broadhurst D J, Grozin A G *Phys.Lett.B* **267** 105 (1991);  
 Rosner J L *Phys.Rev.D* **42** 3732 (1990);  
 Mannel T, Roberts W, Ryzak Z *Phys.Lett.B* **254** 274 (1991);  
 Neubert M *Phys.Lett.B* **264** 455 (1991)
15. Hikasa K et al., PDG. *Phys.Rev.D* **45(II)** S1 (1992)
16. Vainshtein A I et al. *Uspekhi Fiz.Nauk* **123** 214 (1977);  
 Bykov A A, Dremin I M, Leonidov A V *Uspekhi Fiz.Nauk* **143** 3 (1986)
17. Novikov V A et al. *Phys.Rep.C* **41** 1 (1978)
18. Nir Y Preprint SLAC-PUB-5874 (Stanford, 1992)
19. Lee-Franzini L, Franzini P J Preprint LNF-93/064(P) (Frascati, 1993)
20. Eichten E Preprint FERMILAB-Conf-85/29-T (1985)
21. Kiselev V V *Nucl.Phys.B* **406** 340 (1993)
22. Kiselev V V Preprint IHEP 94-63 (Protvino, 1994)
23. Gottfried K *Phys.Rev.Lett.* **40** 598 (1978);  
 Voloshin M B *Nucl.Phys.B* **154** 365 (1979);  
 Peskin M *Nucl.Phys.B* **156** 365 (1979)
24. Yan T-M *Phys.Rev.D* **22** 1652 (1980);  
 Kuang Y-P, Yan T-M *Phys.Rev.D* **24** 2874 (1981), **41** 155 (1990);  
 Kuang Y-P, Tuan S F, Yan T-M *Phys.Rev.D* **37** 1210 (1988)
25. Voloshin M B, Zakharov V I *Phys.Rev.Lett.* **45** 688 (1980);  
 Novikov V A, Shifman M A *Z.Phys.C* **8** 43 (1981)
26. Brown L S, Chan R N *Phys.Rev.Lett.* **35** 1 (1975);  
 Voloshin M B, *JETP Lett.* **21** 347 (1975)

27. Abrams G S et al. *Phys.Rev.Lett.* **34** 1181 (1975);  
 Green J et al., CLEO Collab. *Phys.Rev.Lett.* **49** 617 (1982);  
 Bowcock G et al., CLEO Collab. *Phys.Rev.Lett.* **58** 307 (1987);  
 Brock I C et al., CLEO Collab. *Phys.Rev.D* **43** 1448 (1991);  
 Wu Q W et al., CUSB-II Detector. *Phys.Lett.B* **301** 307 (1993);  
 Albrecht H et al., ARGUS Collab. *Z.Phys.C* **35** 283 (1987)
28. Voloshin M B *Pisma Zh.Exp.Teor.Fiz.* **37** 58 (1983);  
 Belanger G, DeGrand T, Moxhay P *Phys.Rev.D* **39** 257 (1989);  
 Lipkin H J, Tuan S F *Phys.Lett.B* **206** 349 (1988);  
 Moxhay P *Phys.Rev.D* **39** 3497 (1989);  
 Kiselev V V, Likhoded A K Preprint IHEP 94-46 (Protvino, 1994);  
 Zhou H-Y, Kuang Y-P *Phys.Rev.D* **44** 756 (1991)
29. Kiselev V V, Tkabladze A V *Yad.Fiz.* **48** 536 (1988)
30. Kiselev V V, Likhoded A K, Tkabladze A V *Yad.Fiz.* **56** 128 (1993)
31. Kiselev V V, Tkabladze A V *Phys.Rev.D* **48** 5208 (1993)
32. Du D, Wang Z *Phys.Rev.D* **39** 1342 (1989)
33. Jibuti G R, Esakia Sh M, *Yad.Fiz.* **50** 1065 (1989), **51** 1681 (1990)
34. Lusignoli M, Masetti M *Z.Phys.C* **51** 549 (1991)
35. Bagan E et al. Preprint CERN-TH.7141/94, 1994
36. Colangelo P, Nardulli G, Paver N *Z.Phys.C* **57** 43 (1993)
37. Jenkins E et al. *Nucl.Phys.B* **390** 463 (1993)
38. Kiselev V V, Likhoded A K, Tkabladze A V *Yad.Fiz.* **46** 934 (1987)
39. Kiselev V V Preprint IHEP 93-75 (Protvino, 1993)
40. Kartvelishvili V G, Chikovani E G, Esakia Sh M **19** 139 (1988)
41. Clavelli L *Phys.Rev.D* **26** 1610 (1982);  
 Ji Ch-R, Amiri F *Phys.Rev.D* **35** 3318 (1987)
42. Chang C-H, Chen Y-Q *Phys.Rev.D* **46** 3845 (1992); *Phys.Lett.B* **284** 127 (1992)
43. Braaten E, Cheung K, Yuan T C *Phys.Rev.D* **48** 5049 (1993)
44. Kiselev V V, Likhoded A K, Shevlyagin M V, *Yad.Fiz.* **57** 733 (1994)
45. Chen Y-Q *Phys.Rev.D* **48** 5181 (1993)
46. Berezhnoy A V, Likhoded A K, Shevlyagin M V Preprint IHEP 94-48 (Protvino, 1994)



47. Kiselev V V, Likhoded A K, Shevlyagin M V Preprint IHEP 94-10 (Protvino, 1994)
48. Falk A, Luke M, Savage M, Wise M *Phys.Lett.B* **312** 486 (1993);  
Cheung K, Yuan T Ch Preprint NUHEP-TH-94-7 (Evanston, 1994)
49. Lusignoli M, Masetti M, Petrarca S *Phys.Lett.B* **266** 142 (1991)
50. Danilov M Preprint ITEP 92-93, (Moscow, 1993)
51. Likhoded A K, Slabospitsky S R, Mangano M, Nardulli G *NIM A* **333** 209 (1993)
52. Gershtein S S, Kiselev V V, Likhoded A K, Slabospitsky S R, Tkabladze A V  
*Yad.Fiz.* **48** 515 (1988) [*Sov.J.Nucl.Phys.* **48** 326 (1988)];  
Gershtein S S, Likhoded A K, Slabospitsky S R *Int.J.Mod.Phys.A* **6(13)** 2309  
(1991)
53. Eichten E, Quigg C Preprint FERMILAB-PUB-94/032-T, hep-ph/9402210 (1994)
54. Chen Y-Q, Kuang Y-P *Phys.Rev.D* **46** 1165 (1992)
55. Eichten E, Feinberg F *Phys.Rev.D* **23** 2724 (1981)
56. Gromes D *Z.Phys.C* **26** 401 (1984)
57. Kwong W, Rosner J L *Phys.Rev.D* **38** 279 (1988)
58. Stanley D P, Robson D *Phys.Rev.D* **21** 3180 (1980)
59. Kwong W, Rosner J L *Phys.Rev.D* **44** 212 (1991)
60. Kaidalov A B, Nogteva A V *Yad.Fiz.* **47** 505 (1988) [*Sov.J.Nucl.Phys.* **47** 321  
(1988)]
61. Quigg C *FERMILAB-Conf-93/265-T* (1993)
62. Baker M, Ball J S, Zachariassen F Univ. of Washington Preprint (Seattle 1992)
63. Itoh C et al. *Nuovo Cimento A* **105(10)** 1539 (1992)
64. Roncaglia R, Dzierba A R, Lichtenberg D B, Predazzi E *Indiana Univ. Preprint  
IUHET 270* (1994)
65. Martin A in *Heavy Flavours and High Energy Collisions in the 1-100 TeV Range* Eds  
A.Ali, L.Cifarelli (NY:Plenum Press, 1989) p.141; CERN-TH.5349/88 (1988)
66. Kwong W, Rosner J L *Phys.Rev.D* **47** 1981 (1993);  
Nussinov S *Z.Phys.C* **3** 165 (1979);  
Lichtenberg D B, Roncaglia R, Wills J G, Predazzi E *Z.Phys.C* **47** 83 (1990)
67. Aliev T M, Yilmaz O *Nuovo Cimento A* **105(6)** 827 (1992)
68. Eichten E, Godfried K *Phys.Lett.B* **66** 286 (1977)

69. Kiselev V V, Likhoded A K, Tkabladze A V *Yad.Fiz.* **56** 128 (1993);  
Kiselev V V Preprint IHEP 93-64 (Protvino, 1993); Int. J. Mod. Phys.A [in press]
70. Isgur N, Scora D, Grinstein B, Wise M B *Phys.Rev.D* **39** 799 (1989)
71. Wirbel M, Stech B, Bauer M *Z.Phys.C* **29** 637 (1985);  
Bauer M, Stech B, Wirbel M *Z.Phys.C* **34** 103 (1987)
72. Galkin V O, Mishurov A Yu, Faustov R N, *Yad.Fiz.* **53** 1676 (1991)
73. Colangelo P, Nardulli G, Pietroni M *Phys.Rev.D* **43** 3002 (1991)
74. Avaliani I S, Sissakian A N, Slepchenko L A Preprint JINR E2-92-547 (Dubna, 1992)
75. Kartvelishvili V G, Likhoded A K *Yad.Fiz.* **42** 1306 (1985)
76. Kiselev V V, Tkabladze A V *Yad.Fiz.* **50** 1714 (1989)
77. Dominguez C A, Schilcher K, Wu Y L *Phys.Lett.B* **298** 190 (1993)
78. Chabab M Preprint Univ. de Montpellier LPT/93-01 (1993)
79. Reinshagen S, Rückl R Preprint CERN-TH.6879/93 (1993); Preprint MPI-Ph/93-88  
(Max-Plank-Institute 1993)
80. Sheikoleslami S M, Khanna M P *Phys.Rev.D* **44** 770 (1991);  
Masetti M *Phys.Lett.B* **286** 160 (1992)
81. Kiselev V V, Likhoded A K, Slabospitsky S R, Tkabladze A V *Yad.Fiz.* **49** 1100  
(1989);  
Ali A Preprint DESY 93-105 (1993)
82. Suzuki M *Phys.Lett.B* **155** 112 (1985); *Nucl.Phys.B* **258** 553 (1985)
83. Chang Ch-H, Chen Y-Q *Phys.Rev.D* **49** 3399 (1994)
84. Close F E, Wambach A *Nucl.Phys.B* **412** 169 (1994)
85. Ball P, Braun V M, Dosch H G *Phys.Rev.D* **44** 3567 (1991);  
Ball P Heidelberg Preprint HD-THEP-92-10 (1992)
86. Okun L B *Leptons and Quarks* (M.: Nauka, 1990)
87. Buras A J, Gerard J-M, Ruckl R *Nucl.Phys.B* **268** 16 (1986)
88. Gaillard M K, Lee B W *Phys.Rev.Lett.* **33** 108 (1974);  
Altarelli G, Maiani L *Phys.Lett.B* **52** 351 (1974)
89. Shifman M A *Nucl.Phys. B(Proc. Suppl)* **3** 289 (1988)
90. *Handbook of Mathematical Functions*, ed. M.Abramowitz, I.A.Stegun M.: Nauka,  
1979 (in Russian).

91. Chen Y-Q *Phys.Rev.D* **48** 5181 (1993)
92. Bourrely C, Soffer J, Renard F M, Taxil P *Phys.Rep.* **177** 326 (1989)
93. Chang Ch-H, Chen Y-Q *Phys.Rev.D* **48** 4086 (1993)
94. Jaffe R L, Randall L *Nucl.Phys.B* **412** 79 (1994)

*Received September, 1994*

# Contents

1. Introduction	1
2. Spectroscopy of $B_c$ mesons	5
2.1. Mass spectrum of $B_c$ mesons	6
2.1.1. Potential	6
2.1.2. Spin-dependent splitting of the $(\bar{b}c)$ quarkonium	10
2.1.3. $B_c$ meson masses from QCD sum rules	16
2.2. Radiative transitions in the $B_c$ family	18
2.2.1. Electromagnetic transitions	18
2.2.2. Hadronic transitions	20
2.3. Leptonic constant of $B_c$ meson	23
2.3.1. $f_{B_c}$ from potential models	24
2.3.2. $f_{B_c}$ from QCD sum rules	24
3. Decays of $B_c$ mesons	29
3.1. Life time of $B_c$ mesons	29
3.2. Semileptonic decays of $B_c$ mesons	34
3.2.1. Quark models	34
3.2.2. $B_c^+ \rightarrow J/\Psi(\eta_c)e^+\nu$ decay in QCD sum rules	39
3.2.3. Approximate spin symmetry	44
3.3. Hadronic decays of $B_c$ mesons	47
4. Production of $B_c$ mesons	52
4.1. Production of $B_c$ mesons in $e^+e^-$ -annihilation	52
4.2. Hadronic production of $B_c$ mesons	57
4.3. $B_c$ meson production in $\nu N$ -, $ep$ - and $\gamma\gamma$ - collisions	63
4.3.1. $B_c$ production in $\nu N$ -interactions	63
4.3.2. Production of $B_c$ mesons in $ep$ -scattering	64
4.3.3. Photonic production of $B_c$ mesons	65
5. Conclusion	69
6. Appendices	72
I. Covariant quark model	72
II. Spectral densities for three-particle functions	74
III. QCD sum rule scheme for three-point correlators	75
References	76